NOVEL SMALL MOLECULE INDUCES APOPTOSIS IN MALIGNANT PERIPHERAL NERVE SHEATH TUMORS OF NEUROFIBROMATOSIS TYPE I

APPROVED BY SUPERVISORY COMMITTEE

_____

Luis F. Parada, Ph.D. (Mentor)

_____

Lu Q. Le, M.D., Ph.D. (Mentor)

_____

Michael White, Ph.D. (Chair)

_____

Jane Johnson, Ph.D.

DEDICATION

I would like to thank the members of my Graduate Committee for providing guidance along this incredible journey. My two mentors have shaped the way that I think – and for this I will be forever grateful.

# NOVEL SMALL MOLECULE INDUCES APOPTOSIS IN MALIGNANT PERIPHERAL NERVE SHEATH TUMORS OF NEUROFIBROMATOSIS TYPE 1

by

VINCENT CHAU

DISSERTATION

Presented to the Faculty of the Graduate School of Biomedical Sciences

The University of Texas Southwestern Medical Center at Dallas

In Partial Fulfillment of the Requirements

For the Degree of

DOCTOR OF PHILOSOPHY

The University of Texas Southwestern Medical Center at Dallas

Dallas, Texas

July, 2013

NOVEL SMALL MOLECULE INDUCES APOPTOSIS IN MALIGNANT PERIPHERAL NERVE SHEATH TUMOR OF NEUROFIBROMATOSIS TYPE I

Vincent Chau, Ph.D.

The University of Texas Southwestern Medical Center at Dallas, 2013

Supervising Professors: Luis F. Parada, Ph.D. and Lu Q. Le, M.D., Ph.D.

Neurofibromatosis Type 1 (NF1) is an autosomal disease that affects neural crest-derived tissues, leading to a wide spectrum of clinical presentations. Patients commonly present with plexiform neurofibromas, benign but debilitating growths that can transform into malignant peripheral nerve sheath tumors (MPNSTs), a main cause of mortality. Currently, surgery is the primary course of treatment for MPNST, but with the limitation that these tumors are highly invasive. Radiotherapy is another treatment option, but is undesirable because it can induce additional mutations. MPNST patients may also receive doxorubicin as therapy, but this DNA-intercalating agent has relatively low tumor specificity and limited efficacy. In this study, we exploited a robust genetically-engineered mouse model of MPNST that

recapitulates human NF1 associated MPNST to identify a novel small chemical compound that inhibits tumor cell growth. Compound 21 (Cpd21) inhibits growth of all available *in vitro* models of MPNST and human MPNST cell lines, while remaining non-toxic to normally-dividing Schwann cells or mouse embryonic fibroblasts. We show that this compound delays the cell cycle and leads to cellular apoptosis. Moreover, Cpd21 can reduce MPNST burden in a mouse allograft model, underscoring the compound's potential as a novel chemotherapeutic agent.

TABLE OF CONTENTS

PRIOR PUBLICATIONS

Mo, W., Chen, J., Patel, A., Zhang, L., **Chau, V.**, Li, Y., Cho, W., Lim, K., Xu, J., Lazar, Alexander J., Creighton, C. J., Bolshakov, S., McKay, R. M., Lev, D., Le, L. Q., and Parada, L. F. 2013. CXCR4/CXCL12 Mediate Autocrine Cell- Cycle Progression in NF1-Associated Malignant Peripheral Nerve Sheath Tumors. *Cell* 152:1077-1090.

**Chau, V.**, Lim, S.K., Mo, W., Liu, C., Patel, A.J., McKay, R.M., Wei, S., Posner, B.A. Williams, N. S., De Brabander, J. K., Parada, L. F., and Le, L.Q. Novel Small Molecule Induces Apoptosis in Malignant Peripheral Nerve Sheath Tumors of Neurofibromatosis Type I. Manuscript submitted for publication.

LIST OF FIGURES

LIST OF TABLES

LIST OF APPENDICES

# LIST OF DEFINITIONS

| | |
|---|---|
| ATP | adenosine triphosphate |
| BrdU | bromodeoxyuridine |
| BSA | bovine serum albumin |
| CDK | cyclin-dependent kinase |
| CDKI | cyclin-dependent kinase inhibitor |
| cDNA | complementary deoxyribonucleic acid |
| cis-NP | *cis-Nf1*$^{+/-}$*;p53*$^{+/-}$ |
| Cpd21 | Compound 21 or SW106065 |
| CT | computed tomography |
| DMEM | Dulbecco's Modified Eagle Medium |
| DMSO | dimethyl sulfoxide |
| DNA | deoxyribonucleic acid |
| DRG | dorsal root ganglion |
| EC50 | half maximal effective concentration |
| FBS | fetal bovine serum |
| FITC | fluorescein isothiocyanate |
| GAP | guanosine-5'-triphosphatase associated proteins |
| GBM | glioblastoma multiforme |
| GDP | guanosine-5'-diphosphate |
| GEF | guanine nucleotide exchange factor |

| | |
|---|---|
| GFP | green fluorescent protein |
| GPCR | G protein coupled receptor |
| GRD | guanosine-5’-triphosphatase associated protein related domain |
| GTP | guanosine-5’-triphosphate |
| H&E | hematoxylin and eosin |
| IP | intraperitoneal |
| LOH | loss of heterozygosity |
| MAPK | mitogen-activated protein kinase |
| MEF | mouse embryonic fibroblast |
| MPNST | malignant peripheral nerve sheath tumor |
| MPNST-luc+ | luciferase-tagged malignant peripheral nerve sheath tumor |
| MRI | magnetic resonance imaging |
| mRNA | messenger ribonucleic acid |
| MTT | malignant Triton tumor |
| Myc-SC | *Myc*-immortalized Schwann cell |
| NCSC | neural crest stem cell |
| NF1 | Neurofibromatosis Type I |
| NF2 | Neurofibromatosis Type II |
| NP SKPs | $Nf1^{-/-};p53^{-/-}$ skin derived precursors |
| PBS | phosphate buffered saline |
| PCR | polymerase chain reaction |
| PET | positron emission tomography |

| | |
|---|---|
| PFS | progression free survival |
| PH | Plekstrin homology |
| PI3K | phosphatidylinositol 3’-kinase |
| PIP2 | phosphatidylinositol 4,5-biphosphate |
| PIP3 | phosphatidylinositol 3,4,5-triphosphate |
| PMA | phorbol ester 12-myristate 13-acetate |
| qRT-PCR | quantitative real time polymerase chain reaction |
| RNA | ribonucleic acid |
| RNase | ribonuclease |
| S9 | supernatant fraction obtained from liver homogenate by centrifuging at 9000 g for 20 minutes in a suitable medium |
| SCP | Schwann cell precursor |
| SDS-PAGE | sodium dodecyl sulfate polyacrylamide gel electrophoresis |
| SKP | skin derived precursor |
| sMPNST | SKP-derived malignant peripheral nerve sheath tumor |

# CHAPTER ONE
# Introduction and Literature Review

## Introduction to Neurofibromatosis Type I

There are two distinct forms of neurofibromatosis: Neurofibromatosis Type I (NF1) or von Recklinghausen's disease, and Neurofibromatosis Type II (NF2) or bilateral acoustic or central neurofibromatosis. Historically, these two different forms of neurofibromatosis were grouped together clinically to describe patients with café-au-lait spots and nervous system tumors (Ruggieri and Huson, 1999), though it is now understood that NF1 and NF2 are two genetically-distinct diseases (Gutmann, 2001).

NF1 is an autosomal dominant disorder that affects 1 in 3500 people (Crowe et al., 1956; Gutmann et al., 1997; Huson et al., 1989; Szudek et al., 2000), making it the most common form of neurofibromatosis and one of the most common autosomal dominant diseases (Ruggieri and Huson, 1999). NF1 is diagnosed in patients that present with two or more of the following signs and symptoms: six or more café-au-lait spots, two or more neurofibromas, axillary or inguinal freckling, optic glioma, two or more Lisch nodules of the eye, osseous abnormality, or a first-degree relative that was diagnosed with the aforementioned criteria (Gutmann et al., 1997; Ruggieri and Huson, 1999; Stumpf et al., 1988).

NF1 is considered the most common tumor predisposition syndrome since patients may develop a variety of benign and malignant tumors, including neurofibromas (Ferner and Gutmann, 2002; Pinsk et al., 2003), optic gliomas (Hegedus et al., 2008; Listernick et al.,

1997), somatostatinoma (Mao et al., 1995), pheochromocytoma (Vlenterie et al., 2013; Walther et al., 1999), gastrointestinal stromal tumor (Andersson et al., 2005; Pinsk et al., 2003; Vlenterie et al., 2013), rhabdomyosarcoma (Coffin et al., 2004; Ferrari et al., 2007), leimyosarcoma (Bernardis et al., 1999), leukemia (Bader and Miller, 1978; Bollag et al., 1996; Side et al., 1997; Zvulunov et al., 1995), astrocytoma (Ruggieri and Packer, 2001), and malignant peripheral nerve sheath tumors (MPNSTs) (Ferrari et al., 2007; Menon et al., 1990).

In addition to a predisposition to neoplasms, NF1 patients commonly experience hypertension due to narrowing of the renal artery, coarctation of the aorta, or secondary to pheochromocytoma (Bausch et al., 2007; Zinnamosca et al., 2011). Many NF1 patients are cognitively-impaired or have learning difficulties (Ozonoff, 1999).

**Genetic Basis of NF1**

NF1 occurs in patients that have germline mutations in the *NF1* tumor suppressor gene, which was originally identified by positional cloning (Cawthon et al., 1990; Viskochil et al., 1990; Wallace et al., 1990). *NF1* encodes for a protein called Neurofibromin. The product of the *NF1* gene was identified by finding protein sequence homology between the encoded product and members of the GTPase-activating protein (GAP) family, including mammalian p120-GAP (Xu et al., 1990a; Xu et al., 1990b) and yeast IRA1 and IRA2 (Ballester et al., 1990; Xu et al., 1990b).

Neurofibromin contains two domains, the Sec14 domain (Mousley et al., 2007) and the RASGAP-related domain (RAS-GRD) (Ballester et al., 1990; Xu et al., 1990b). The

Sec14 domain has been reported to be involved in lipid signaling in yeast (Mousley et al., 2007), but its role in NF1 remains unknown (Le and Parada, 2007). The RAS-GRD is involved in the inactivation of RAS signaling (Figure 1). RAS is located at the inner leaflet of the plasma membrane and its activity is active when bound to GTP and inactive when bound to GDP. Two families of proteins determine whether RAS is bound to GTP or GDP. The first are guanine nucleotide exchange factors (GEFs) such as SOS (Egan et al., 1993), which catalyze the exchange of GDP for GTP, thereby activating RAS. The second are GTPase associated proteins (GAPs), which catalyze the hydrolysis of GTP to GDP, thereby inactivating RAS.

Binding of specific ligands to growth factor receptors such as epidermal growth factor receptors (EGFRs) and platelet derive growth factor receptors (PDGFRs) causes the association of adaptor proteins Shc (Rozakis-Adcock et al., 1992) and GRB2 (Lowenstein et al., 1992), which in turn activate SOS (Egan et al., 1993). SOS then exchanges the GDP for GTP to activate RAS, which in turn activates downstream phosphatidylinositol 3'-kinase (PI3K) and mitogen-activated protein kinase (MAPK) signaling (Basu et al., 1992; Dasgupta et al., 2005; DeClue et al., 1992; Le and Parada, 2007; Weiss et al., 1999; Wittinghofer, 1998). PI3K and MAPK signaling are commonly understood to regulate cell proliferation, death, differentiation, and migration, and dysregulated signaling in these pathways is known to play an important role in tumorigenesis (Bennett et al., 2009). The RAS-GRD of Neurofibromin normally maintains RAS in an inactive state, preventing overactive Ras signaling (Le and Parada, 2007), and thereby acts as a potent tumor suppressor. Loss of heterozygosity (LOH) in *NF1* due to genetic mutation thus results in activated RAS signaling

(Basu et al., 1992; Bollag et al., 1996; DeClue et al., 1992; Guha et al., 1996), which then drives neurofibroma formation (Serra et al., 1997).

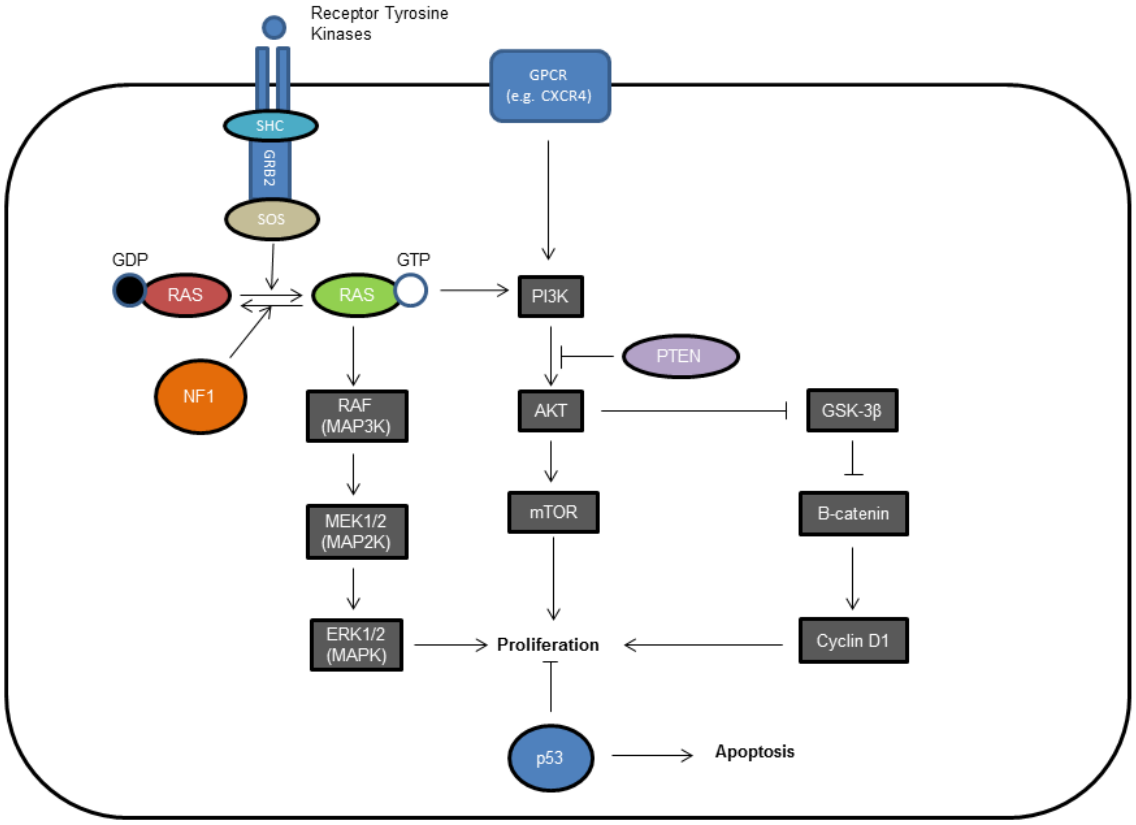


**Figure 1 Signaling Pathways in Neurofibromatosis Type I.** Receptor tyrosine kinases such as EGFR and PDGFR bind to extracellular ligands and activate SHC, which then recruits GRB2 and SOS. SOS exchanges the GDP that is bound to RAS for GTP, thereby activating RAS. RAS then activates RAF, which in turn activates the MAPK pathway, leading to cellular proliferation. In addition, RAS activates PI3K, leading to the activation of AKT and mTOR, which also result in cellular proliferation and growth. PI3K may also be activated by GPCRs. The activation of RAS is normally opposed by NF1, which contains a RAS-GRD that inactivates RAS by increasing the rate of hydrolysis of GTP to GDP. Therefore, when the *NF1* gene is deficient, the activation of RAS is unopposed, leading to cellular proliferation. PTEN also normally opposes the activation of AKT, and PTEN expression may be lost or decreased in the context of Neurofibromatosis Type I. p53 also normally prevents unchecked proliferation and induces apoptosis. Therefore, loss of both *p53* and *NF1* leads to unchecked proliferation and escape from apoptosis, two hallmark signs of cancer (Hanahan and Weinberg, 2011). Recently, it was demonstrated in the context of MPNST that CXCR4, which is a GPCR, activates PI3K and leads to the activation of β-Catenin and Cyclin D1, which leads to cellular proliferation (Mo et al., 2013). Figure adapted from Le and Parada (2007).

**Neurofibromas**

Neurofibromas are the hallmark sign that is observed in NF1 patients. These are benign lesions that expand and that can appear throughout the body (Ruggieri and Huson, 1999). Neurofibromas can appear as nodules either on physical examination or as tumors in imaging modalities. Neurofibromas have complex cellular architecture, including Schwann lineage cells, fibroblasts, perineurial cells, and mast cells enmeshed in collagen deposits with physical proximity to peripheral nerves (Le et al., 2009). Though all subtypes of neurofibromas appear similar at the cellular level, the differences in clinical presentation are suspected to reflect either differences in the source cells or their anatomical location at the time of tumor formation (Le et al., 2009).

Neurofibromas can be classified into two groups: cutaneous (dermal) and plexiform. Cutaneous neurofibromas are nodules that appear in the epidermis and/or dermis of the skin (Ruggieri and Huson, 1999), and are observed in virtually all adult NF1 patients (Huson, 1999; Le et al., 2009). These neurofibromas can expand rapidly, especially during puberty or pregnancy (Dugoff and Sujansky, 1996; Ferner, 2007; Lakkis and Tennekoon, 2000), and may retreat into quiescence in unpredictable ways (Ruggieri and Huson, 1999), perhaps suggesting a contribution by hormones to pathogenesis. Studies that have been done to elucidate the role of hormones, such as progesterone (Fishbein et al., 2007; McLaughlin and Jacks, 2003), estrogen (Fishbein et al., 2007; McLaughlin and Jacks, 2003), testosterone (Fishbein et al., 2007), and growth hormone (Cunha et al., 2003) in neurofibromas have generally correlated the expression of the respective hormonal receptors in certain cell types within neurofibromas. These studies raise the question of whether some of all of these

hormones and receptors are necessary for the development of neurofibromas. More broadly, they raise the question of how the body's neuroendocrine organs and products intersect with neurofibroma formation.

Plexiform neurofibromas develop along nerves and may involve multiple nerve branches, and are typically painful (Korf, 1999; Ruggieri and Huson, 1999). Plexiform neurofibromas develop in about 30% of NF1 patients (Huson et al., 1988). These tumors tend to develop congenitally and grow throughout life (Le et al., 2009). These tumors may compress critical anatomic structures, leading to life-threatening complications. Unfortunately, surgical resection is often difficult because of the invasive nature of plexiform neurofibromas into surrounding structures (Korf, 1999). Plexiform neurofibromas often transform into MPNSTs, which are aggressive tumors that metastasize widely (Ducatman et al., 1986). Whereas dermal neurofibromas are known to arise from a type of adult stem cell called skin-derived precursors (SKPs) (Le et al., 2009), plexiform neurofibromas are believed to arise from embryonic neural crest lineage Schwann cell progenitors (Zhu et al., 2002). Whether the two cell types are related or the same remains unclear (Mo et al., 2013).

## Brief History of Mouse Modeling and Its Relations to Neurofibromatosis Type I and Cancer

In the 1980s, technological advances in generating genetically-engineered mice allowed the introduction of single oncogenes into the mouse genome (Van Dyke and Jacks, 2002). Two early groups showed that mice harboring single oncogenes can develop spontaneous tumors. The first group expressed c-Myc fused to a mouse mammary tumor

virus (MTV) promoter in mammary epithelium, and showed that this transgene expression led to spontaneous mammary adenocarcinoma (Stewart et al., 1984). Later, this work was expanded to show that mice expressing c-Myc coupled to immunoglobulin mu or kappa develop lymphoma (Adams et al., 1985). The second group showed that expression of SV40 early region genes fused to the metallothionein gene in mice led to tumor development in the choroid plexus of the brain (Brinster et al., 1984). In addition, expression of SV40 along with the rat insulin II gene leads to development of pancreatic beta cell tumors (Hanahan, 1985). These pioneering experiments demonstrated the utility of studying cancer using mice that could be engineered with specific genetic components.

A few years later, mutation of tumor suppressor genes was shown to lead to tumor development. For example, mice lacking one copy of *Rb* develop pituitary adenomas (Jacks et al., 1992), and mice lacking both copies of *p53* develop a wide variety of tumors, including lymphomas, hemangiosarcoma, mammary adenocarcinoma, alveolar and bronchiolar adenoma, malignant Schwannoma, osteosarcoma, embryonal carcinoma, choriocarcinoma, and Leydig cell tumor (Donehower et al., 1992). These early experiments were critical in determining that the absence of a normal gene could also lead to tumorigenesis.

Since a single genetic change is generally not sufficient to induce tumorigenesis (Van Dyke and Jacks, 2002), many groups have combined multiple genetic changes by intercrossing different mouse strains to interrogate the cooperating events leading to cancer development. For instance, combining deletions of *p53* with expression of SV40, which inactivates pRB, leads to faster tumor development in the choroid plexus and decreased survival compared with mice without *p53* deficiency (Symonds et al., 1994). This experiment

determined that perturbations of p53 and pRB function collaborate in cancer development, and demonstrate that combinations of genetic changes can lead to tumorigenesis.

Manipulating the mouse genome has since become increasingly sophisticated. Transgenes can now be introduced into the entire organism or into specific cell types or during specific time windows. To attain spatial control of a gene in specific cell type, the gene of interest is flanked by recombinase sites (loxP or frt) in one mouse and mated with a second mouse that contains the recombinase (Cre or flp) transgene that is driven by a cell-type specific promoter (Gorman and Bullock, 2000; Nagy, 2000; Rossant and McMahon, 1999). Progeny will have deletions of that gene (as determined by the first mouse) in the specific cell type (as determined by the second mouse). Another approach is to create a fusion protein between Cre recombinase and a mutant form of the ligand-binding domain of the estrogen receptor that is controlled by a tissue-specific promoter (Feil et al., 1997). This fusion protein can bind to and be activated by an exogenous source of tamoxifen. The delivery of tamoxifen to the mouse allows the fusion protein to shuttle into the nucleus and to induce recombination, thereby allowing genetic manipulation in a temporally-controlled fashion (Brocard et al., 1997). These technical advances allow the examination of particular cellular compartments and specific cell-cell and cell-microenvironment interactions *in vivo*. In addition, there are model systems that allow a transgene to be reversibly expressed such as the Tet-Off or Tet-On systems (Baron and Bujard, 2000).

In the case of the *Nf1* gene, homozygous knock out of both copies of *Nf1* in mice results in embryonic death at E13.5, with embryos exhibiting severe structural defects of the heart (Brannan et al., 1994; Jacks et al., 1994), delayed development of the abdominal wall

and smooth muscle in the stomach, and hyperplasia of the paravertebral sympathetic neurons (Brannan et al., 1994). Mice that are heterozygous at the *Nf1* locus ($Nf1^{+/-}$) develop pheochromocytoma, myeloid leukemia, lymphomas, lung adenocarcinoma, fibrosarcomas, and hepatomas. However, $Nf1^{+/-}$ mice do not develop many of the canonical features seen in NF1 patients, including neurofibromas, MPNST, optic gliomas, pigmentation defects, or Lisch nodules (Jacks et al., 1994). Approximately half of the tumors seen in the $Nf1^{+/-}$ mice, including all of the pheochromocytomas and myeloid leukemias, showed LOH in the *Nf1* gene (Jacks et al., 1994). Therefore, this result is consistent with the Knudson "two-hit" model and is consistent with the view that loss of both copies of *Nf1* contributes to tumorigenesis (Jacks et al., 1994).

**Mouse Models of Neurofibromas**

Cichowski *et al*. (1999) then created chimeric mice harboring $Nf1^{+/-}$;$Nf1^{+/+}$ genotype to bypass the embryonic lethality caused by homozygous deletion of *Nf1*. These mice could be categorized into three groups based on phenotype. The first group, which showed the highest proportion of chimerism, died within 1 month from unknown etiology. The second group, which had the lowest degree of chimerism, survived to adulthood without detectable pathology. The third group, which was moderately chimeric, exhibited reduced life span, myelodysplasia, neuromotor deficits, and neurofibromas (Cichowski et al., 1999). These neurofibromas arose from the dorsal root ganglia and resembled plexiform neurofibromas. Interestingly, dermal neurofibromas were not detectable. These neurofibromas contained cells that were $Nf1^{-/-}$ as demonstrated by β-galactosidase staining, and also stained positively

for S100, a Schwann cell marker. Examination of these tumors by electron microscopy revealed that they were composed of Schwann cells and perineurial cells, two important cell types that are found in human neurofibromas.

Numerous groups then proceeded to generate tissue-specific knockouts of *Nf1*. When *Nf1* is conditionally deleted in myelinating Schwann cells driven by *Krox20-Cre* (*Krox20-Cre-Nf1*$^{f/-}$) , the peripheral nerves were enlarged (Zhu et al., 2002). Histological analysis revealed that there was a proliferation of bipolar cells that stained positively for Schwann cell, neural crest, perineurial, fibroblast, and neuronal markers. There was collagen deposition and mast cell infiltration, and all of these signs are consistent with human neurofibromas. In addition, *Krox20-Cre-Nf1*$^{f/f}$ mice had fewer and smaller hyperplastic lesions, less collagen deposition, less mast cell infiltration. These results imply that the haploinsufficient tissues surrounding the *Nf1*-deficient Schwann cells play an important role in neurofibroma formation.

Another model of neurofibroma can be generated by deleting *Nf1* in fetal stem/progenitor cells during nerve development (Joseph et al., 2008; Zheng et al., 2008). *P0A-Cre* drives recombination in the Schwann cell precursors (SCPs), which are also known as neural crest stem cells (NCSCs) for their ability to give rise to Schwann cells and myofibroblasts (Joseph et al., 2004; Morrison et al., 1999). *P0A-Cre-Nf1*$^{f/-}$ mice develop enlarged nerves, and 71% of these mice develop plexiform neurofibromas with spindle-shaped cells, collagen deposition, and mast cell infiltration. The other 29% of *P0A-Cre-Nf1*$^{f/-}$ mice develop hyperplasia with focal neurofibroma. Surprisingly, the SCPs/NCSCs of *P0A-Cre-Nf1*$^{f/-}$ mice did not undergo increased proliferation. Rather, the Remak bundles in *P0A-*

*Cre-Nf1*$^{f/-}$ mice were disorganized with axons segregating abnormally. Lastly, these authors showed that continuous growth of *Nf1*-deficient, non-myelinating Schwann cells drive neurofibroma progression. Despite the propensity of *P0A-Cre-Nf1*$^{f/-}$ mice for developing neurofibromas, one group argues that differentiated glia, such as nonmyelinating Schwann cells, but not NCSCs, which they claim could not be cultured or detected postnatally, are the cells that give rise to plexiform neurofibroma (Joseph et al., 2008). This group also reported that knockout of *Nf1* from the neural tube (*Wnt1-Cre-Nf1*$^{f/-}$) leads to death at birth with no neurofibromas detected, and that knockout of *Nf1* from the Schwann cell lineage (*3.9Periostin-Cre-Nf1*$^{f/-}$) leads to early death at 4 weeks with no neurofibromas detected (Joseph et al., 2008).

Yet another group showed that knocking out *Nf1* in boundary cap cells and Schwann cell precursors generates neurofibromas (Wu et al., 2008). *Desert Hedgehog Cre (Dhh-Cre)* is expressed in the boundary cap cells and Schwann cell precursors at E12.5 but not in neural crest cells, neurons, or CNS cells. *Dhh-Cre-Nf1*$^{f/f}$ mice have reduced survival, whereas *Dhh-Cre-Nf1*$^{f/+}$ mice have normal survival time. *Dhh-Cre-Nf1*$^{f/f}$ mice also had enlarged peripheral and cranial nerve trunks and nerve roots. Plexiform neurofibromas were detected in all of the *Dhh-Cre-Nf1*$^{f/f}$ mice, and contained a mixture of S100+ and S100- cells and classic neurofibroma histology. Dermal neurofibromas were detected in 46.4% of *Dhh-Cre-Nf1*$^{f/f}$ mice, and showed numerous S100+ cells with abundant collagen and mast cell infiltration. In addition, 39.3% of *Dhh-Cre-Nf1*$^{f/f}$ mice had pigmentation defects overlying the spinal cord. Finally, the nerves from *Dhh-Cre-Nf1*$^{f/f}$ mice showed abnormal morphology and contain Schwann cells that demonstrate increased proliferation.

In addition to work in Schwann cells and their precursors, another group suggested that the microenvironment is also important in demonstrating that *Nf1* heterozygosity in bone-marrow derived cells is sufficient to allow neurofibroma formation when Schwann cells are *Nf1*-deficient (Yang et al., 2008). It was known that *Nf1*-deficient Schwann cells secrete a factor that stimulates Nf1 heterozygous mast cell migration (Yang et al., 2003). When *Krox20-Cre-Nf1*$^{f/f}$ mice were lethally-irradiated and then transplanted with *Nf1*$^{+/-}$ bone marrow, survival was decreased compared to either *Krox20-Cre-Nf1*$^{f/f}$ or *Krox20-Cre-Nf1*$^{f/-}$ mice that were transplanted with wildtype bone marrow. *Krox20-Cre-Nf1*$^{f/f}$ mice transplanted with *Nf1*$^{+/-}$ bone marrow develop enlarged spinal cords and neurofibromas with disruption of normal architecture, collagen deposition, and infiltration of donor mast cells and small numbers of macrophages, T lymphocytes, and B lymphocytes. This experiment demonstrated that *Nf1*$^{+/-}$ bone marrow cells are both sufficient and required for neurofibroma progression. Furthermore, this group showed that transplantation of Nf1$^{+/-}$ bone marrow with disrupted c-kit receptors (either genetically or pharmacologically) into *Krox20-Cre-Nf1*$^{f/-}$ mice abrogates neurofibroma formation.

Another model of neurofibroma can be generated from skin-derived precursors (SKPs), which are stem cells that are present in the skin and that can differentiate into neuronal and glial lineages (Fernandes et al., 2006; Fernandes et al., 2004; McKenzie et al., 2006; Toma et al., 2001; Toma et al., 2005). When *Nf1*$^{-/-}$ SKPs were transplanted subcutaneously into mice with *Nf1*$^{+/-}$ background, neurofibromas did not form. However, when *Nf1*$^{-/-}$ SKP that were transplanted into the sciatic nerve of mice with *Nf1*$^{+/-}$ background, tumors formed and contained spindle-shaped cells, expressed S100, and had mast cell

infiltration (Le et al., 2009). These tumors were consistent with neurofibroma, and indicate that *Nf1*-deficency and a proper microenvironment are required for the formation of neurofibromas from SKPs. Furthermore, if the ubiquitously driven *CMV-CreER-Nf1*$^{f/-}$ mice are painted with 4-OH-tamoxifen, a tumor that resembles dermal neurofibroma forms. Interestingly, when *CMV-Cre-ER-Rosa26-Nf1*$^{f/-}$ SKP that were treated with 4-OH-tamoxifen *ex vivo* were implanted back into the original mouse, only pregnant female mice develop tumors that resembled dermal neurofibromas. These results indicate that SKPs are the cell of origin of dermal neurofibromas, and that hormones play an important role in neurofibroma development.

Taken together, these data suggest that the microenvironment plays an essential role in the development of neurofibromas, with mast cells performing critical functions. Moreover, deletion of *Nf1* during an early point in Schwann cell development can overcome the necessity of a favorable microenvironment for neurofibroma formation. Therefore, *Nf1* has both a temporal and spatial complexity in driving neurofibroma development.

**Malignant Peripheral Nerve Sheath Tumors**

NF1 patients may also develop a variety of malignant tumors, with MPNST being the most common (Brems et al., 2009; Gutmann et al., 1997). MPNST is a soft tissue sarcoma that may arise within 8-13% of NF1 patients with pre-existing plexiform neurofibromas (Ferner and Gutmann, 2002). This cancer typically arises at ages 30-40 in NF1 patients or ages 60-70 in sporadic cases (Angelov et al., 1998; Evans et al., 2002). MPNSTs most commonly arise in the pelvic region or in the extremities (Anghileri et al., 2006), and

typically present as painful, growing masses (Grobmyer et al., 2008). Neurological symptoms tend to correlate with the anatomical location of the tumor.

Unfortunately, it is generally difficult to differentiate MPNST from the surrounding benign neurofibromas. Some claim that magnetic resonance imaging (MRI) (Bhargava et al., 1997), computed tomography (CT) (Grobmyer et al., 2008), and positron emission tomography (PET) (Cardona et al., 2003; Gregorian et al., 2009) may aid in diagnosis of MPNST. However, many NF1 patients are often diagnosed with MPNST after the cancer has already metastasized, most commonly to the lungs (Anghileri et al., 2006), and sometimes to the liver and brain (Ducatman et al., 1986; Vauthey et al., 1995). The current gold standard for diagnosing MPNST is usually with histological analysis (Gutmann et al., 1997; Katz et al., 2009), and MPNSTs usually contain spindle-shaped cells, mitotic figures, atypical nuclei, with areas of necrosis (Lin et al., 1997).

**Mouse Models of MPNST**

The two most common cancer-associated mutations present in MPNST in addition to *Nf1* mutation are *TP53* (Berghmans et al., 2005; Birindelli et al., 2001; Greenblatt et al., 1994; Jhanwar et al., 1994; Menon et al., 1990) and *CDKN2A* (Berner et al., 1999; Birindelli et al., 2001; Buchstaller et al., 2012; Kourea et al., 1999; Nielsen et al., 1999; Perrone et al., 2003), which are both well-known tumor suppressor genes. Both genes have been perturbed in efforts to generate murine models of MPNST.

The well-known p53 protein regulates multiple cellular processes whose dysregulation lead to cancer, and this tumor suppressor gene is linked to *Nf1* on chromosome 11 in mice (Buchberg et al., 1992). Two groups generated the pioneering murine models of

MPNST by mutating both *Nf1* and *p53* (Cichowski et al., 1999; Vogel et al., 1999). Mice that have mutations of *Nf1* and *p53* in trans (*trans-Nf1*$^{+/-}$*;p53*$^{+/-}$) survive on average 10 months, underwent LOH at either the *Nf1* or *p53* locus, and developed tumors seen in mice with either single mutation, including osteosarcoma, fibrosarcoma, rhabdomyosarcoma, and hemangiosarcoma (Cichowski et al., 1999). Mice with *Nf1*$^{+/-}$ and *p53*$^{+/-}$ genotype in *cis* configuration (*cis-Nf1*$^{+/-}$*;p53*$^{+/-}$) survive on average 5 months, underwent LOH at both loci, and developed several soft tissue sarcomas, including malignant triton tumor (MTT), leiomyosarcoma, and MPNST (Cichowski et al., 1999; Vogel et al., 1999). These MPNSTs were invasive, displayed histology that is consistent with human MPNST such as interweaving bundles of spindle-shaped cells, and stained positively for S100 (Cichowski et al., 1999; Vogel et al., 1999).

Deficiency in *Nf1* is known to induce increased expressed of *Ink4a* and *Arf* (known as *CDKN2A* in humans) in neural crest cells cultured from the sciatic nerve or sympathetic chain (Joseph et al., 2008). The *Ink4a* gene encodes p16$^{INK4a}$, which inhibits CDK4 and CDK6, and this inhibition in turn prevents the phosphorylation of Rb, leading to arrest at the G1 phase (Quelle et al., 1995; Serrano et al., 1993). *Arf* encodes p19$^{Arf}$, which is induced by oncogenic RAS and activates p53, leading to cell cycle arrest (Palmero et al., 1998; Quelle et al., 1995). Mice harboring genotypes of either *Nf1*$^{+/-}$*;Ink4a/Arf*$^{+/-}$ or *Nf1*$^{+/-}$*;Ink4a/Arf*$^{/-}$ spontaneously develop MPNST on the shoulders, ribs, and legs (Joseph et al., 2008). These MPNSTs displayed tightly packed spindle-shaped cells, hyperchromatic nuclei, mitotic figures, and stained positively for S100. One group argues that the lack of p75+ (a marker of

SCPs/NCSCs) cells in adult *Nf1*$^{+/-}$*;/Ink4a/Arf*$^{-/-}$ tissues before the development of MPNSTs suggests that MPNSTs do not arise from SCPs/NCSCs (Joseph et al., 2008).

In an effort to interrogate the downstream effectors of *Nf1* in MPNST development, another group showed that *K-Ras* activation combined with *Pten*$^{+/-}$ leads to MPNST formation in mice (Gregorian et al., 2009). This group used the *mGFAP-Cre* to upregulate *K-Ras* and to delete *Pten* at the differentiation stage between the Schwann cell precursor and immature Schwann cell stages. Crossing the *mGFAP-Cre* line to *LSL-Rosa26* mice, followed by subsequent β-galactosidase staining showed that *mGFAP-Cre* is active in the intercostal nerve, dorsal root ganglia (DRG), and trigeminal ganglia. Mice with genotype of *mGFAP-Cre-LSL-K-Ras*$^{G12D/+}$*;Pten*$^{f/+}$ develop plexiform neurofibromas and MPNSTs with 100% penetrance. All MPNSTs developed within the plexiform neurofibromas, and showed increased expression of pS6, pAKT, and pERK. Mice with genotype of *mGFAP-Cre-LSL-K-Ras*$^{G12D/+}$, of *mGFAP-Cre-Pten*$^{f/f}$, or of *mGFAP-Cre-Nf1*$^{f/f}$ did not develop neurofibromas or MPNSTs. Pten negatively regulates the PI3K pathway, which controls cellular growth and survival (Cantley and Neel, 1999).

To find novel drivers of MPNST development, another group employed a forward-genetic screening approach by employing the Sleeping Beauty (SB) mutagenesis system (Dupuy et al., 2005). This group verified that *Nf1* and *Pten* are important players in MPNST development (Keng et al., 2012a; Rahrmann et al., 2013; Watson et al., 2013). This group used the *Dhh-Cre* drivers to conditionally delete *Nf1* and *Pten* in Schwann cell precursors at E12.5. Mice with genotype of *Dhh-Cre-Nf1*$^{f/f}$*;Pten*$^{f/f}$ develop high grade MPNSTs in the brachial plexus, trigeminal nerve, sciatic nerve, and sacral plexus (Keng et al., 2012a). Other

allelic combinations of mice with *Nf1* and *Pten*, including *Dhh-Cre-Nf1*$^{f/f}$*;Pten*$^{f/+}$, *Dhh-Cre-Nf1*$^{f/f}$, *Dhh-Cre-Nf1*$^{f/+}$*;Pten*$^{f/f}$, and *Dhh-Cre-Pten*$^{f/f}$, develop low grade tumors. Mice with genotype of *Dhh-Cre-Nf1*$^{f/+}$*;Pten*$^{f/+}$ do not develop tumors. Tumors from *Dhh-Cre-Nf1*$^{f/f}$*;Pten*$^{f/f}$ and *Dhh-Cre-Nf1*$^{f/f}$*;Pten*$^{f/+}$ mice are positive for S100 and Olig2, reflecting the Schwann cell and/or precursor origin. Tumors from *Dhh-Cre-Nf1*$^{f/f}$*;Pten*$^{f/f}$ mice were also positive for pERK, pAKT, and pS6k, reflecting the upregulation of RAS/MEK/ERK and PI3K/AKT/mTOR pathways. Finally, this group showed that human MPNST also have reduced *PTEN* expression.

This same group was also able to generate sporadic MPNSTs in a mouse model that both overexpresses *Egfr* and is deficient in *Pten* in Schwann cells (Keng et al., 2012b). Mice with genotypes *Dhh-Cre-Pten*$^{f/f}$*;Cnp-Egfr* or *Dhh-Cre-Pten*$^{f/+}$*;Cnp-Egfr* were generated, and both types of mice exhibited enlarged dorsal root ganglia and trigeminal nerves. *Dhh-Cre-Pten*$^{f/f}$*;Cnp-Egfr* mice developed MPNST, whereas *Dhh-Cre-Pten*$^{f/+}$*;Cnp-Egfr* mice developed neurofibromas. Moreover, *Pten* expression was found to be dramatically decreased and *Egfr* was increased in MPNST compared to Schwann cells purified from plexiform neurofibromas, Schwann cells purified from dermal neurofibromas, and wildtype Schwann cells (Keng et al., 2012b).

Recently, this group reported additional genetic drivers of MPNST development (Rahrmann et al., 2013; Watson et al., 2013). Using the *Cnp-Cre* transgene, the SB transposon was conditionally activated in Schwann cells and their precursors. This screen identified many cooperating mutations in the Wnt/β-catenin, PI3K/AKT/mTOR, and growth factor receptor pathways that drive MPNST development (Rahrmann et al., 2013). In

addition, *Foxr2* (a gene of unknown function) was identified as a proto-oncogene and was shown to be more highly expressed in human MPNSTs compared to neurofibromas. Overexpression of *Foxr2* in immortalized Schwann cells leads to tumor formation in a xenograft model, whereas knockout of *Foxr2* rescues this phenotype. It will be exciting to see whether mice with germline knockin of *Foxr2* will develop MPNSTs.

One of the goals of this project is to generate a new mouse model of MPNST (Chau *et al*., manuscript submitted for publication). Recently, it was reported that skin-derived precursors (SKPs) are the cell of origin of dermal neurofibromas, and when implanted next to the sciatic nerve, could also give rise to plexiform neurofibromas (Le et al., 2009). Since neural-crest progenitors have the potential to give rise to MPNST, we tested the depletion of *Nf1* and *p53* in SKPs. The resultant cells give rise to highly aggressive, malignant tumors that express all known markers of MPNST, including embryonic Schwann cell, glial cell, and neural-crest associated markers. Therefore, these SKP-derived MPNST (sMPNST) are physiologically relevant and are an ideal tool for drug discovery.

**Current Therapy for MPNST**

Complete excision of the tumor is currently the mainstay of therapy for MPNST. Unfortunately, surgery may not always be possible because MPNSTs are highly invasive (Katz et al., 2009). Since MPNSTs are difficult to diagnose when they arise from plexiform neurofibromas, patients that are diagnosed with MPNST often have advanced disease (Katz et al., 2009). Routine surgical removal of pre-cancerous plexiform neurofibromas is not

desirable since doing so could severely compromise the associated nerve (Bhargava et al., 1997).

Radiation therapy is another treatment option, but is undesirable because it can induce additional mutations. One group reported that radiation substantially increases the risk of developing a second nervous system tumor (most commonly optic glioma) in NF1 patients, especially when the treatment was completed in childhood (Sharif et al., 2006). Therefore, radiation therapy is avoided for NF1 patients without evidence of MPNST (Katz et al., 2009).

First-line chemotherapy for MPNST patients is currently doxorubicin (Katz et al., 2009), but this DNA-intercalating agent is nonspecific for MPNST and has limited efficacy. Combining doxorubicin with ifosfamide yields slightly improved patient outcomes, but this therapy is not generally curative (Kroep et al., 2011). Despite these chemotherapeutic regimens, ten-year survival is 31.6% for primary MPNST, 25.9% for recurrent MPNST, and 7.5% for metastatic MPNST (Zou et al., 2009a). Other groups have tested doxorubicin in combination with RAD001 (mTOR inhibitor) in mice, but there was no observed difference in tumor volume compared to RAD001 alone. When doxorubicin was tested in combination with bevacizumab (anti-VEGF antibody) in patients, there was no increase in response rate compared to doxorubicin alone (D'Adamo et al., 2005). Considered together, these treatment modalities have much room for improvement, and prognosis for MPNST patients therefore currently remains poor.

**Drug Discovery and Exploration of Pathogenesis**

Since there is difficulty in treating patients with MPNST, there is an urgent need for novel chemotherapy that is specific to the tumor. In this study, a high throughput screening approach was taken to test a library of chemical compounds on sMPNST cells to find compounds that can specifically target MPNST cells but spare normal cells. A standing concern is that tumor cells will drift from their original intrinsic cellular and molecular properties in unpredictable and unmeasurable ways when cultured over successive passages. One way to circumvent this potential problem is to use cells that are of low passage to avoid long term exposure to culture conditions. Since sMPNSTs can be easily generated and explanted, a large number of cells with low cell passage could be generated for high throughput screening. In this study, Compound (Cpd21) was identified and validated to inhibit a variety of primary cells from mouse models of MPNST, but was nontoxic to Schwann cells and fibroblasts. In addition, Cpd21 decreases the growth of MPNSTs *in vivo*, and induces apoptosis both *in vitro* and *in vivo*. Cpd21 has the potential to become a new class of chemotherapy, and can be used to further study the pathogenesis of MPNST.

**Interaction with Other Therapies of MPNST**

Another goal of this study is to explore how Cpd21 interacts with other inhibitors of MPNST. Multiple groups are experimenting with novel inhibitors for MPNST, and these inhibitors can be grouped according to the specific pathway that is perturbed.

First, groups have interrogated the RAS/RAF/MEK/ERK pathway in MPNST, and have tested MEK inhibitors in various malignancies associated with NF1. When *Nf1* is

deficient, RAS is overactive, leading to the phosphorylation and activation of MEK and downstream ERK (Ambrosini et al., 2008), which controls cellular proliferation. There are several MEK inhibitors that are currently undergoing testing in MPNST. For instance, MEK inhibitors, including PD98059, PD184352, and U0126, have been shown to be effective at inhibiting pERK in various MPNST cell lines (ST88-14, NF90-8, and STS26-T), and to decrease the proliferation of these cell lines (Mattingly et al., 2006). Another MEK inhibitor, PD0325901, has been shown to inhibit the growth of neurofibromas that develop in Dhh-Cre-$Nf1^{f/f}$ mice and to modestly inhibit growth of human MPNST in mouse xenograft models (Jessen et al., 2013). In addition, others have shown that U0126, another MEK inhibitor, is effective at inhibiting growth of MPNST cells from *cis-*$Nf1^{+/-}$;$p53^{+/-}$ mice, and can attenuate the colony-forming ability of these cells in soft agar (Li et al., 2002).

Others have tested PI3K/AKT pathway inhibitors, including LY294002, on MPNST. Activated RAS in turn upregulates PI3K, which is an enzyme that is involved in the conversion of phosphatidylinositol 4,5-biphosphate [PtdIns $(4,5)P_2$] or PIP2 to phosphatidylinositol 3,4,5-triphosphate [PtdIns $(3,4,5)P_3$] or PIP3 (Li et al., 2000), which activates downstream AKT and mTOR, key mediators of cellular proliferation (Hennessy et al., 2005). LY294002 was effective at inhibiting three MPNST cells lines, including T265, ST88, and STS26T (Zou et al., 2009b).

The third pathway that has been investigated for potential inhibitor intervention is the mTOR pathway. *Nf1* deficiency leads to the activation of RAS, which upregulates the activity of PI3K and AKT, which in turn lead to mTOR activation and cellular proliferation in MPNST (Hennessy et al., 2005; Johannessen et al., 2005; Sarbassov et al., 2005).

Rapamycin, which is an mTOR inhibitor, decreased the growth of human MPNST cell lines and *Nf1*$^{-/-}$;*p53*$^{-/-}$ mouse embryonic fibroblasts (MEFs) (Johannessen et al., 2005). In another study, rapamycin and RAD001, another inhibitor of mTOR, inhibited MPNST cell growth and decreased tumor xenograft growth only transiently (Johansson et al., 2008).

Finally, the ligand CXCL12 and its receptor CXCR4 was recently reported to promote MPNST growth by stimulating Cyclin D1 via P13K and β-Catenin signaling (Mo et al., 2013). Using a microarray approach, the gene expression profiles of sMPNST, wildtype SKPs, *Nf1*$^{-/-}$ SKP, and *Nf1*$^{-/-}$;*p53*$^{-/-}$ SKP were compared. CXCR4 was found to be highly expressed in sMPNST and upregulated in both the pretumorigenic *Nf1*$^{-/-}$ and *Nf1*$^{-/-}$;*p53*$^{-/-}$ SKP compared to wildtype SKPs. Knockdown of CXCR4 caused decreased tumorigenesis in both sMPNST and human MPNST cells when implanted in nude mice. Also, knockdown of CXCR4 leads to growth arrest and a decrease in cyclin D1 protein levels. Importantly, it was shown that CXCR4 depletion leads to decreased β-catenin activity, which is a known regulator of cyclin D1 (Sherr, 1995). The inhibitor of CXCR4, AMD3100, decreases Cyclin D1 levels via the AKT/GSK-3β/β-catenin pathway, decreases MPNST cell growth in culture, and inhibits tumorigenesis of MPNST (Mo et al., 2013).

One aim of this study was to test each inhibitor in combination with Cpd21. The PI3K inhibitor, LY294002, was shown to interact with Cpd21 in inhibiting MPNST. The PI3K pathway, and specifically, the phosphorylation of AKT, is commonly understood to regulate cellular proliferation. Therefore, it is not surprising that coupling the induction of apoptosis by Cpd21 with the inhibition of proliferation by LY294002 produces a decrease in growth of

MPNSTs that is greater than either inhibitor alone. This inhibitor combination shows promise in the treatment of MPNST.

# CHAPTER TWO
# Drug Discovery, Validation, and In Vitro Characterization


## ABSTRACT

MPNSTs are the main cause of mortality in NF1 patients. They arise from plexiform neurofibromas, and are derived from the Schwann cell lineage. Currently, surgery is the only curative option for MPNST, but this approach is limited because MPNSTs are highly invasive. Radiation therapy has the capacity to induce additional mutations, and is therefore used only in palliative circumstances. MPNST patients may also receive doxorubicin as therapy, but this DNA-intercalating agent is nonspecific for MPNST and has limited efficacy. Since the three mainstays of cancer therapy are often not effective for MPNST patients, there is an urgent need for novel therapies that can effectively target MPNST. Autograft implantation of skin-derived precursors (SKPs) that are deficient in *Nf1* and *p53* leads to formation of SKP-derived MPNSTs (sMPNST), which recapitulate human MPNST. To identify novel therapies for MPNST, a high-throughput approach is taken, whereby a library of 4480 compounds is screened to identity compounds that can inhibit sMPNST but not Schwann cells. Compound 21 (Cpd21) inhibits growth of all available *in vitro* models of MPNST and human MPNST cell lines, while remaining non-toxic to normally-dividing Schwann cells or mouse embryonic fibroblasts. We show that this compound delays the cell cycle and leads to cellular apoptosis *in vitro*.

# BACKGROUND

## Goals and General Approach

There are two main goals of this project. First is to identify novel compounds that can specifically target MPNST but spare normal tissue. Second is to use these newly identified small molecules to probe the pathogenesis of MPNST. The sMPNST model was chosen for use in the identification of novel therapeutic compounds that can inhibit MPNST but not Schwann cells using a high throughput screening approach. A longstanding concern with cultured tumor cells is that they will drift from their original properties in unpredictable ways over time in culture. These uncontrollable and unmeasurable changes may inadvertently change fundamental properties of the original tumor cells. To mitigate these concerns, the relative facility of generating *Nf1*$^{-/-}$*;p53*$^{-/-}$ sMPNSTs afforded the advantage of propagating sufficient numbers of cells for high throughput screening while keeping the cell passage number low. Using this mouse model, one novel compound, Compound 21 (Cpd21), was identified and validated to inhibit MPNST but not Schwann cells or fibroblasts.

## MPNST and the Schwann Cell Lineage

Schwann cells were chosen as the control cell type for this high throughput screen because MPNSTs are believed to arise from the Schwann-cell lineage based on multiple lines of evidence. First, MPNSTs express S100β, which is a marker for Schwann cells (Kahn et al., 1983; Stefansson et al., 1982). S100β is a protein that regulates target proteins in

response to calcium, and has been reported to modulate cell-cell communication, cell growth, morphology, metabolism, and contraction (Zimmer et al., 1995).

Second, neurofibromas are known to arise from the Schwann cell lineage (Zhu et al., 2002), and plexiform neurofibromas are known to give rise to MPNSTs in NF1 patients (Ferner and Gutmann, 2002). Neurofibromas are composed of Schwann cells, fibroblasts, perineurial cells, mast cells, endothelial cells, collagen deposits, and proximity to axonal processes (Le and Parada, 2007). Zhu et al. (2002) demonstrated that Krox20-Cre driven ablation of *Nf1* in Schwann cells that are surrounded by a microenvironment of $Nf1^{+/-}$ cells was sufficient for the development of neurofibromas (Zhu et al., 2002).

Third, mice that are deficient in *Pten* in Schwann cells develop low grade MPNST, and mice that are deficient in *Pten* and that overexpress *EGFR* in Schwann cells using a *Dhh-Cre* driver develop high grade MPNSTs (Keng et al., 2012a; Keng et al., 2012b). Mice with Schwann cells that were deficient in both copies of *Pten* and that overexpressed *EGFR* had a median survival of 26 days, showed enlarged dorsal root ganglia (DRGs), and had high tumor grades along the brachial plexus, trigeminal nerves, sciatic nerves, and sacral plexus (Keng et al., 2012a; Keng et al., 2012b).

Finally, MPNSTs can be generated from SKPs, which are derived from the neural crest and can be differentiated into Schwann cells. SKPs are adult stem cells that reside in the dermis of both mice (Toma et al., 2001) and humans (Toma et al., 2001; Toma et al., 2005), and can be differentiated in culture to generate neurons, glial cells, smooth muscle cells, adipocytes (Toma et al., 2001), and osteoblastic cells (Buranasinsup et al., 2006). SKPs are believed to be neural crest in origin because of several lines of evidence (Fernandes et al.,

2004; Fernandes et al., 2008). First, SKPs express the same transcription factors as the neural crest, including Pax3, Slug, Snail, Sox9, and Twist (Fernandes et al., 2008). Second, the neural cells that can be differentiated from SKPs are mostly Schwann cells and catecholeminergic neurons, both of which are derived from the neural crest (Fernandes et al., 2008). Interestingly, when SKPs are treated with forskolin and neuregulin, they differentiate into Schwann cells (which are of neural crest lineage) that can associate with neuron axons in culture (McKenzie et al., 2006). These Schwann cells also associate with and remyelinate crushed axons when injected into mice (McKenzie et al., 2006), highlighting their potential as treatment for neurological diseases and trauma. Third, SKPs can follow the neural crest migration pathways into ganglia, nerves, and the skin when injected into embryonic chicks (Fernandes et al., 2008). Finally, SKPs express β-galactosidase when derived from Wnt1-Cre;R26R mice, which are known to express β-galactosidase in all neural crest derived tissues (Fernandes et al., 2008).

Taken together, these lines of evidence show that MPNSTs are derived from the Schwann cell lineage. Identification of compounds that can inhibit MPNST but not Schwann cells could aid the discovery of potential new classes of drugs that are effective and specific for this tumor.

**The Cell Cycle and MPNST**

Cpd21 is shown in this study to decrease the percentage of cells in S phase and thereby decrease proliferation. The cell cycle is composed of four phases: G1, S, G2, and M. Complexes of cyclins and cyclin-dependent kinases (CDKs) are the main players in the cell

cycle and are responsible for signaling other proteins to carry out functions at particular stages of the cell cycle. There are three interphase CDKs (Cdk2, Cdk4, and Cdk6), one mitotic CDK (Cdk1 or Cdc2), and multiple associated cyclins (cyclins A, B, D, and E) that regulate the cell cycle (Malumbres and Barbacid, 2009). DNA damage initiates signaling pathways that ultimately inhibit CDKs to stop the cell cycle so that the damage can be repaired. If the damage is too great, then cells become senescent or undergo apoptosis. Buildup of DNA damage leads to cellular transformation and cancer (Kastan and Bartek, 2004).

In the historical cell cycle model, cells that trigger cell division are sensed by Cyclins D1, D2, and D3, which activate CDK4 and CDK6 during G1 (Malumbres and Barbacid, 2001). CDK4 and CDK6 then phosphorylate Rb. Cyclin E is concurrently expressed and activates CDK2, which continues to phosphorylate Rb, leading to its release of E2F and progression past the G1/S boundary (Harbour et al., 1999; Lundberg and Weinberg, 1998). Cyclin A is then expressed during late S phase and G2 and activates CDK2 and later CDK1. Cyclin B is then expressed to activate CDK1, which regulates mitosis (Malumbres and Barbacid, 2005). Interestingly, knockout mice with deficiencies in CDK2, CDK4, and CDK6 were recently generated, and it was shown that loss of these CDKs did not affect the cell cycles of most cell types. Instead, loss of these CDKs only generated cell cycle defects in specialized cell types, suggesting that other cellular components may play important roles in cell cycle progression (Malumbres and Barbacid, 2009).

These CDKs are in turn regulated by CDK inhibitors (CDKIs), which can be grouped into two protein families: the INK4 family and the Kip and Cip family (Sherr and Roberts,

1999). The INK4 family is composed of four members: $p16^{INK4a}$, $p15^{INK4b}$ $p18^{INK4c}$, and $p19^{INK4d}$. This family of proteins binds and inhibits CDK4 and CDK6, but not other CDKs. The Kip/Cip family of CDKIs include $p21^{Cip1}$, $p27^{Kip1}$, and $p57^{Rip2}$. These proteins bind to both cyclins and CDKs, specifically CDKs that are associated with Cyclin A, D, and E. CDKIs are in turn responsive to DNA damage, and prevent cell cycle progression before the previous phase has been completed successfully (Malumbres and Barbacid, 2009).

**Apoptosis and MPNST**

Cpd21 is also found to induce apoptosis in this study. Apoptosis is a form of cell death that is characterized by biochemical and morphological changes. There are two main biochemical pathways that execute apoptosis: the intrinsic (mitochondrial) pathway and the extrinsic (death receptor) pathway (Fesik, 2005). In the intrinsic pathway, cytochrome c is released from the mitochondria and aggregates with APAF1 to activate Caspase 9 (Wei et al., 2001). The release of cytochrome c is determined by members of the BCL2 family of proteins, which includes members that are either pro-apoptotic (BAX or BAK) or anti-apoptotic (BCL2 and BCL-$X_L$). In the extrinsic pathway, extracellular ligands such as TNF, Fas ligand (CD95L), or TRAIL (APO2L or TNFSF10) interact with their respective receptors, leading to the activation of the Fas-associated death domain (FADD) (Fesik, 2005). This ultimately leads to the activation of Caspase 8. The intrinsic and extrinsic pathways then converge and cleave caspase 3, leading to its activation. Activated caspase 3 has a variety of functions. Caspase 3 causes the externalization of phosphatidylserine to the outer leaflet of the plasma membrane (Mandal et al., 2002), and hence detection by

macrophages. Another function of caspase 3 is the cleavage of PARP (Nicholson et al., 1995; Tewari et al., 1995), which is the negative regulator of the endonuclease responsible for internucleosomal DNA cleavage (Tanaka et al., 1984; Yoshihara et al., 1975; Yoshihara et al., 1974). Activated caspase 3 also cleaves and activates ROCK-I (Coleman et al., 2001; Sebbagh et al., 2001), leading to morphological changes that characterize apoptosis (Leverrier and Ridley, 2001), including cellular contraction and blebbing (Coleman et al., 2001).

In this study, Cpd21 is shown to inhibit MPNSTs, to decrease the proliferative capacity of this tumor, and to induce apoptosis. MPNSTs currently have a poor prognosis and can only be completely cured with early surgery. This underscores the need for new, potential compounds like Cpd21.

# METHODS

## Cell Culture

MPNST cells from all human and murine sources were cultured in DMEM, 10% fetal bovine serum (FBS), 1% L-glutamine, 1% sodium pyruvate, and 1% penicillin/streptomycin. Schwann cells were obtained from ScienCell and cultured in Schwann Cell Medium (ScienCell) according to manufacturer's instructions. Schwann cells were immortalized by infecting with *Myc* retrovirus according to procedures outlined by (Takahashi and Yamanaka, 2006). The human MPNST cells, S462 and SNF96.2, were a gift from Karen Cichowski.

## High Throughput Screening

sMPNST and Schwann cells were each passaged from initial sources and frozen in 1 mL fractions with 10% DMSO. Cells were revived, passaged once, and seeded at 400 cells/50 uL/well in 384 well plates, and grown overnight. Compounds were added at a final concentration of 2.5 µM using Biomek FX, and incubated at 37$^{o}$C for 96 h. Plates were then allowed to cool to room temperature for 20 min. CellTiter-Glo$^{TM}$ (Promega) was added (20 uL/well), and plates were read using an Envision 2102 Multilabel Reader (Perkin Elmer). High throughput screening was done in collaboration with Shuguang Wei and Bruce A. Posner.

**Dose response studies**

Cells were plated at a density of 1500 cells/50uL/well in 96-well plates. Cpd21 (ChemBridge) was serially diluted in DMSO and then added to the cellular layer to produce a final volume of 150 uL and 0.5% DMSO in each well. Final compound concentrations tested are as follows: 0.125, 0.25, 0.5, 1, 2.5, 5, 10, and 20 µM. Plates were incubated at 37$^{o}$C under normoxic conditions for 96 h. At 96 h, plates were incubated at room temperature for 20 min. 20 uL CellTiter-Glo$^{TM}$ (Promega) was added to each well, and plates were read using PolarStar OPTIMA (BMG Labtech) luminometer.

**Soft Agar Assay**

Experiments were plated in two layers in 6 well plates. The bottom layer is an acellular layer made up of 0.6% Bacto-agar (BD Biosciences) in MPNST media (see above), and this layer was plated one day in advance. To plate the top, cellular layer, cells were trypsinized, pelleted, and resuspended to a density of 2 x $10^4$ cells/mL. Resuspended cells were then mixed in 1:1 ratio with agar to a final cell density of 1x $10^4$ cells/mL in 0.6% agar. Plates were allowed to solidify at room temperature for 45 min before being incubated at 37$^{o}$C for 10 days. Experiments were done in triplicate. Plates were stained with 0.5 mL of 0.005% crystal violet for 1 h to visualize colonies. All colonies in each well were counted for quantification.

**Cell Cycle Analysis**

BrdU at 10 µM was added to cells for 30 min. Any floating cells were collected, and adherent cells were trypsinized. Both fractions were then pelleted, washed in cold PBS, and resuspended in 100 uL cold PBS. Cells were then fixed in 5 mL ice cold ethanol while being vortexed. Samples were stored overnight at $4^{o}$C. Samples were then pelleted, and vortexed while 2N HCl/Triton X-100 was added to denature DNA. After an incubation at room temperature for 30 min, samples were pelleted, resuspended in 1 mL 0.1 M $Na_2B_4O_7$, pH 8.5 to neutralize the sample, and pelleted again. Each sample was then incubated with 50 uL 0.5% Tween 20/1%BSA/PBS, 20 uL anti-BrdU-FITC (BD Biosciences), and 5 uL of 10 mg/mL RNAse overnight. Samples were then pelleted, resuspended in 1 mL 5 ug/mL propidium iodide (Sigma), and analyzed by flow cytometry.

**Quantitative Real-Time PCR**

Cells were seeded at 5 x $10^4$ cells/2 mL/well in 6-well plates and treated with Cpd21 for 24 h. Media was aspirated and discarded, and 600 uL RLT Buffer Plus (Qiagen) was added to each well to harvest RNA. Manufacturer's instructions for purifying RNA were followed (Qiagen). 1 ug of RNA was used to synthesize cDNA using iScript cDNA Synthesis Kit (BioRad), according to manufacturer's instructions. Reaction product was diluted 1:20 using water, and 5 uL diluted cDNA was loaded into each well of qPCR plate, along with 10 uL Power SYBR Green (Applied Biosystems), and 5 uL of diluted primer mix at a final concentration of 0.5 µM. Plates were sealed and processed by 7500 Real Time PCR

System (Applied Biosystems).

**Western Blotting**

Cells were seeded at 5 x $10^4$ cells/2 mL/well in 6-well plates and treated with Cpd21 for indicated time points. Media was collected and centrifuged at 14,000 rpm. Supernatant was discarded. Cells were trypsinized, collected along with 10% FBS media, and centrifuged at 1500 rpm for 5 min. Supernatant was discarded. Cells were lysed with 600 uL RIPA buffer (ThermoScientific), containing Complete Mini (Roche) and 1% Halt Phosphatase Inhibitor Cocktail (ThermoScientific). LDS Sample Buffer (Thermo Scientific) containing 2% beta-mercaptoethanol (Sigma) were added to a final concentration of 25% in each sample, which was then boiled for 10 min. Prepared samples were run on 5-20% SDS-PAGE gel (BioRad), and transferred to nitrocellulose membrane (Whatman) using wet transfer. Membranes were blocked with 5% non-fat dry milk in PBS-T for 1 h, and antibodies were added in PBS-T overnight at 4$^o$C with shaking. The following antibodies were used: Cyclin D1 (Millipore), Caspase 3 (Cell Signaling), PARP (Novus Biologicals and Millipore), pAKT (Cell Signaling), AKT (Cell Signaling), alphaTubulin (Sigma), GAPDH (Santa Cruz), and H3 (Millipore). Membranes were washed with PBS-T three times. Secondary antibody added in PBST-T. Secondary antibodies include: anti-mouse (Vector) and anti-rabbit (Vector). Membranes were washed with PBS-T three times, and developed using Pierce ECL Substrate (Thermo Scientific) or ChemiGlow (protein simple).

**Annexin V Staining**

Media from cells that were treated with Cpd21 were collected, and adherent cells were washed with cold PBS, trypsinized, and collected in the same tube. Samples were centrifuge and supernatant was aspirated, and samples were processed according to manufacturer (MACS Miltenyi Biotec). Briefly, samples were resuspended in Binding Buffer (0.01 M Hepes/NaOH (pH 7.4), 0.14 M NaCl, 2.5 mM $CaCl_2$), and 300 uL of this suspension was added to 5 uL of Annexin V antibody (MACS Miltenyi Biotec) and 2.5 uL propidium iodide. Samples were stored in the dark for 15 min and analyzed by flow cytometry.

## RESULTS

### *Nf1* and *p53* Deficient Skin-Derived Precursors (SKPs) Form MPNST

NF1-associated dermal and plexiform neurofibromas are histologically indistinguishable despite having significantly different natural history and tumor progression properties. Recently, we reported that SKPs are the cell of origin of dermal neurofibromas (Le et al., 2009). Given the potential in mice for neural crest progenitors to give rise to MPNST after additional loss of the *p53* tumor suppressor, we tested the consequences of dual *Nf1* and *p53* loss of function (NP) in SKPs. In vitro, SKPs from mice with $Nf1^{f/f};p53^{f/f}$ genotype were cultured and infected with adenovirus containing Cre-GFP (Ad-Cre) to induce tumor suppressor recombination (Biernaskie et al., 2006) (Figure 2Aa). The majority of infected cells displayed green fluorescence, indicating effective viral entry and expression (Figure 2Ab). We confirmed effective Cre-mediated recombination of all floxed alleles by PCR analysis (Figure 2Ab).

The $Nf1^{-/-};p53^{-/-}$ cells (NP SKPs) were then reimplanted into the same mouse from which they were derived (autograft) and highly aggressive, malignant tumors developed in all cases (Figure 2Ac). These tumors could be successfully cultured as either spheres or adherent cells (data not shown), or allografted into nude mice (Figure 2Ad). These tumors (termed sMPNST; for SKP derived MPNST) were assayed for human MPNST-associated genes including embryonic Schwann cell markers, S100 (Cichowski et al., 1999; Vogel et al., 1999), Krox20 (Zhu et al., 2002), PLP (Mayes et al., 2011), and GAP43 (Kioussi and Gruss, 1996; Stemple and Anderson, 1992); developing glial cell marker, Dhh (Wu et al., 2008); and neural-crest-associated marker, snail (Fernandes et al., 2004). The RT-qPCR data

demonstrated expression of all markers in all sMPNSTs analyzed (Figure 2Ae). Thus, sMPNSTs exhibit molecular characteristics of human NF1 associated MPNST.

Hematoxylin and eosin (H&E) staining of sMPNSTs showed presence of spindle-shaped cells that interweave in a poorly-differentiated, wavy appearance, reminiscent of human MPNST histology (Figure 2Ba). Additionally, the commonly used MPNST markers, S100 and GAP43, were present (Figure 2Bb-2Be). Therefore, our results indicate that SKPs, cells that give rise to neurofibromas upon loss of *Nf1*, can also give rise to MPNST with additional loss of *p53*. The facility of generating and explanting sMPNSTs made this a favorable system for performing chemical compound screens.

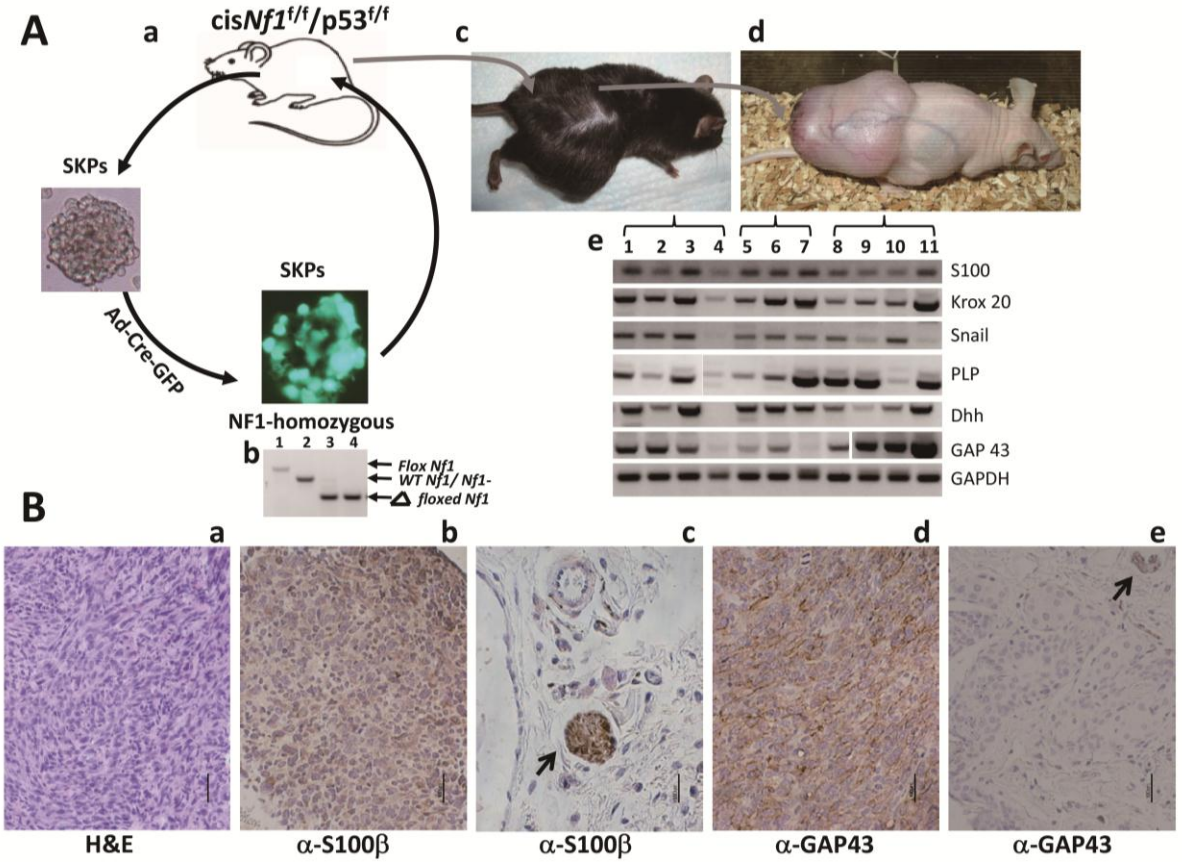


**Figure 2 MPNSTs can be Generated from SKPs that are Deficient in *Nf1* and *p53*.** (A) a. SKPs are isolated from the skin of cis-Nf1$^{f/f}$;p53$^{f/f}$ mice, cultured, and infected with Ad-Cre-GFP. b. Infected SKPs were screened for expression of GFP, and genotyped for the deletion of Nf1. Lane 1 represents Nf1$^{f/f}$ control. Lane 2 represents wildtype Nf1$^{+/+}$ control. Lane 3 represents Nf1$^{-/-}$ control. Lane 4 represents Nf1$^{-/-}$ SKPs that were infected with Ad-Cre-GFP. c. These Nf1$^{-/-}$;p53$^{-/-}$ SKPs are then autologously transplanted back into the original mouse. d. Resultant tumors are transplanted into nude mice via xenotransplantation. e. RT-qPCR results. Lanes 1-4 represent MPNSTs derived from cis-Nf1$^{+/-}$;p53$^{+/-}$ mice. Lanes 5-7 represent MPNSTs derived from PLP-CreERT-Nf1$^{f/f}$;p53$^{f/f}$ mice that have been injected with tamoxifen to induce recombination. Lanes 8-11 represent sMPNSTs. (B) a. H&E staining of sMPNST. b-e. Immunohistochemical staining for S100B in sMPNST (b) and skin (c), and for GAP43 in sMPNST (d) and skin (e).

**Novel MPNST inhibitory Small Molecule**

We hold the concern that over time in culture, tumor cells will drift from their original intrinsic cellular and molecular programs in unpredictable ways. These uncontrollable and unmeasurable changes may inadvertently alter fundamental properties of the original tumor cells. To mitigate these concerns, the relative facility of generating primary cultures from sMPNSTs afforded the advantage of propagating sufficient numbers of cells for a high throughput screening while keeping the cell passage number low. We performed a limited high-throughput, small-molecule screen using sMPNST cells produced above in an extension of a related ongoing large scale screen in our research group. We carried out a 200,000 compound screen on primary mouse glioblastoma multiforme (GBM) cells that are deficient for *Nf1*, *p53*, and *Pten* (KL and LFP, unpublished data). This original GBM screen yielded 4480 compounds, identified as inhibitory to GBM cell growth. We reasoned that since sMPNST cells are deficient in two of these same tumor suppressors, some compounds might have conserved sMPNST cell growth inhibitory properties.

A well-established luminescence assay for measuring ATP levels (an indication of cellular metabolic activity) was adopted (CellTiter-Glo$^{TM}$, Promega), and performed 96 hours after compound exposure. 1515 compounds exhibited a greater than 20% decrease in ATP levels at 2.5 μM (Figure 3A and 3B). To exclude compounds that exert general cell toxicity, or perturb the generic cell cycle or mitotic machinery, we counter-screened the 1515 compounds against *Myc*-immortalized Schwann cells (Ridley et al., 1988; Takahashi and Yamanaka, 2006) and eliminated compounds that showed greater than 20% lower ATP levels. The resultant 119 compounds were rescreened on sMPNSTs but with a cutoff at 70%

inhibition. 28 compounds passed this test and were further tested in dose response studies ranging from 125 nM to 20 µM. The twenty-first compound (Figure 3C) (Cpd21 or identification number SW106065) was capable of inhibiting ATP consumption of sMPNST and all other models of MPNST tested (Figure 3D) with an EC50 of 1 µM. In a second approach, an additional 29 compounds that inhibit sMPNST cells were identified, bringing the total number of compounds that are effective on sMPNST cells to 57 (Figure A1). These compounds were also validated in dose response studies ranging from 125 nM to 20 µM (Figure A2). However, these compounds were found to be toxic to Schwann cells, MEF cells, or both.

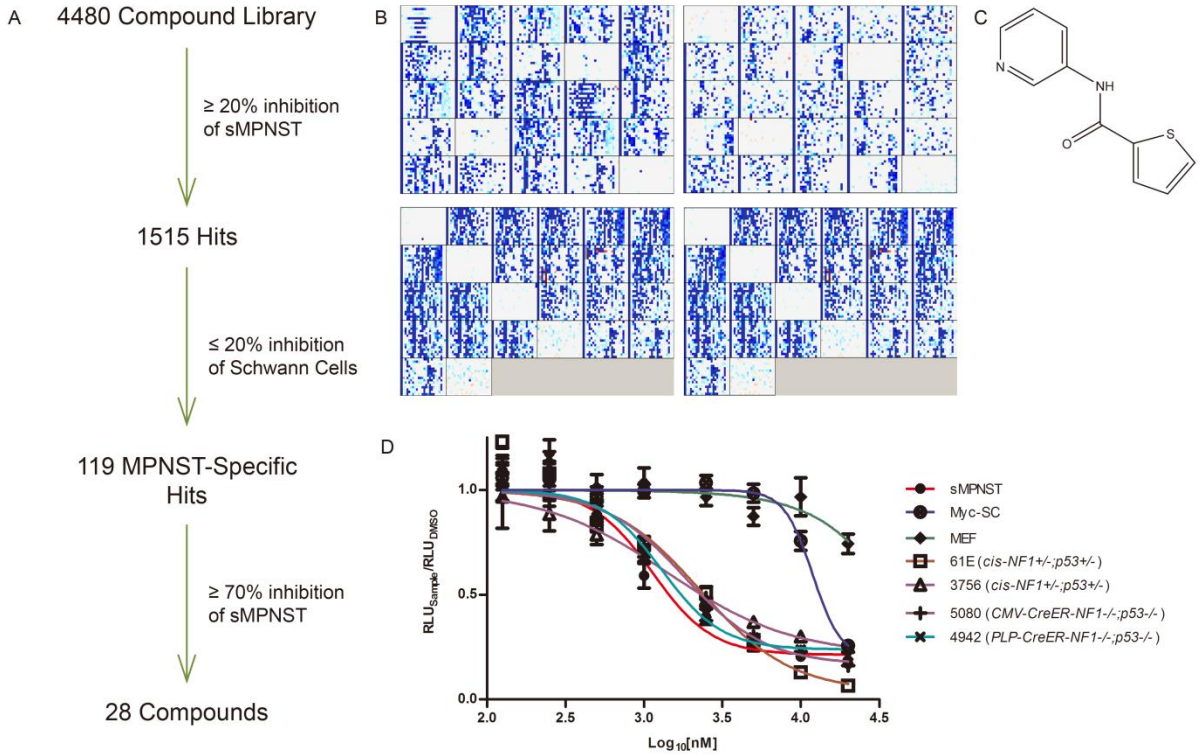


**Figure 3 Identification of Cpd21 by high-throughput, small-molecule screening.** (A) Summary of screening procedure. (B) Sample data from high-throughput screening of sMPNST cells (upper panels) and Schwann cells (lower panels). Intensity of blue or red signal correlates with degree of inhibition or induction of ATP levels by small molecules, respectively. (C) Structure of Cpd21. (D) Dose-response curve of Cpd21 at 0.125, 0.25, 0.5, 1, 2.5, 5, 10, and 20 μM in sMPNST cells, MEF, Schwann cells, and tumor cells generated from other models of MPNST.

**Cpd21 was Validated to Specifically Inhibit Human MPNST Growth and Anchorage-Independent Growth**

We extended the functional analysis of Cpd21 to additional cell lines. Human MPNST cell lines, S462 (Figure 4A) and SNF96.2 (Figure 4B), were assayed for dose-dependent growth, and EC50 concentrations of 439.0 nM and 753.6, respectively, were determined. In contrast, NIH3T3 cells and wildtype Schwann cells showed a considerably higher dose resistance (Figure 4C). We also tested sMPNST response to Cpd21 in anchorage independent soft agar growth assays and found Cpd21-mediated inhibition of colony formation (Figure 4D and 4E). This effect was also observed in MPNST cells derived from *cis-Nf1*$^{+/-}$*;p53*$^{+/-}$ mice (Figure 4F and 4G). Thus Cpd21 has general toxic activity on *Nf1* and *p53* deficient MPNST cells but not on diverse non-tumorigenic, mitotically active fibroblasts or Schwann cells.

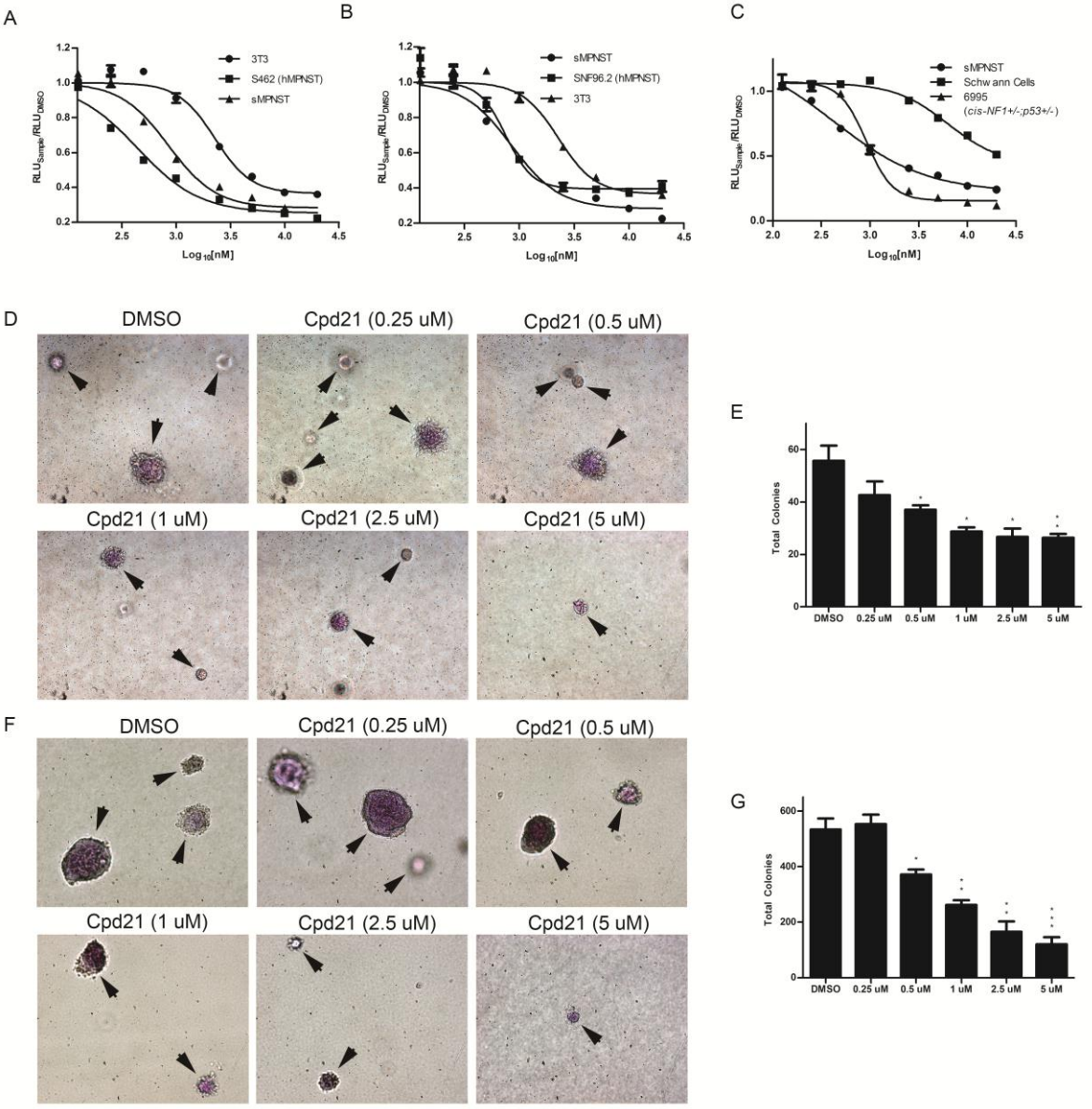


**Figure 4 Effect of Cpd21 in vitro.** (A, B) Dose-response curves of Cpd21 treatment on two human MPNST cell lines, S462 and SNF96.2, respectively, compared with mouse NIH 3T3 cells and sMPNST cells. (C) Dose-response curves of Cpd21 treatment on wildtype Schwann cells, compared with sMPNST and MPNST from *cis-Nf1*$^{f/f}$*;p53*$^{f/f}$ mice. (D) Soft agar assay of sMPNST cells that were treated with DMSO or Cpd21 at 0.25, 0.5, 1, 2.5, or 5 µM for 2 weeks in triplicate. Representative images shown. Arrows indicate colonies, which may be out of plane in agar. Images at 20X. (E) Number of colonies per well were counted for soft agar assays and averaged. (F) Soft agar assay of MPNST cells from *cis-Nf1*$^{+/-}$*;p53*$^{+/-}$ mice, and that were treated with DMSO or Cpd21 at 0.25, 0.5, 1, 2.5, or 5 µM for 2 weeks in triplicate. Representative images shown. Arrows indicate colonies, which may be out of

plane in agar. Images at 20X. (G) Number of colonies per well were counted for soft agar assays and averaged. All values represent the mean ± standard deviation. Student's t-test was used to test for significance (*$p<0.05$, **$p<0.01$,***$p<0.001$).

**Cpd21 Delays the Cell Cycle in sMPNST**

To address the mechanism of action of Cpd21, we treated sMPNST cells at 0.25, 0.5, 1, 2.5, and 5 μM for 24 h, and pulsed with BrdU for 30 min. Subsequent flow cytometry analysis revealed a decreased percentage of cells in the S phase, and a corresponding increased percentage in G1/G0 and G2/M, compared to treatment with DMSO alone (Figure 5A).

Several cell cycle regulatory genes exhibited decreased mRNA in the presence of Cpd21 including: *cyclin A2, cyclin B1, cyclin D1, cyclin E, cdk4, and cdk6* (Figure 5B and 5C). Also, increased levels of *cdkn1a* and *cdkn2a* mRNA were observed in a dose-dependent manner (Figure 5D). In addition, levels of Cyclin D1 protein, which is known to interact with CDK4/6 in regulating G1/S progression, were decreased (Bates et al., 1994; Tam et al., 1994) (Figure 5E). These results indicate that following exposure to Cpd21 cells in S phase are underrepresented, consistent with a delay in the cell cycle and an arrest of the mitotic machinery.

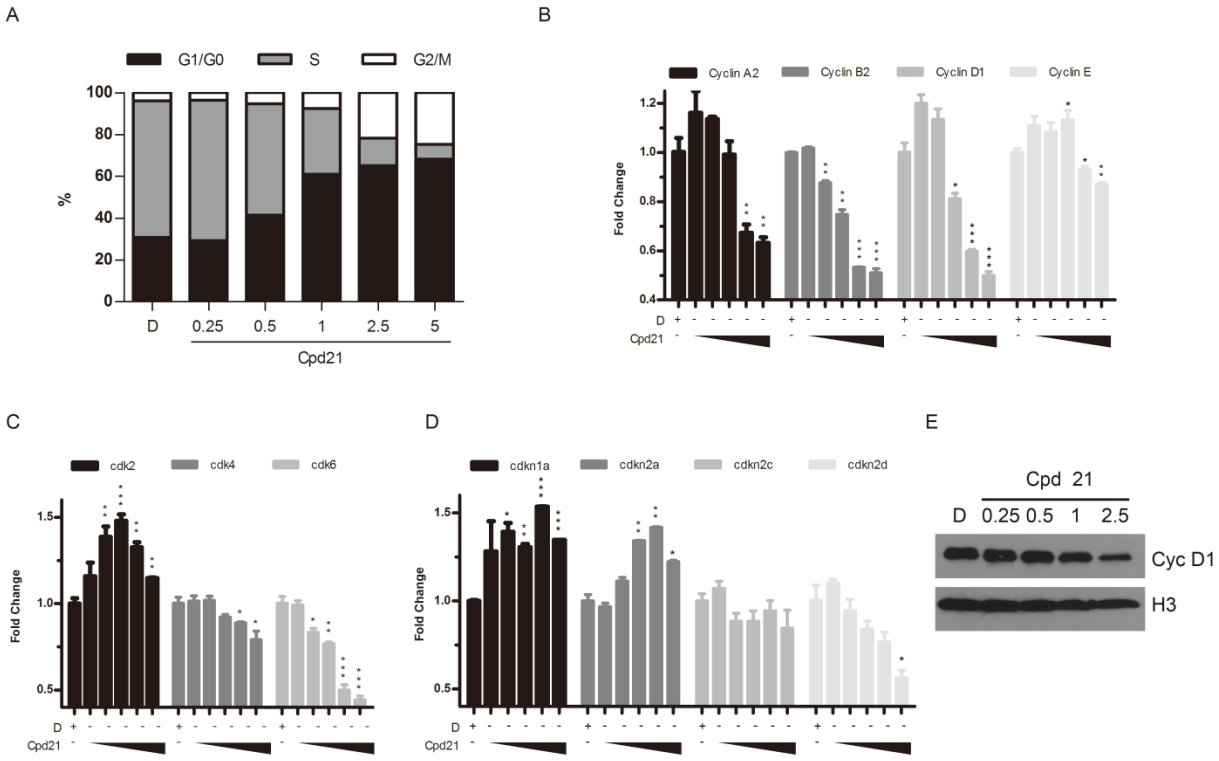


**Figure 5 Effect of Cpd21 on Cell Cycle Machinery.** (A) Effect of Cpd21 on cell cycle distribution. sMPNST cells were treated with DMSO alone, D, or Cpd21 at 0.25, 0.5, 1, 2.5 or 5 µM for 24 h and pulsed with BrdU for 30 min. Cells were analyzed by flow cytometry and percentage of cells in each phase is shown. (B, C, D) sMPNST Cells were treated with DMSO alone, D, or with Cpd21 at 0.25, 0.5, 1, 2.5, or 5 µM for 24 h and RNA harvested for qRT-PCR for cyclins (B), CDKs (C), or CDKIs (D). (E) Western blot for cyclin D1 for sMPNST cells that were treated with DMSO alone, D, or Cpd21 at 0.25, 0.5, 1, and 2.5 µM. All values represent the mean ± standard deviation. Student's t-test was used to test for significance (*$p<0.05$, **$p<0.01$, ***$p<0.001$).

**Cpd21 Induces Apoptosis in MPNST**

We examined Cpd21 treated sMPNST cells for apoptosis by annexin V-FITC-conjugated flow cytometry (Vermes et al., 1995). Tumor cells treated with Cpd21 concentrations at or above 0.5 µM showed a statistically-significant increase in the percentage of apoptotic cells (Figure 6A). At the EC50 concentration of 1 µM, 11.23 ± 1.56% of the cells were annexin V positive, compared to 5.02% ± 0.83% in DMSO-treated control cells.

We also performed Caspase-3 Western blotting of Cpd21-treated sMPNST cells and found evidence of protein cleavage, consistent with induced apoptosis (Figure 6B). Similar results were confirmed via PARP cleavage assays. sMPNST cells that were treated with Cpd21 at 0.25, 0.5, 1, 2.5, and 5 µM showed the presence of cleaved PARP, which was nearly undetectable when sMPNST cells were treated with DMSO alone (Figure 6C). We further validated this mechanism in MPNST cells cultured from spontaneous MPNSTs from our *cis-Nf1*$^{+/-}$*;p53*$^{+/-}$ mouse model (Figure 6D), and in the human MPNST cell line, S462 (Figure 6E). Other cell types, including *Myc*-immortalized Schwann cells (Figure 6F) and MEF cells (Figure 6G) did not undergo caspase 3 cleavage. Together, these data indicate that, *in vitro*, Cpd21 induced mitotic arrest of MPNST cells that ultimately results in cellular apoptosis, and that this phenotype was not observed in untransformed dividing cells.

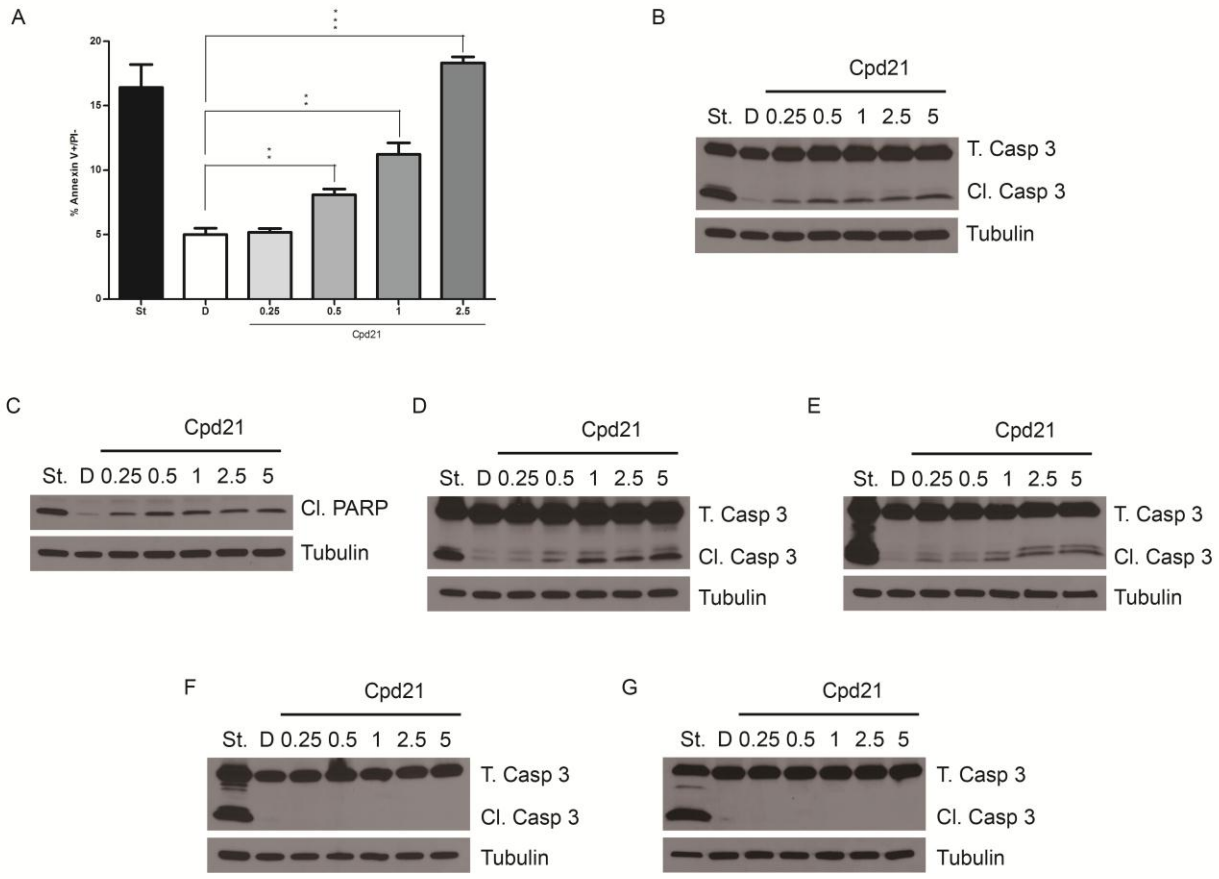


**Figure 6 Cpd21 Induces Apoptosis in vitro.** (A) Annexin V staining as detected by flow cytometry. sMPNST cells were treated with DMSO, D, alone or with Cpd21 at 0.25, 0.5, 1, and 2.5 µM. sMPNST cells treated with staurosporine, St, were used as positive control. (B-F) Western blotting for cleavage of caspase 3 in sMPNST cells (B), for cleavage of PARP in sMPNST cells (C), for cleavage of caspase 3 in MPNSTs generated from *cis-Nf1*$^{+/-}$*;p53*$^{+/-}$ mice (D), for cleavage of caspase 3 in human MPNST cell line, S462 (E), for cleavage of caspase 3 in *Myc*-SC (F), and for cleavage of caspase 3 in MEF cells (G). Each cell type was treated with staurosporine, St, as a positive control for caspase 3 cleavage. Total caspase 3 (T. Casp 3) and cleaved caspase 3 (Cl. Casp 3) were assayed in each case. All values represent the mean ± standard deviation. Student's t-test was used to test for significance (*$p<0.05$, **$p<0.01$, ***$p<0.001$).

**DISCUSSION**

A high throughput screening approach was taken to identify novel small molecules that could inhibit MPNST but not Schwann cells. This screen was done in the context of another screen performed on GBM cells (KL and LFP, unpublished data). The initial hypothesis for this study was that since sMPNSTs are deficient in *Nf1* and *p53*, and GBMs are deficient in *Nf1*, *p53*, and *Pten*, the screening process could be shortened by testing the subset of compounds that inhibited GBM on MPNST. It was expected that this cherry-picked library would be enriched in hits that would be effective against MPNST. It was therefore surprising to find that only one hit, Cpd21, was found to inhibit MPNST but not Schwann cells or MEF cells. One possible hypothesis to explain this discrepancy is that there are fundamental differences between MPNST and GBM despite similarities in genotype. Perhaps the presence of *Pten* in the sMPNST model is enough to abrogate the efficacy of many of the compounds that could inhibit the *Pten*-deficient GBM.

Cpd21 was validated to inhibit other models of MPNST, hence confirming its general effectiveness. In addition, it was validated to be effective in inhibiting human MPNST cell lines, S462 and SNF96.2. Cpd21 was also able to decrease the number and size of colonies formed in soft agar by MPNST cells.

Cpd21 was observed to decrease the proliferation of MPNST cells as evidenced by its ability to decrease the percentage of cells in S phase and to increase the percentage in G1/G0 and G2/M. Several cell cycle regulatory genes exhibited decreased mRNA, including *cyclin A2, cyclin B1, cyclin D1, cyclin E, cdk4, and cdk6*. Increased levels of *cdkn1a* and *cdkn2a* mRNA were observed in a dose-dependent manner. In addition, levels of Cyclin D1 protein,

which is known to interact with CDK4/6 in regulating G1/S progression, were decreased. These changes are consistent with a decrease in proliferative capacity of MPNST cells.

In addition, Cpd21 was shown to induce apoptosis in mouse and human MPNST but not Schwann and MEF cells. It is interesting that Cpd21 could induce apoptosis in the context of *p53* deficiency since *p53* is widely known to mediate apoptosis in response to cellular stress (Vogelstein et al., 2000). One possible explanation is that Cpd21 may induce *p53*-independent apoptosis, a process that has been reported by others (Clarke et al., 1993; Peled et al., 1996; Strasser et al., 1994) and that can be triggered by cytokine withdrawal, and various exogenous chemical compounds such as dexamethasone, ionomycin, and phorbol ester 12-myristate 13-acetate (PMA) (Villunger et al., 2003). Both p53-dependent and p53-independent apoptosis are mediated by PUMA (Jeffers et al., 2003; Villunger et al., 2003; Yu and Zhang, 2003) and NOXA (Villunger et al., 2003), which inhibit the anti-apoptotic protein, Bcl-2. This disinhibits Bax/Bak, leading to apoptosis (Villunger et al., 2003). Therefore, an interesting extension of the work in this study is to determine whether one, some, or all of the components of the p53-independent apoptotic pathway are involved in mediating the effects of Cpd21.

# CHAPTER THREE
# Metabolic Properties, Pharmacokinetic Properties, and *In Vivo* Effects of Cpd21


## ABSTRACT

The purpose of this study is to determine the *in vivo* effect of Cpd21. For any cancer drug to be efficacious, it must resist degradation by metabolic enzymes, remain long enough in the body to be effective, and must be able to reach the target tumor cells. To assess the metabolic profile of Cpd21, the rates at which Cpd21 is broken down by hepatocytes or its S9 enzymatic fraction were measured. These metabolic half-lives were found to be sufficiently long in duration for further *in vivo* delivery and testing. Next, Cpd21 was injected into nude mice harboring sMPNSTs, and was observed to distribute rapidly from the serum into tumors and to remain at high concentrations for an extended period of time. These pharmacokinetic properties were thus favorable for *in vivo* delivery. Upon efficacy testing, tumor size was found to be decreased by treatment with Cpd21 compared to vehicle. In addition, Cpd21 treatment decreased the number of BrdU and Ki67 positive cells, confirming a decrease in proliferation, and increased the number of cleaved caspase 3 and cleaved PARP positive cells, confirming an induction of apoptosis as observed *in vitro*. Finally, this apoptotic effect of Cpd21 was specific to tumors and did not affect any other organs.

## BACKGROUND

### Escape From Apoptosis and Relationship to Cancer

When bodily cells experience cell cycle arrest and decline in proliferation, they often enter apoptosis (Fesik, 2005). Loss of *Nf1* increases RAS signaling and upregulates MAPK and PI3K signaling, which leads to increased cellular growth and invasion. Loss of *p53* prevents cells that have sustained DNA damage from triggering apoptosis and being eliminated. Therefore, the combined loss of *Nf1* and *p53* allows cells to increase proliferation, invade, and escape apoptosis, culminating in the formation of MPNST, a cancer with poor prognosis in NF1 patients (Ferner and Gutmann, 2002).

Apoptosis is a form of cell death that involves morphological and biochemical changes. Cells undergo shrinkage, nuclear pyknosis, membrane blebbing, and formation of apoptotic bodies (Hacker, 2000). The biochemical changes involve a cascade of caspases (Slee et al., 2001; Thornberry and Lazebnik, 1998). The two main signaling pathways involved in apoptosis are the intrinsic (mitochondrial) and extrinsic (death receptor) pathways (Fesik, 2005). The intrinsic pathway is activated by pro-apoptotic proteins such as BID, BAD, BAK, and BAX, which activate apoptosis by inducing the release of cytochrome c from the mitochondria (Wei et al., 2001). Cytochrome c then binds APAF1 and activates caspase 9, which then activates a downstream common apoptotic pathway (Hakem et al., 1998; Wei et al., 2001). BAX and BAK also inhibit the activity of anti-apoptotic proteins such as BCL2 and BCL-$X_L$, which normally prevent the release of cytochrome c from the mitochondria. The extrinsic pathway is activated by the binding of extracellular ligands such as TNF, FAS ligand (CD95L), TRAIL (APO2L), or THFSF10 (Fesik, 2005). These ligands

bind to their respective receptors, including TNFR1, FAS, DR4 (TRAILR1), and DR5 (TRAILR2) (Fesik, 2005). The binding of these ligands to their respective receptors activates the FAS-associated death domain (FADD) and caspase 8.

Ultimately, both the intrinsic and extrinsic pathways converge and activate the common apoptotic pathway, which involves the cleavage of procaspase-6, -7, and -3 (Slee et al., 2001) into 'executioner' caspases. These activated caspases cleave a variety of cellular substrates, leading to the morphological changes observed in apoptosis. The first substrates to be cleaved are inhibitors of apoptosis proteins, including BCL2, BCL-$X_L$ (Wolf and Green, 1999), and X-linked inhibitor of apoptosis protein (X-IAP) (Slee et al., 2001). The active caspases then cleave gelsolin and DNA fragmentation factor (DFF45)/inhibitor of caspase-activated DNase (ICAD) in CAD, which cleaves DNA and promotes chromatin condensation (Wolf and Green, 1999). In addition, these active caspases cleave structural proteins, including lamins, NuMa, and SAF-A, thereby causing the nucleus to disintegrate (Wolf and Green, 1999). Cleavage of cytoskeletal proteins, including fodrin, keratins, actin, and others breaks down the structural integrity of the cell (Wolf and Green, 1999).

**Restoring Apoptosis in MPNST**

Restoring proper apoptosis to cancer cells with a small molecule may eliminate one means by which cancer cells stay alive (Fesik, 2005). Different groups have proposed the perturbation of particular components of the apoptotic cascade for benefit in cancer therapy. At the death domain receptor level, for instance, TRAIL and anti-TRAIL antibodies are currently in clinical trials for a variety of tumors (Fesik, 2005). These candidates are

attractive because the extrinsic apoptotic pathway is believed to be independent of p53, which is commonly mutated. Interestingly, one group has found that MPNST cell lines are sensitive to treatment with TRAIL (Reuss et al., 2013). Other groups are targeting BCL2 (Fesik, 2005), which is known to prevent apoptosis. BCL2 has been reported to be expressed in MPNST (Suster et al., 1998), but its role in MPNST pathogenesis has not been elucidated. Another target is the anti-apoptotic X-IAP (Fesik, 2005), but the role of this family of proteins has not been explored in MPNST.

In this study, the metabolic and pharmacokinetic properties of Cpd21 are explored. Cpd21 is then delivered *in vivo* and found to inhibit MPNSTs. Consistent with findings *in vitro*, Cpd21 decreases proliferation and induces apoptosis in MPNST. This apoptotic effect is shown to be specific to the tumor and does not affect any other tissues.

## METHODS

### Cell and Tissue Samples

MPNST cells from all human and murine sources were cultured in DMEM, 10% fetal bovine serum, 1% L-glutamine, 1% sodium pyruvate, and 1% penicillin/streptomycin. Schwann cells were obtained from ScienCell and cultured in Schwann Cell Medium (ScienCell) according to manufacturer's instructions. Schwann cells were immortalized by infecting with *Myc* retrovirus according to procedures outlined by (Takahashi and Yamanaka, 2006). sMPNST-luc+ cells were generated by Wei Mo (LFP).

### Metabolic Stability Studies

Metabolic studies were done in collaboration with Noelle Williams (NSW). Cpd21 levels for metabolic stability and pharmacokinetic studies were monitored by LC-MS/MS using an AB/Sciex (Applied Biosystems) 3200 Qtrap mass spectrometer coupled to a Shimadzu Prominence LC. The compound was detected with the mass spectrometer in positive MRM (multiple reaction monitoring) mode by following the precursor to fragment ion transition 205.0 to to 111.1. An Agilent C18 XDB 5 micron packing column (50 X 4.6 mm) was used for chromatography with the following conditions: Buffer A: $dH_20$ + 0.1% formic acid, Buffer B: methanol + 0.1% formic acid, 0-1.5 min 3% B, 1.5-3 min gradient to 100% B, 3.0-4.0 min 100% B, 4.0-4.1 min gradient to 3% B, 4.1-5.0 min 3% B. N-benzyl benzamide (Sigma) was used as an internal standard (transition 212.1 to 91.1). For S9 studies, Cpd21 (2 □M) was incubated in a 1 ml incubation volume with 1 mg of murine CD-1 S9 (combined cytosol and microsome) fractions (Celsis/In Vitro Technologies) and Phase I

(the NADPH regenerating system) cofactors (Sigma) for 0-240 min. Reactions were quenched by mixing the incubation mixture with 1 mL of methanol/0.2 ng/μL n-benzylbenzamide/0.2% formic acid. The quenched mixture was vortexed for 15 s, incubated at room temperature for 10 min and spun for 5 min at 986 x g. Supernatants were then transferred to a tube and spun in a refrigerated microcentrifuge for 5 min at 16,100 x g. The second supernatant was transferred to an HPLC vial and analyzed by LC-MS/MS.

Metabolic stability studies with hepatoctyes were conducted similarly. Male ICR/CD-1 mouse hepatocytes, InVitroGRO HI and HT Medium, and Celsis Torpedo Antibiotic Mix were purchased from Celsis/In Vitro Technologies. Cryopreserved hepatocytes were thawed in HT Media containing antibiotics, resuspended in HI media at 2 x $10^6$/mL and plated in 96-well plates at 0.05 mL ($10^5$ cells)/well. Compounds to be tested were dissolved in DMSO at 2 mM, further diluted to 4 μM in HI media, and added to the cells in 50 μL so that the final compound concentration was 2 μM. The cells were then placed in a $37^0$C, 5% $CO_2$ incubator. At the time points indicated, the well contents were harvested and a 2-fold volume of methanol added to lyse the cells and precipitate proteins. The samples were incubated 10 min at RT and then spun at 16,100 x g for 5 min in a microcentrifuge. The supernatant was analyzed by LC-MS/MS. Metabolism of 7-ethoxycoumarin was used to monitor S9 and hepatocyte performance.

**Pharmacokinetic Studies**

Pharmacokinetic studies were done in collaboration with NSW. These studies were performed by first implanting 6-7 week old NCR-nu/nu female mice (Charles River

Laboratories) with 2.5 x $10^5$ MPNST tumor cells in the left flank, subcutaneously. When tumors reached 800 $mm^3$, the animals were injected with Cpd21 at 20 mg/kg in 0.2 ml 10% ethanol, 10% PEG400, 80% of a solution of 5% dextrose, pH 7.4. Blood was drawn at each time point (0, 10, 30, 60, 180, 360, 1440 min) using the anticoagulant, ACD (acidified citrate dextrose) and plasma isolated by centrifugation. 100 □L of plasma was mixed with 200 □L of acetonitrile containing 0.15% formic acid and 37.5 ng/mL n-benzylbenzamide IS. The samples were vortexed 15 sec, incubated at room temp for 10 min and spun twice at 16,100 x g at $4^0$C in a refrigerated microcentrifuge. The amount of Cpd21 present in plasma was quantified by LC-MS/MS to determine the rate of clearance from mouse blood. A Cpd21 standard curve was generated using blank plasma spiked with known concentrations of Cpd21 and processed as described above. The concentrations of Cpd21in each time-point sample were quantified using Analyst 1.4.2. A value of 3-fold above the signal obtained from blank plasma was designated the limit of detection (LOD). The limit of quantitation (LOQ) was defined as the lowest concentration at which back calculation yielded a concentration within 20% of theoretical. The LOQ for plasma was 5 ng/mL and 1 ng/mL for tumor. Back-calculation of points on the standard curve yielded values within 15% of theoretical over 4 orders of magnitude (5000 to 5 or 1 ng/mL). Pharmacokinetic parameters were calculated using the noncompartmental analysis tool of WinNonLin (Pharsight).

**Bioluminescent Imaging**

sMPNST-luc+ cells were injected at 2 x $50^5$ cells/200 uL on both left and right flanks of nude mice that were age- and sex-matched. Mice were imaged after one week by injecting

160 uL of 20 mg/mL luciferin (Promega), which was pre-diluted in 0.9% sterile NaCl in order to obtain baseline images and values. Total flux was quantified using IVIS Lumina II (Caliper Life Sciences). Mice were then injected with 40 mg/kg Cpd21 or vehicle (10% ethanol, 10% PEG400, and 80% of 5% dextrose in water) twice per day for 4 weeks. Mice were imaged each week and at the end of the treatment period.

**Immunohistochemistry**

Tissue samples were fixed in 10% formalin and processed in tissue processor for 30 min intervals (45 min for brain tissues). Tissues were embedded in paraffin blocks, sectioned with microtome, collected on slides, and dried at room temperature overnight. Slides were de-paraffinized, and heated in microwave with antigen retrieval buffer (0.18 mM citric acid, 0.82 mM sodium citrate pH 6.0) until boiling, and allowed to cool at room temperature for 1 h. Slides were then washed with PBS, and treated with 3% $H_2O_2$ for 15 min. Slides were washed three times with PBS, and blocked with 10% goat serum for 1 h. Primary antibody (1:500) was added overnight at 4$^{o}$C. Primary antibodies include: S100 (DAKO), GAP43 (Abcam), Ki67 (Thermo Scientific), Caspase 3 (Cell Signaling), and PARP (Novus Biologicals or Millipore). Slides were washed three times with PBS, and biotinylated goat secondary antibody (Jackson) was added (1:500) for 1 h. ABC amplification was done according to manufacturer's instructions (Vector), and slides were then washed with PBS three times. DAB staining was done according to manufacturer's instructions (Vector). Slides were counterstained with hematoxylin for 20 s, and dehydrated with 100% and 95% ethanol,

followed by treatment with xylene. Slides were then coverslipped, allowed to dry, and imaged.

**Western Blotting**

Cells were seeded at 5 x $10^4$ cells/2 mL/well in 6-well plates and treated with Cpd21 for indicated time points. Media was collected and centrifuged at 14,000 rpm. Supernatant was discarded. Cells were trypsinized, collected along with 10% FBS media, and centrifuged at 1500 rpm for 5 min. Supernatant was discarded. Cells were lysed with 600 uL RIPA buffer (ThermoScientific), containing Complete Mini (Roche) and 1% Halt Phosphatase Inhibitor Cocktail (ThermoScientific). LDS Sample Buffer (Thermo Scientific) containing 2% beta-mercaptoethanol (Sigma) were added to a final concentration of 25% in each sample, which was then boiled for 10 min. Prepared samples were run on 5-20% SDS-PAGE gel (BioRad), and transferred to nitrocellulose membrane (Whatman) using wet transfer. Membranes were blocked with 5% non-fat dry milk in PBS-T for 1 h, and antibodies were added in PBS-T overnight at 4$^o$C with shaking. The following antibodies were used: Cyclin D1 (Millipore), Caspase 3 (Cell Signaling), PARP (Novus Biologicals and Millipore), pAKT (Cell Signaling), AKT (Cell Signaling), αTubulin (Sigma), GAPDH (Santa Cruz), and H3 (Millipore). Membranes were washed with PBS-T three times. Secondary antibody added in PBST-T. Secondary antibodies include: anti-mouse (Vector) and anti-rabbit (Vector). Membranes were washed with PBS-T three times, and developed using Pierce ECL Substrate (Thermo Scientific) or ChemiGlow (protein simple).

# RESULTS

## Metabolic Stability of Cpd21

To determine whether Cpd21 could be directly tested *in vivo*, we sought to define the metabolic properties *in vitro* according to previously published methods (Lu et al., 2009; Tso et al., 2013). To examine stability, Cpd21 was incubated with purified, hepatic, enzymatic S9 fraction over a period of 240 min, and measured over time (Figure 7A) (NSW). The half-life in the S9 fraction is 22.65 min. In addition, we also incubated Cpd21 with cultured hepatocytes and found that the half-life is 121.6 min (Figure 7B) (NSW). These assays demonstrate that Cpd21 would have reasonable stability in vivo.

## Pharmacokinetic Properties of Cpd21

We next sought to define the pharmacokinetic (PK) properties of Cpd21 according to previously published methods (Williams et al., 2007). sMPNST ($2.5 \times 10^5$) cells were injected subcutaneously into nude mice, and when tumors reached 800 $mm^3$, a single dose of Cpd21 was injected IP at 20 mg/kg. Plasma and tumor samples were collected after 10, 30, 90, 180, 360, and 960 minutes and assayed by mass spectrometry (Figure 7C) (NSW). We observed that Cpd21 rapidly distributes from the plasma into the sMPNST tissues, and that the half-life in the sMPNST tissues is 6-8 hours once the compound is completely distributed. Importantly, Cpd21 concentration remains above 1 μM (204 ng/mL, which is the EC50 in sMPNST cells) in the sMPNSTs for over 6 hours. These results indicate that Cpd21 is successfully delivered to the tumor tissue in adequate concentrations and with an adequate half-life for *in vivo* studies.

**Chronic Administration of Cpd21**

We next determined a dose tolerable for chronic *in vivo* administration of Cpd21. Compound dissolved in a mixture of ethanol, PEG400, and dextrose was delivered intraperitoneally (IP) at 20 or 40 mg/kg twice per day, into nude mice over the course of two weeks for comparison with vehicle administration. These concentrations were selected because 40 mg/kg is the maximum solubility in the aforementioned formulation. Over this period, the mice were weighed daily and observed for signs of toxicity. Neither concentration of Cpd21 produced measurable weight loss or distress in the mice (data not shown). Therefore, we selected 40 mg/kg twice per day IP as the dosing regimen for efficacy studies.

**Efficacy of Cpd21 *in vivo***

We then tested the effects of Cpd21 administration on tumor burden *in vivo*. Nude mice were injected with sMPNST cells that carried a luciferase gene (MPNST-luc+) to permit non-invasive *in vivo* tumor growth assessment by luminescence. One week after allograft, recipient mice were IP injected with either 40 mg/kg of Cpd21 or vehicle twice daily over a 4 week period, and mice were imaged on a weekly basis. We observed that treatment with Cpd21 reduced the tumor burden as measured by total flux normalized to baseline flux levels (Figure 7D and 7E). Cpd21 administratation also decreased tumor weight (Figure A3A) and tumor volume (Figure A3B) compared to vehicle control.

**Cpd21 Decreases Proliferation of sMPNSTs**

BrdU was injected into mice prior to necropsy. Both BrdU and Ki67 evaluation indicated a significant decrease in tumor cell proliferation following Cpd21 treatment (Figure 7F-7I). These results are consistent with our observations that Cpd21 inhibits the cell cycle *in vitro*, resulting in a decrease in the proliferative capacity of sMPNSTs.

**Cpd21 Induces Apoptosis in sMPNSTs**

Consistent with the *in vitro* data, Cpd21-treated sMPNSTs exhibited elevated activated caspase 3 and PARP (Figure 7J-7M). These results were confirmed by Western blotting to detect cleaved caspase 3 and cleaved PARP in tumors from our *in vivo* model (Figure 7N). Taken together, our results demonstrate that Cpd21 can be delivered to mice in concentrations to sufficiently penetrate sMPNST tissue, and inhibit tumor development.

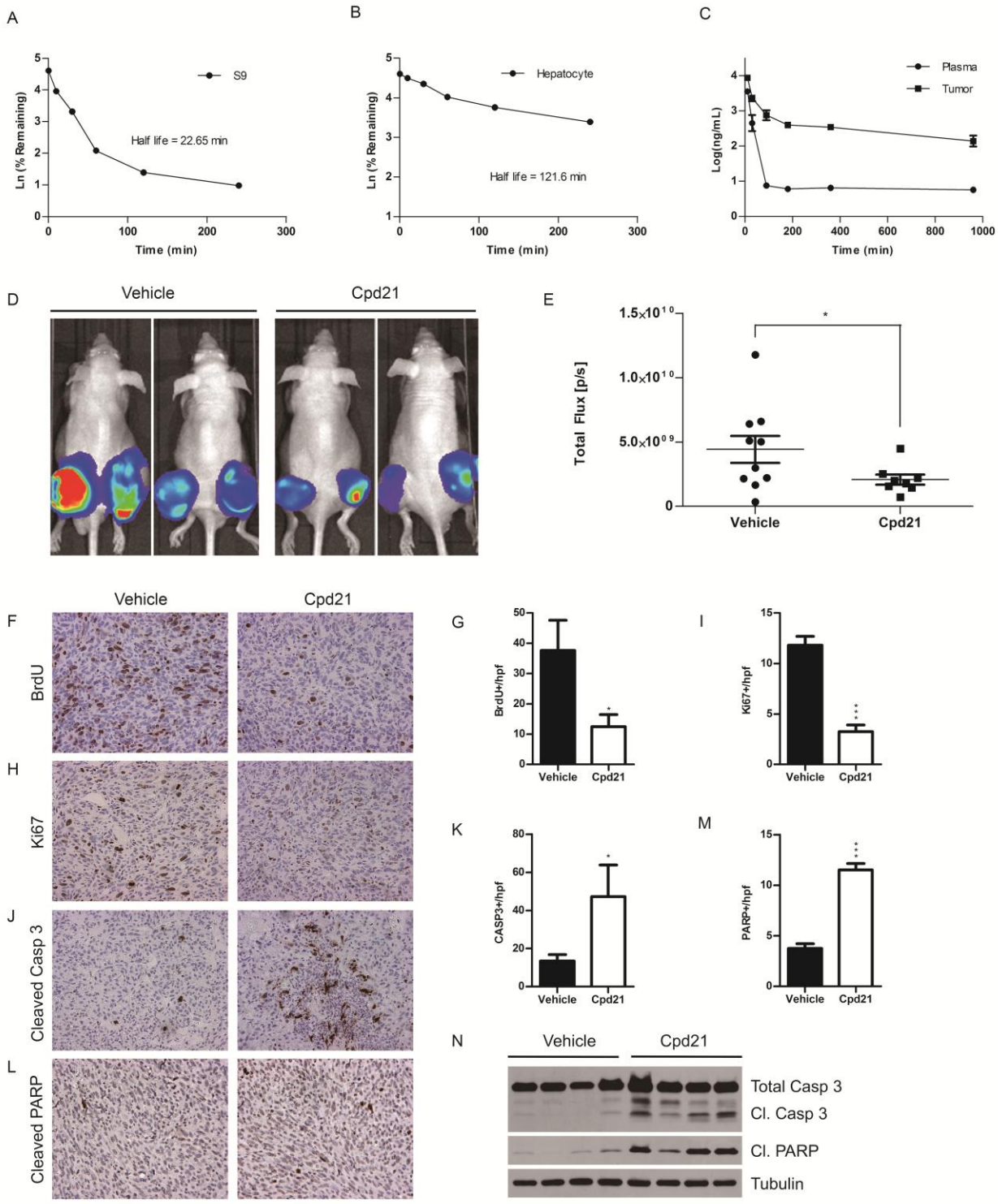


**Figure 7 Effect of Cpd21 in vivo.** (A and B) Cpd21 was incubated with murine, hepatic S9 fractions (A) or murine hepatocyte (B) for indicated times. Amount of Cpd21 remaining was

quantified by mass spectrometry (NSW). (C) Cpd21 was injected at 20 mg/kg IP and quantified in plasma or tumor over time. PK parameters were quantified using the noncompartmental analysis tool in WinNonlin (Pharsight) (NSW). (D) sMPNST-luc+ cells were injected subcutaneously in nude mice. Cpd21 at 40 mg/kg or vehicle was injected IP twice per day for 4 weeks. Mice were imaged using a bioluminescent imager every 7 days, and images shown are from week 4. (E) Quantification of tumor images in D by normalizing total flux at week 4 with baseline flux (n=10 for vehicle, n=8 for Cpd21). (F) BrdU staining of Cpd21- or vehicle-treated tumors (G) Quantification of BrdU staining. (H) Immunohistochemistry of Ki67. (I) Quantification of Ki67 staining. (J) Immunohistochemistry of cleaved caspase 3. (K) Quantification of cleaved caspase 3 staining. (L) Immunohistochemistry of cleaved PARP. (M) Quantification of cleaved PARP staining. (N) Western blot analysis of tumor sample lysates for cleavage of caspase 3 and PARP. All values represent the mean ± standard deviation. Student's t-test was used to test for significance (*$p<0.05$, **$p<0.01$, ***$p<0.001$).

**Apoptotic Effect of Cpd21 is Specific to sMPNSTs**

To extend the previous observation that extended exposure to Cpd21 did not appear to cause general toxicity, we also examined various tissues following necropsy for histological evidence of Cpd21 induced toxicity. In addition to tumor tissue (Figure 8A), we examined liver (Figure 8B), kidney (Figure 8C), brain (Figure 8D), skin (Figure 8E), and sciatic nerve (Figure 8F), and found no evidence of abnormal histology. Activated caspase 3 could only be detected in tumor samples (Figure 8G) and not in other tissues examined (Figure 8H-8L). In contrast to other chemotherapeutic agents such as doxorubicin that induce toxicity in a variety of tissues (Brenner et al., 1984), Cpd21 appears to act most notably on malignant tumor tissue.

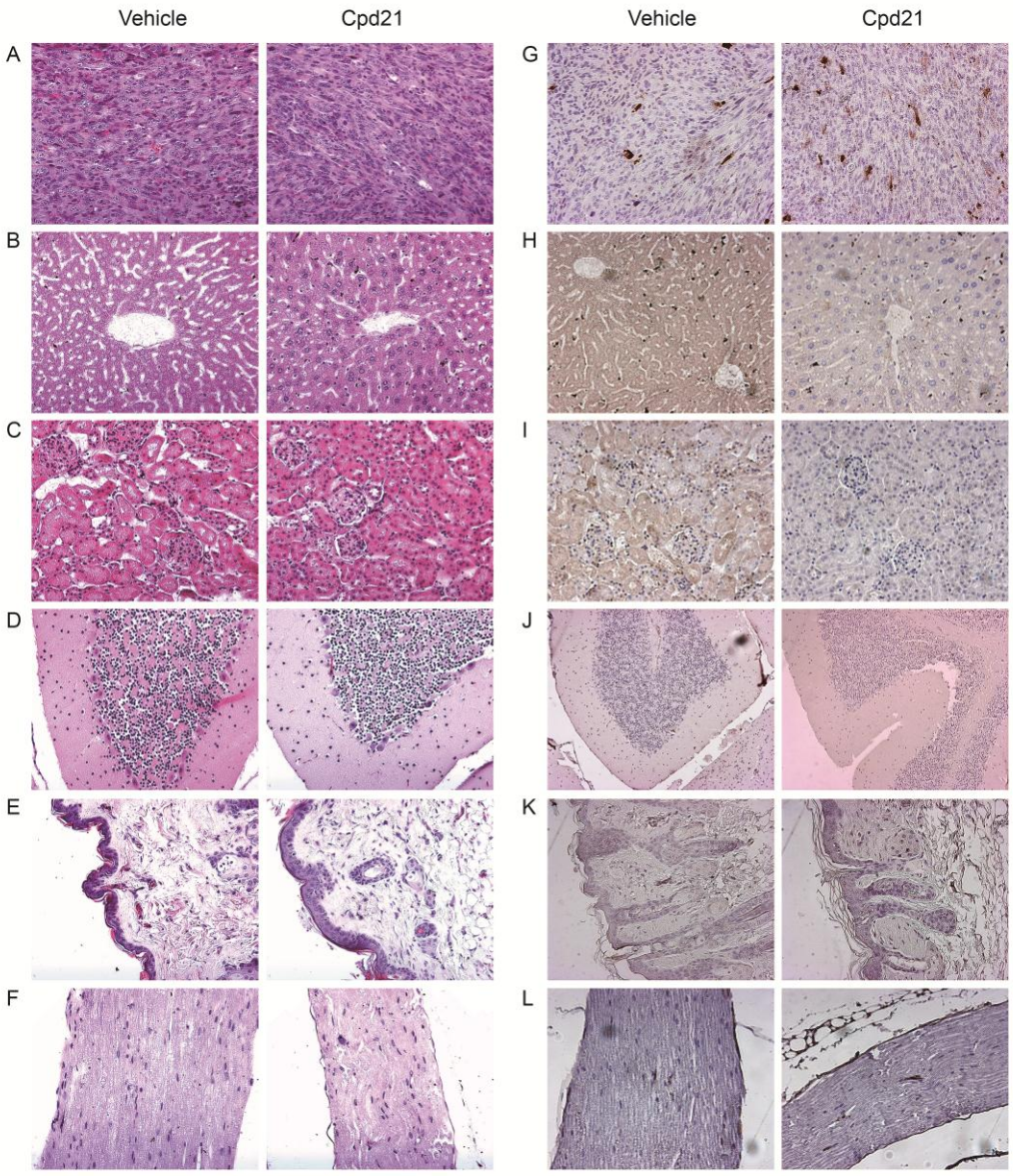


**Figure 8 Apoptotic effect of Cpd21 is specific to tumor tissue.** (A-F) H&E staining of tumors (A), liver (B), kidney (C), brain (D), skin (E), and sciatic nerve (F) from mice treated with either Cpd21 or vehicle. (G-L) Immunohistochemitry for cleaved caspase 3 is only detected in tumor tissue (G), but not in liver (H), kidney (I), brain (J), skin (K), or sciatic nerve (L). All images captured at 20X objective.

## DISCUSSION

Increased proliferation, activation of invasion, and evasion of apoptosis are important hallmarks of cancer (Hanahan and Weinberg, 2011). In the sMPNST model, cancer cells are deficient in *Nf1* and *p53*. The absence of *Nf1* causes RAS to be overactive, leading to activation of RAF and PI3K (Le and Parada, 2007). The upregulation of RAF activates MAPK signaling, while the upregulation of PI3K activates AKT, mTOR, and RAC. MAPK signaling and mTOR both drive cellular proliferation, and RAC is known to mediate cell migration. In addition, the absence of *p53* prevents the cells from ceasing proliferation and entering apoptosis after DNA damage (Kastan et al., 1991). Therefore, the combined loss of both *Nf1* and *p53* leads to unchecked proliferation, invasive capacity, and escape from apoptosis.

Given this cellular context, a high throughput screening approach was taken to identify compounds that inhibit MPNST but not Schwann cells or MEF cells. One compound, Cpd21, was found to inhibit proliferation and to induce apoptosis. Of course, an obvious hypothesis is that Cpd21 first inhibits proliferation by inducing cell cycle arrest, which leads to subsequent apoptosis. However, it remains a possibility that Cpd21 may act through multiple mechanisms, perhaps leading to cell cycle arrest and apoptosis in parallel amongst different subpopulations in MPNST.

In this study, Cpd21 was also shown to act specifically on MPNSTs. Cpd21 did not induce any structural changes that were detected by H&E staining. In addition, Cpd21 only induced apoptosis in MPNSTs and not any other tissues as evidenced by activated caspase 3 staining. Though Cpd21 does not induce histological changes, it remains a possibility that

Cpd21 may still affect organ function, though observation of mice for the duration of Cpd21 treatment showed no signs of distress or other illness, and therefore a deficit in organ function is unlikely.

At this point, the specific mechanism of Cpd21 action on MPNSTs is not known. Therefore, an area of further research is to chemically alter the structure of Cpd21 to determine the structure-activity relationship of this small molecule. Doing so would yield insight into how the structure may be altered for increased efficacy and decreased toxicity. In addition, structure-activity relationship studies may be useful into determining where a potential substrate may be attached for future biochemical studies of the molecular target. Such studies would help elucidate the mechanism by which Cpd21 functions and generate new leads that may play an essential role in MPNST biology.

# CHAPTER FOUR
# Probing Interactions with Other Inhibitors of MPNST


## ABSTRACT

MPNSTs are a main cause of mortality in NF1 patients. MPNSTs are typically treated with surgery when discovered early. Radiation therapy is usually reserved for palliative treatment because of its ability to induce additional mutations, and is therefore reserved for palliative treatment. MPNST patients may also receive doxorubicin as therapy, but this DNA-intercalating agent has shown limited efficacy and has relatively low tumor specificity. Therefore, there is an urgent need for novel chemotherapeutic agents. Cpd21 inhibits MPNST cells but not Schwann and MEF cells, and decreases MPNST tumorigenesis by inhibiting proliferation and inducing apoptosis. To improve on the efficacy profile of Cpd21, known inhibitors of MPNST were tested in conjunction with Cpd21 to identify potential interactions. The phosphatidylinositol-3-kinase (PI3K) inhibitor, LY294002, was shown to interact with Cpd21 in inhibiting MPNST. This combined treatment offers promising potential as a new chemotherapeutic option.

**BACKGROUND**

MPNST is a malignancy that arises in NF1 patients (Ducatman et al., 1986). Currently, early surgery is the mainstay of treatment (Ducatman et al., 1986; Ferner and Gutmann, 2002), with chemotherapy demonstrating some limited benefit (Katz et al., 2009), and radiation therapy being offered palliatively due to its potential induction of additional mutation (Ducatman et al., 1986). Various groups have tested and reported the efficacy and toxicity of other inhibitors of MPNST (Table 1). Authors have selected inhibitors for pathways that have been implicated in MPNST.

**Table 1 Compounds Reported to Inhibit MPNST**

| Inhibitor | MPNST Cells Reported | Reported Concentration Range of Efficacy (μM) | Authors |
|---|---|---|---|
| Doxorubicin | ST88-14 | 0.1-10 | (Johansson et al., 2008; Slomiany et al., 2009) |
| U0126<br>(MEK Inhibitor) | ST88-14<br>NF90-8 | 10 (ST88-14)<br>15 (NF90-8) | (Jessen et al., 2013; Mattingly et al., 2006) |
| LY294002<br>(PI3K/AKT Inhibitor) | ST88-14<br>T265 | 3.5-12.2 | (Zou et al., 2009b) |
| Rapamycin<br>(mTOR Inhibitor) | ST88-14<br>T265 | 0.001-0.01 | (Johansson et al., 2008; Zou et al., 2009b) |
| AMD3100<br>(CXCR4 Inhibitor) | sMPNST<br>MPNST-cisNP<br>S462<br>SNF96.2 | ~0.5 (sMPNST)<br><0.5 (MPNST-cisNP)<br>~0.5 (S462)<br>~10 (SNF96.2) | (Mo et al., 2013) |

Doxorubicin is considered a first-line chemotherapeutic agent for MPNST (Katz et al., 2009). In one study, doxorubicin in combination with ifosfamide showed a limited longer progression free survival (PFS) compared with doxorubicin alone or ifosfamide alone (Kroep et al., 2011). Other groups have tested doxorubicin in combination with RAD001 (mTOR inhibitor) in mice, but there was no observed difference in tumor volume compared to RAD001 alone. When doxorubicin was tested in combination with bevacizumab (anti-VEGF antibody) in patients, there was no increase in response rate compared to doxorubicin alone (D'Adamo et al., 2005).

Multiple pathway-specific inhibitors have also been tested in MPNST. First, groups have tested inhibitors to the RAS/RAF/MEK/ERK pathway on MPNST. When *Nf1* is deficient, RAS activity is upregulated, leading to RAF activation, which activates MEK and leads to the phosphorylation of ERK (Ambrosini et al., 2008). The activation of ERK, in turn, leads to cellular proliferation. MEK inhibitors have been shown to be effective at inhibiting pErk in various MPNST cell lines (ST88-14, NF90-8, and STS26-T), and to decrease the proliferation of these cell lines (Mattingly et al., 2006). There are several MEK inhibitors that have been tested in MPNST. For instance, MEK inhibitors, including PD98059, PD184352, and U0126, have been shown to be effective at inhibiting the proliferation of MPNST cells lines (ST88-14, NF90-8, and STS26-T) by inhibiting pERK (Mattingly et al., 2006). A fourth MEK inhibitor, PD0325901, has been shown to inhibit the growth of neurofibromas that develop in Dhh-Cre-$Nf1^{f/f}$ mice and to modestly inhibit growth of human MPNST in mouse xenograft models (Jessen et al., 2013). Moreover, others have shown that U0126 is effective at inhibiting growth of MPNST cells from *cis-*$Nf1^{+/-}$*;*$p53^{+/-}$ mice, and can

attenuate the colony-forming ability of these cells in soft agar (Li et al., 2002). U0126 was selected for testing in conjunction with Cpd21 in this study to determine whether there is any interaction between the two inhibitors.

Second, activated RAS can also directly activate PI3K. Overactive RAS is known to activate PI3K, which is an enzyme that is involved in the conversion of phosphatidylinositol 4,5-biphosphate [PtdIns $(4,5)P_2$] or PIP2 to phosphatidylinositol 3,4,5-triphosphate [PtdIns $(3,4,5)P_3$] or PIP3 (Li et al., 2000). PIP3 binds to the plekstrin homology (PH) domain of AKT, causing AKT to move to plasma membrane (Brazil and Hemmings, 2001; Kandel and Hay, 1999; Scheid and Woodgett, 2001), where AKT is then phosphorylated by PDK1(Hay and Sonenberg, 2004). Mice that are deficient of AKT showed that AKT is upstream of mTOR (Peng et al., 2003). Moreover, mTOR is negatively regulated by TSC1 and TSC2, and it was demonstrated that AKT can inhibit TSC2 (Inoki et al., 2002; Manning et al., 2002). Therefore, activated AKT is upregulates mTOR, and both proteins are key mediators of cellular growth and proliferation (Hennessy et al., 2005). Inhibitors of the PI3K/AKT pathway, including LY294002, have been tested on MPNST. LY294002 was effective at inhibiting three MPNST cells lines, including T265, ST88, and STS26T (Zou et al., 2009b). In this study, LY294002 was tested in combination with Cpd21 to test for potential interaction.

The third pathway that has been investigated for potential inhibitor intervention is the mTOR pathway. Overactive RAS as a result of *Nf1* deficiency leads to PI3K and AKT activation, which lead to mTOR pathway upregulation and cellular proliferation in MPNST (Hennessy et al., 2005; Sarbassov et al., 2005). mTOR is composed of two complexes of

proteins called mTORC1 and mTORC2, and is bound to Raptor and Rictor (Katz et al., 2009). mTOR is known to integrate the signals from receptor tyrosine kinases, which sense growth factors in the extracellular environment, with metabolic signals, which reflect the nutrition status of the cell (Hay and Sonenberg, 2004; Katz et al., 2009). In the absence of nutrients, mTOR is bound tightly to Raptor and mLST8, which prevents mTOR from signaling its downstream effectors (Hay and Sonenberg, 2004). An influx of nutrients triggers a conformational change between the three proteins and allows mTOR to interact with its targets, 4E-BP1 and S6K1, which ultimately results in regulation of protein translation (Hay and Sonenberg, 2004). mTOR inhibitors have been tested on MPNST, including rapamycin and RAD001. Rapamycin binds to FKBP12, which binds a region located near the C-terminus on mTOR called FRB (Hay and Sonenberg, 2004). When mTOR inhibitors were injected into mice implanted with MPNST xenografts, the inhibitor delayed tumor growth but only transiently (Johansson et al., 2008). Therefore, rapamycin was selected and tested in combination with Cpd21 to determine whether these two inhibitors interact.

Finally, the ligand CXCL12 and its receptor CXCR4 was recently reported to promote MPNST growth by stimulating Cyclin D1 via P13K and β-Catenin signaling (Mo et al., 2013). By comparing the gene expression profiles, CXCR4 was found to be highly expressed in sMPNST and upregulated in both the pretumorigenic *Nf1*$^{-/-}$ and *Nf1*$^{-/-}$;*p53*$^{-/-}$ SKP compared to wildtype SKPs. Knockdown of CXCR4 caused decreased tumorigenesis in both sMPNST and human MPNST cells when implanted in nude mice. Also, knockdown of CXCR4 leads to growth arrest and a decrease in cyclin D1 protein levels. Importantly, it was

shown that CXCR4 depletion leads to decreased β-catenin activity, which is a known regulator of cyclin D1 (Sherr, 1995). Recently, one other group confirmed the importance of the β-catenin signaling pathway using a forward genetic screening approach (Rahrmann et al., 2013). The inhibitor of CXCR4, known as AMD3100, decreases MPNST cell growth in culture and inhibits tumorigenesis of MPNST (Mo et al., 2013). AMD3100 was tested in combination with Cpd21 to determine potential interactions.

In this study, each inhibitor was verified *in vitro*, and tested alone and in combination with Cpd21. The PI3K inhibitor, LY294002, was shown to interact with Cpd21 in inhibiting MPNST survival. This inhibitor combination shows promise in the treatment of MPNST.

## METHODS

### Cell Samples

MPNST cells are cultured in DMEM, 10% FBS, 1% L-glutamine, 1% sodium pyruvate, and 1% penicillin/streptomycin.

### Additivity Studies

Cells were treated with Cpd21 alone, given inhibitor alone, or Cpd21 combined with inhibitor at stated concentrations below at a final volume of 150 uL in 96 well plates, and incubated for 96 h or other indicated time points. Conditions were plated in quadruplicate. 20 uL of CellTiter-Glo$^{TM}$ (Promega) was then added to each well, and plates were read by PolarStar OPTIMA (BMG Labtech) luminometer. Data were averaged, and interaction was determined using the Loewe additivity model (Straetemans et al., 2005).

### Western Blotting

Cells were seeded at 5 x $10^4$ cells/2 mL/well in 6-well plates and treated with Cpd21 for indicated time points. Media was collected and centrifuged at 14,000 rpm. Supernatant was discarded. Cells were trypsinized, collected along with 10% FBS media, and centrifuged at 1500 rpm for 5 min. Supernatant was discarded. Cells were lysed with 600 uL RIPA buffer (ThermoScientific), containing Complete Mini (Roche) and 1% Halt Phosphatase Inhibitor Cocktail (ThermoScientific). LDS Sample Buffer (Thermo Scientific) containing 2% beta-mercaptoethanol (Sigma) were added to a final concentration of 25% in each sample, which was then boiled for 10 min. Prepared samples were run on 5-20% SDS-PAGE gel (BioRad),

and transferred to nitrocellulose membrane (Whatman) using wet transfer. Membranes were blocked with 5% non-fat dry milk in PBS-T for 1 h, and antibodies were added in PBS-T overnight at 4$^{o}$C with shaking. The following antibodies were used: pERK (Cell Signaling), ERK (Cell Signaling), pAKT (Cell Signaling), AKT (Cell Signaling), pS6 (Cell Signaling), S6 (Cell Signaling), Cyclin D1 (Millipore), αTubulin (Sigma), GAPDH (Santa Cruz), and H3 (Millipore). Membranes were washed with PBS-T three times. Secondary antibody added in PBST-T. Secondary antibodies include: anti-mouse (Vector) and anti-rabbit (Vector). Membranes were washed with PBS-T three times, and developed using Pierce ECL Substrate (Thermo Scientific) or ChemiGlow (protein simple).

## RESULTS

### Cpd21 Interacts with Other Chemotherapeutic Agents in MPNST

Mutation of the *NF1* gene, which encodes a RAS-GTPase activating enzyme (Ballester et al., 1990), has been noted to cause activation of RAS downstream effectors including the ERK, PI3K, and mTOR pathways (Basu et al., 1992; Dasgupta et al., 2005; DeClue et al., 1992; Le and Parada, 2007; Weiss et al., 1999; Wittinghofer, 1998). In addition, the DNA intercalating agent doxorubicin (Mattingly et al., 2006) and inhibition of the CXCR4 receptor (Mo et al., 2013) have been reported to inhibit MPNST growth. We therefore examined whether specific inhibitors or doxorubicin, in conjunction with Cpd 21 might better inhibit sMPNST cell growth. Combinations of doxorubicin (Slomiany et al., 2009); U0126, a MEK inhibitor (Mattingly et al., 2006); LY294002, an AKT inhibitor (Zou et al., 2009b); rapamycin, an mTOR inhibitor (De Raedt et al., 2011; Johansson et al., 2008; Zou et al., 2009b); and AMD3100, a CXCR4 inhibitor (Mo et al., 2013), together with Cpd21, were added to cells and assessed for ATP consumption. We found the inhibition of the PI3K pathway combined with Cpd21 treatment resulted in a decrease in cellular growth and survival that is greater than either inhibitor alone (Figure 9A and 9B) (Straetemans et al., 2005). Phospho-AKT Western blots of sMPNST cells treated with LY294002 at 20 μM for 30 or 60 minutes verified effective pAKT inhibition in sMPNST cells (Figure 9C). None of the other tested reagents produced measurable additive or synergistic effects (Figure A4). These inhibitors were verified to specifically inhibit their respective targets (Figure A4). We extended the above studies of dual LY294002 and Cpd21 treatment to MPNST cells derived from *cis-Nf1*$^{+/-}$*;p53*$^{+/-}$ mice (Figure 9D). Again, the data show that the combined effect of

both inhibitors is greater than that of each individual inhibitor. We tested the effects of both inhibitors on phosphorylation of AKT, and found that pAKT was inhibited only when LY294002 is present (Figure 9C and 9E). Thus, in contrast to published reports of successful application of MEK inhibitors to suppress NF1 based solid tumors and leukemias, in the context of Cp21, co-inhibition of the PI3K pathway was most effective in impeding tumor cell growth and survival.

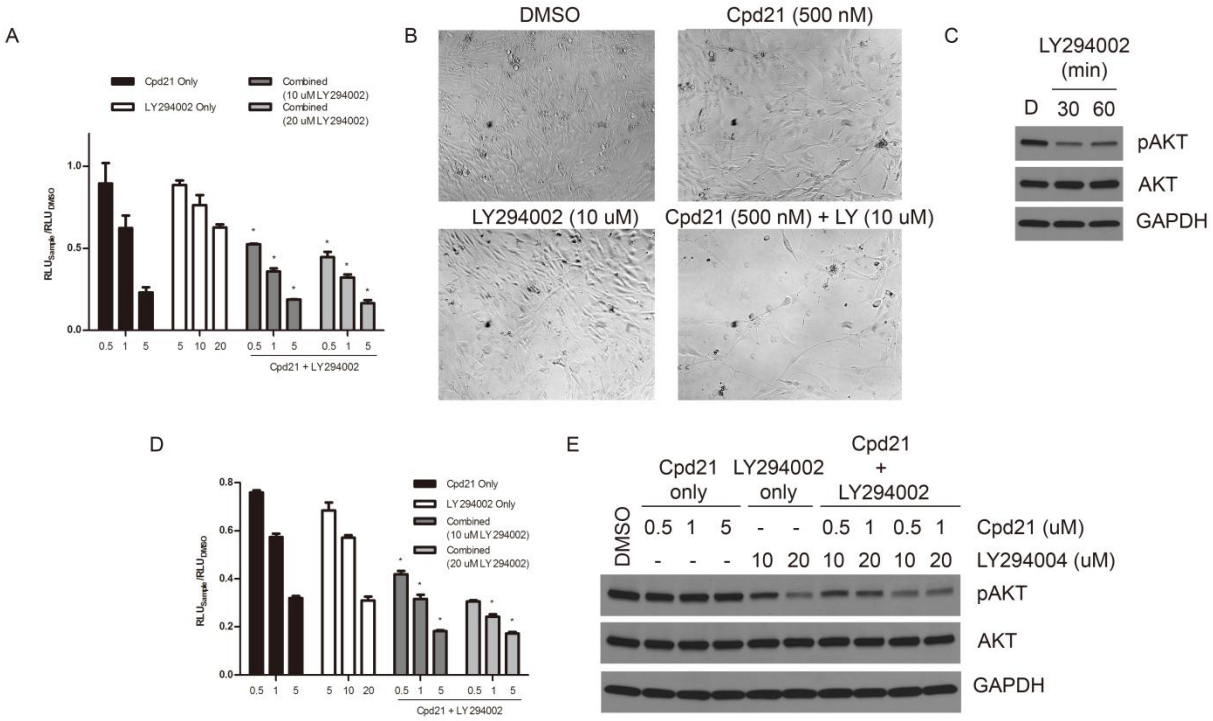


**Figure 9 Cpd21 Interacts with PI3K Inhibitor.** (A) ATP assay of combined treatment of Cpd21 and LY294002 in sMPNST cells. Synergism determined by Loewe method. (B) Phase contrast pictures of sMPNST cells that were treated with DMSO, Cpd21 alone, LY294002 (LY) alone or a combination of both inhibitors. (C) Western blotting for pAKT in sMPNST cells that are treated with 10 μM LY294002 for 30 or 60 min (D) ATP assay following combined treatment of MPNST cells from *cis-Nf1*$^{+/-}$*;p53*$^{+/-}$ mice with Cpd21 and LY294002. (E) Western blotting for pAKT and AKT for sMPNST cells that were treated with Cpd21 alone, LY294002 alone, or with both inhibitors.

**DISCUSSION**

In this study, the dual PI3K/AKT inhibitor, LY294002 was shown interact with Cpd21 to inhibit MPNST survival. In addition, AKT was only phosphorylated when LY294002 was present. In contrast to the published reports that MEK inhibitors can suppress solid tumors and leukemias of NF1 disease, inhibition of the PI3K pathway along with Cpd21 treatment was most effective strategy in impeding tumor cell growth and survival.

MPNSTs are deficient in *Nf1*, which is a tumor suppressor gene that encodes for a protein that normally inhibits RAS signaling (Xu et al., 1990a; Xu et al., 1990b), leading to overactive RAS. This increased RAS signaling leads to activation of RAF and downstream MAPK signaling and activation of PI3K and downstream AKT and mTOR signaling (Le and Parada, 2007). In this molecular model of MPNST, activated AKT drives increased cellular proliferation. At the same time, Cpd21 has been shown to induce apoptosis in MPNSTs. Therefore, it is not surprising that LY294002 interacts with Cpd21 since they perturb two different cellular processes, leading to an effect that is greater than sum of its parts.

One caveat of this study is that LY294002 has been reported to have some off-target effects in other cell types (Hennessy et al., 2005), though this has not been demonstrated in MPNST specifically. Therefore, it remains theoretically possible that interactive effects observed when LY294002 is combined with Cpd21 is a result of some other, unidentified cellular target that is perturbed by LY294002 and that may play an important role in MPNST.

# CHAPTER FIVE
# Discussion and Future Directions

## Implications of the SKP-Model of MPNST

Malignant peripheral nerve tumors are the major source of mortality in NF1. Like most malignant sarcomas, these tumors are resistant to all current chemotherapeutic and radiotherapeutic strategies. It has long been recognized that MPNSTs harbor tumor suppressor mutations in addition to *NF1* loss. Notably, loss of function mutations of the *p53* tumor suppressor have been reported (Berghmans et al., 2005; Birindelli et al., 2001; Greenblatt et al., 1994; Jhanwar et al., 1994; Menon et al., 1990). This has led to the successful generation of spontaneous mouse models of MPNST by mutation of both *Nf1* and *p53* tumor suppressor genes (Cichowski et al., 1999; Vogel et al., 1999). Mice with *cis-Nf1*$^{+/-}$*;p53*$^{+/-}$ background have somatic cells that are deficient in one copy of *Nf1* and one copy of *p53*, and undergo LOH in a subset of cells at both the *Nf1* and *p53* loci, leading to the development of sarcomas, including MPNSTs (Cichowski et al., 1999; Vogel et al., 1999).

A further refinement of MPNST modeling came about by the identification of SKPs as a source for dermal neurofibromas in the skin and by the capacity of SKPs to engender plexiform neurofibromas when placed in the sciatic nerve (Le et al., 2009). Additive mutation of *p53* together with *Nf1* turned SKPs into progenitors of MPNST, thus facilitating high throughput screens for chemical compounds that might inhibit early passage cell growth. Therefore, in both murine models, *Nf1* and *p53* need to be perturbed at both alleles to give rise to MPNST. Both models are thus consistent with the Knudson "two-hit" hypothesis.

In the sMPNST model, MPNSTs form when *Nf1*$^{-/-}$;*p53*$^{-/-}$ SKPs are implanted into nude mice with a genetic background that is wildtype at both *Nf1* and *p53* loci. This observation suggests that MPNSTs may develop from SKPs in a cell-autonomous fashion. One interesting caveat of the sMPNST model is that these mice do not develop other tumor types (e.g. rhabdomyosarcoma, leiomyosarcoma, and MTT) that were observed in mice with *cis*-*Nf1*$^{+/-}$;*p53*$^{+/-}$ background. Instead, only MPNSTs are observed when *Nf1* and *p53* are perturbed in SKPs. A unifying hypothesis for these results is that the loss of *Nf1* and *p53* drive MPNST tumorigenesis whether the genetic background is *Nf1*$^{+/-}$;*p53*$^{+/-}$ or wildtype, and that a tumor microenvironment with a genotype of *Nf1*$^{+/-}$;*p53*$^{+/-}$ may contribute additional factors that are needed to drive the development of other cancers, such as rhabdomyosarcoma, leiomyosarcoma, and MTT.

In this study, the sMPNST model was selected as a tool for drug discovery because of its robustness in displaying all of the histological and molecular properties that are typically observed in human MPNST. In addition, this murine model demonstrated relative facility in generating tumors, allowing the propagation of sufficient numbers of cells for high throughput screening while keeping cell passage number low. Using this model, a high-throughput screening approach was taken to identify novel small molecule compounds that are specific for MPNST but remain nontoxic to other cell types.

**Drug Discovery Using High Throughput Screening**

A limited high-throughput, small-molecule screen using sMPNST cells was performed in an extension of a related ongoing large scale screen on primary mouse GBM

cells with 200,000 compounds (KL and LFP, unpublished data). Since these GBM are deficient for *Nf1*, *p53*, and *Pten*, it was hypothesized that since sMPNST cells are deficient in two of these same tumor suppressors, some compounds might have conserved sMPNST cell growth inhibitory properties. Therefore, a high throughput screen was performed using the small-molecule chemical library composed of the 4480 compounds that were considered toxic to GBM.

One compound, Cpd21, was found to inhibit multiple mouse and human MPNST cell types, but not Schwann and MEF cells. Despite having similarities in genotype, there may differences between MPNST and GBM at the epigenetic or proteomic levels that cause MPNST and GBM cells to behave differently in the presence of compounds from the chosen library. As a result, it is possible that the full 200,000 compound library may contain additional hits that were not present, and thus not screened, in the 4480 cherry-picked library subset. Therefore, a future direction for this work may be an exploration of the remainder of the compounds in the 200,000-compound library that was screened on GBM cells. This approach may allow the identification of many more compounds that are specific to MPNST.

### *In Vitro* and I*n Vivo* Effects of Cpd21

It was a surprise that this compound originating from a 200,000 chemical compound library, had, without chemical modification a repertoire of desirable *in vivo* properties including: low micromolar EC50, adequate stability, manageable toxicity, and adequate accumulation in solid tumor tissue. These serendipitous favorable properties allowed allograft analysis of antitumor efficacy and demonstrated a significant reduction in tumor

burden by this compound. Future efforts to assess the effectiveness of Cp21 on human MPNST xenografts will provide additional insight into the potential for this compound as a therapeutic agent. This chemical compound is a novel contribution to the soft-tissue sarcoma field because MPNSTs are notoriously difficult to treat, and Cpd21 demonstrates potential to be a novel class of chemotherapy. In addition, this compound could be used to further understand MPNST biology in order to uncover novel strategies to target this aggressive cancer.

Although Cpd21 was effective at decreasing the tumor burden of MPNST *in vivo*, there were still some remaining tumors after treatment with this compound. One explanation for this observation is that the bioavailability of Cpd21 may need to be increased. In this study, Cpd21 was injected at a dose that corresponded to its maximum solubility in its respective formulation. Therefore, a possible extension of this work is to modify the chemical structure of Cpd21 in order to create a compound that has increased bioavailability. By adding different chemical moieties to the chemical structure of Cpd21, its structure-activity relationship can be studied and optimized for increased efficacy and reduced toxicity.

At present, the specific mechanism whereby Cpd21 exerts its inhibitory action on MPNST cells is unknown. Compound exposure to tumor cells results in a cell cycle delay manifested by depletion of certain cell cycle related molecules and eventually leading to cellular apoptosis. A similar course of events is seen when tumor-bearing mice are treated with compound. However, the precise molecular target and mechanistic mode of compound action remains a topic of investigation. Empirical chemical compound screens to identify cancer cell inhibitory compounds have been applied for several decades. A significant

proportion of such empirically derived cancer cell inhibitory small molecules that have reached the clinic, have turned out to mechanistically impinge on various aspects of cell division including mitotic spindle machinery, cell cycle machinery and DNA replication and repair machinery. These cellular properties are not unique to cancer cells and are shared by many normally dividing cells in the body that are essential for organ health. Chemotherapeutic toxicity to normal cells represents a major impediment to effective cancer treatment. In this regard, our screen departs from traditional high throughput screens in that we limited our cells assayed to early passage cells rather than to established cell lines. It is also noteworthy that the cellular specificity of Cpd21 renders it relatively innocuous to the normally dividing cells we tested (MEFs, Myc-Schwann Cells, and wildtype SKPs). This feature is consistent with the idea that the compound target(s) relates to the "cancer state" of the MPNST cells rather than to more general properties of mitotically active cells.

**Cpd21 Interacts with PI3K Inhibitor**

Recent advances in MPNST research have pointed to additional potential therapeutic targets including the CXCR4 cytokine axis (Mo et al., 2013) and the RAS/MEK/ERK pathways (Ambrosini et al., 2008; Basu et al., 1992; Cichowski and Jacks, 2001; Dilworth et al., 2006; Jessen et al., 2013; Katz et al., 2009; Katz and McCormick, 1997; Mattingly et al., 2006; Rahrmann et al., 2013). Interestingly, when such compounds were tested in conjunction with Cp21, we found no additive value. Instead, blockade of the PI3K pathway did cooperate with Cpd21 action to inhibit tumor growth. This intriguing result points to the potential plasticity of cancer cells and to the complexity of tumor pathway interactions. For

example, it may be that Cpd21 activity somehow unveils a synthetic dependence on PI3K signaling that is not present in the absence of compound. Continued studies of Cpd21, it specific mode of action, and the mechanistic basis for its activity on MPNST cells but not on non-tumorigenic cells may shed light on novel anticancer pathways.

**Conclusion**

Current first-line treatment for MPNST is surgical intervention. Doxorubicin is also used therapeutically, and radiation therapy is deployed palliatively. Both of the latter treatments, however, have drawbacks due to limited efficacy and adverse side effects. In this study, the sMPNST model was used to successfully identify a compound that is highly specific to this type of MPNSTs. Cpd21 inhibits MPNST cells but not Schwann cells and MEF cells *in vitro*, and decreases the burden of MPNSTs *in vivo* by triggering apoptosis. Furthermore, Cpd21 interacts with LY294002 in inhibiting MPNST cells, suggesting that the PI3K pathway may play a role that is yet to be described. These unique molecular and cellular properties show promising potential for the future treatment of MPNSTs.

## APPENDIX A
## Supplementary High Throughput Screening Information

A high throughput screen involving 4480 compounds identified 1515 compounds that inhibited the ATP metabolism of sMPNST cells greater than 20% at 2.5 µM. Two parallel approaches were then undertaken to exclude compounds that are generally cytotoxic (Figure A1). In the first approach (also discussed in Chapter 3), a counter screen was performed on *Myc*-immortalized Schwann cells (Myc-SC), and compounds that showed greater than 20% inhibition were eliminated. The resultant 119 compounds were rescreened on sMPNSTs but with a cutoff at 70% inhibition. 28 compounds passed this test, and these comprised part of the 57 compounds that were validated in subsequent dose response studies. In the second approach, 848 compounds were identified as inhibiting ATP metabolism of sMPNST cells greater than 70%. A counter screen was performed on MEF cells (KL and LFP, unpublished data), and 320 compounds were found to inhibit ATP metabolism in sMPNST cells greater than 70% and MEF cells less than 25%. These compounds were then tested at a low dose of 167 nM on sMPNST cells. 29 compounds were found to inhibit ATP metabolism of sMPNST cells greater than 30%, and these comprised the second part of the 57 compounds that were validated in subsequent dose response studies. Of these 57 compounds, 42 were validated in dose response studies on sMPNST, Myc-SC, and MEF cells ranging from 125 nM to 20 µM (Figure A2).

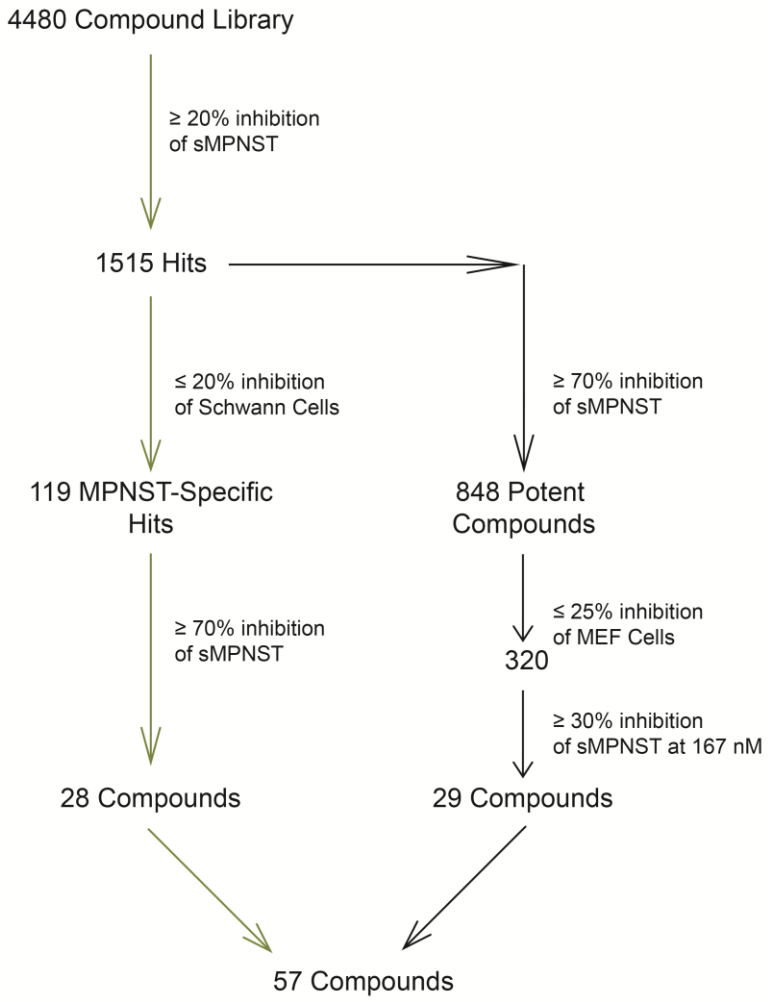


**Figure A1 Schematic of Hit Selection Procedure.** Green arrows denote the hit selection procedure described in Chapter 2. Black arrows denote a second hit approach at selecting hits for validation. In this approach, 848 of 1515 hits were observed to inhibit ATP metabolism of sMPNST cells greater than 70%. A counter screen on MEF cells was then performed (KL and LFP, unpublished data), and 320 of 848 compounds were observed to inhibit ATP metabolism of MEF cells less than 25%. These 320 compounds were tested at a low dose of 167 nM on sMPNST cells, and 29 compounds were found to inhibit ATP metabolism of sMPNST cells at this concentration. Together with the 28 compounds selected in the first approach, these 29 compounds comprise a total list of 57 compounds that are candidates for further dose response validation.

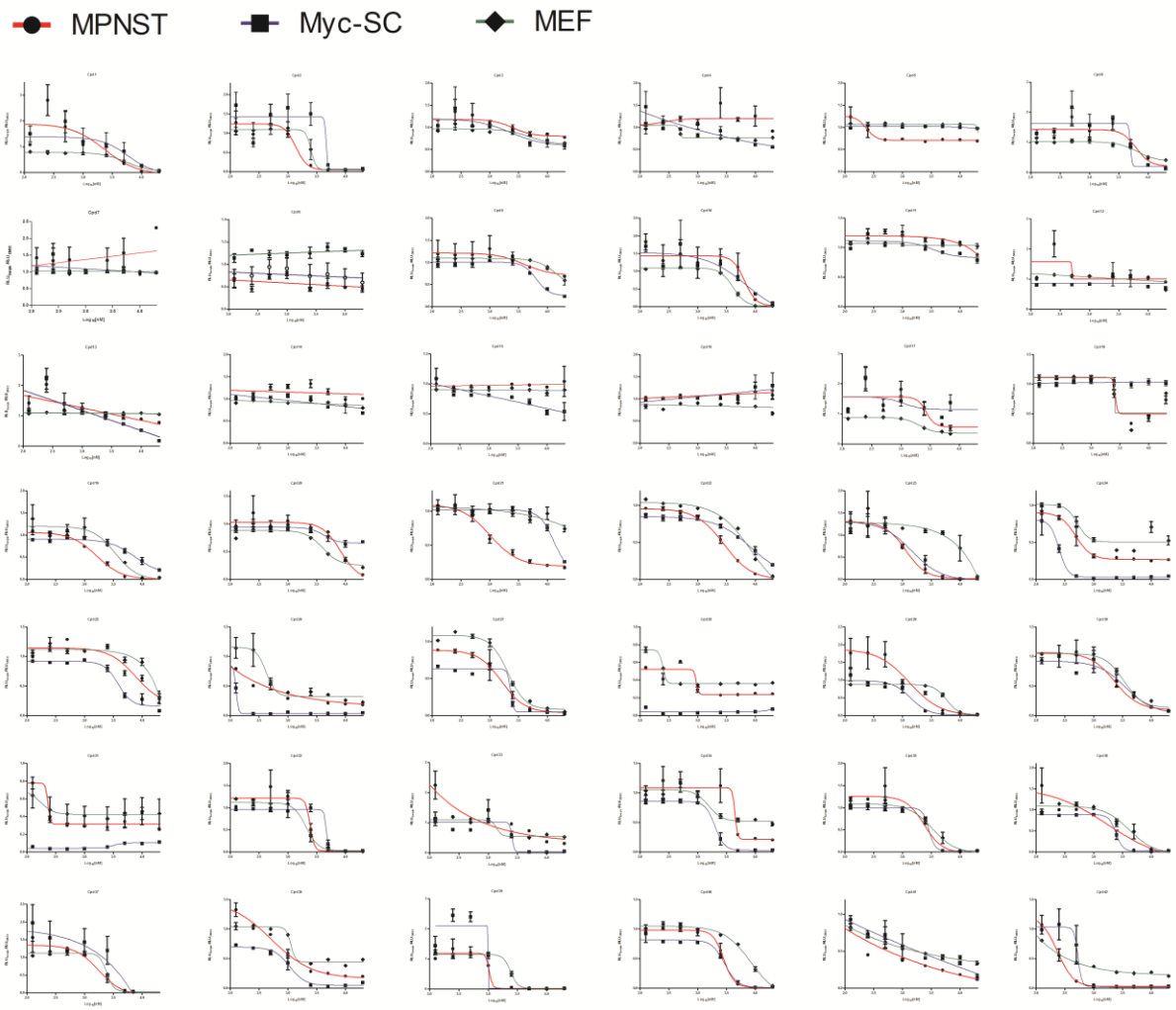


**Figure A2 Validation of High Throughput Screening via Dose Response Studies.** 42 of 57 compounds were validated in dose response studies on sMPNST, Myc-SC, and MEF cells, ranging from 125 nM to 20 µM. The twenty-first compound, Cpd21, showed the greatest separation between the dose response curves of sMPNST cells and the control Myc-SC and MEF cells. The EC50 of Cpd21 on sMPNST cells is 1.0 µM.

# APPENDIX B
## Supplementary Information for In Vivo Effect of Cpd21

Cpd21 was delivered at 40 mg/kg IP twice per day over 4 weeks to mice implanted with MPNST-luc$^{+}$ cells (discussed in Chapter 3). Tumor burden was assessed using three methods. The first is by imaging and quantifying the total flux from bioluminescence signal produced by MPNST-luc$^{+}$ cells (Chapter 3). This signal was decreased by treatment with Cpd21. Mice were also assessed for tumor burden by the measurement of tumor weight and volume, which were both decreased with Cpd21 treatment (Figure A3). Therefore, these three measures of tumor burden are consistent and demonstrate that Cpd21 inhibits MPNST *in vivo*.

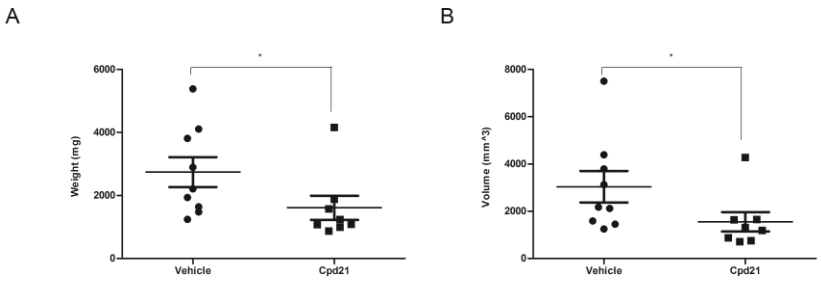


**Figure A3 Cpd21 decreases tumor weight and volume.** (A) Mice are implanted with MPNST-luc$^{+}$ cells and then injected with 40 mg/kg Cpd21 IP twice per day over 4 weeks. Tumor weight is measured and is decreased by Cpd21 treatment. (B) Mice are implanted with MPNST-luc$^{+}$ cells and then injected with 40 mg/kg Cpd21 IP twice per day over 4 weeks. Tumor volume is measured and is decreased by Cpd21 treatment.

## APPENDIX C
## Other Inhibitors Tested for Interaction with Cpd21

As discussed in Chapter 4, we systematically tested Cpd21 in conjunction with compounds that are known to inhibit MPNST, including doxorubicin (Slomiany et al., 2009); U0126, a MEK inhibitor (Mattingly et al., 2006); LY294002, an AKT inhibitor (Zou et al., 2009b); rapamycin, an mTOR inhibitor (De Raedt et al., 2011; Johansson et al., 2008; Zou et al., 2009b); imatinib mesylate, a PDGFR inhibitor (Aoki et al., 2007); and AMD3100, a CXCR4 inhibitor (Mo et al., 2013) (Figure A4). Only LY294002 was observed to interact with Cpd21 in inhibiting MPNST (discussed in Chapter 4, Figure 9).

sMPNST cells were treated with either Cpd21 alone, the given inhibitor alone, or a combination of Cpd21 and the given inhibitor. Cells were incubated for 96 h, and then ATP assay was performed. In parallel, protein was harvested from sMPNST cells treated with the given inhibitor, and Western blotting was performed to evaluate the effect of the inhibitor on its reported target.

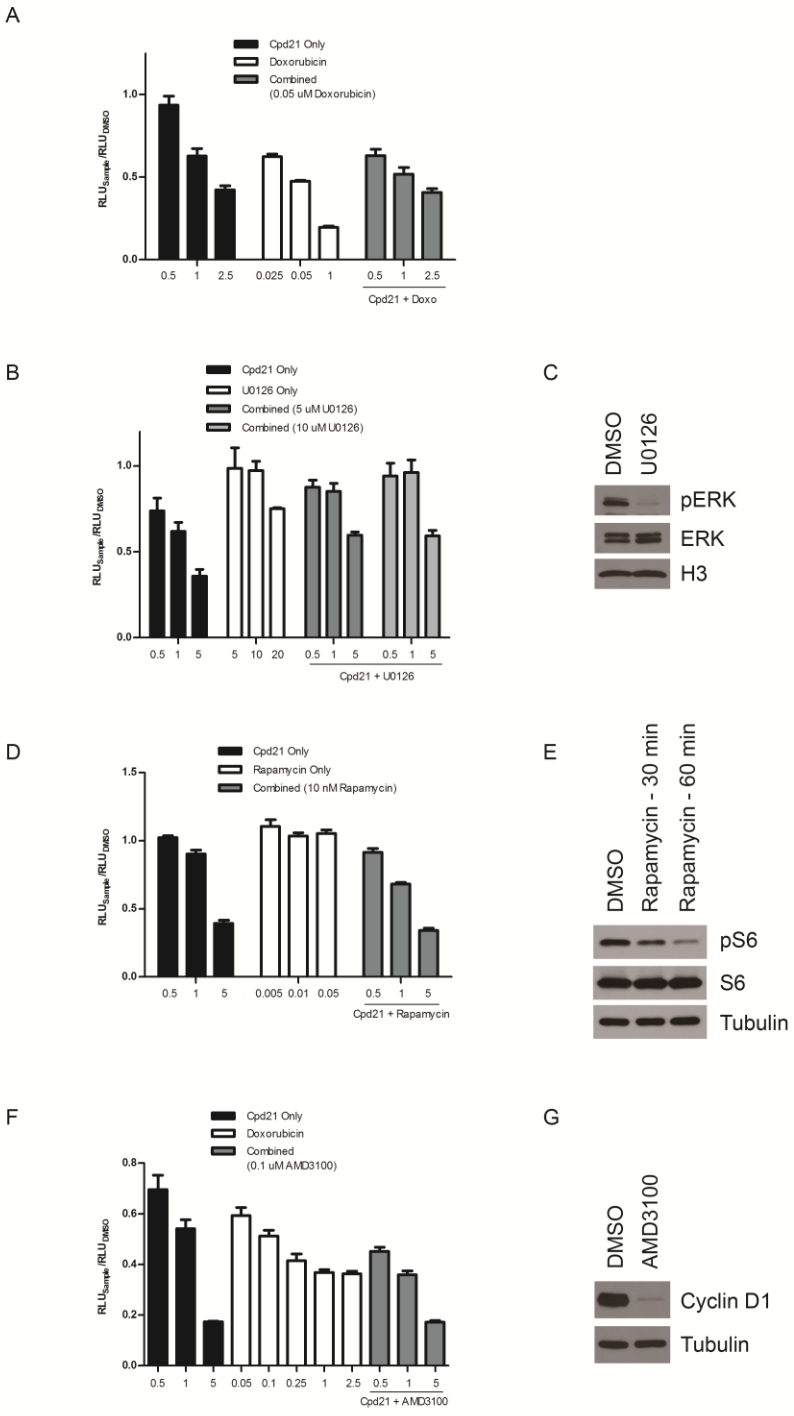


**Figure A4 Other Inhibitors Tested for Interaction with Cpd21.** Other inhibitors were tested, including (A) Doxorubicin, (B and C) U0126, (D and E) Rapamycin, and (F and G) AMD3100. Data tested for synergism by Loewe method. (C, E, G) Inhibitors were verified

for efficacy by Western blotting for downregulation of (C) pERK, (E) pS6, and (G) Cyclin D1, respectively.

## BIBLIOGRAPHY


Adams, J.M., Harris, A.W., Pinkert, C.A., Corcoran, L.M., Alexander, W.S., Cory, S., Palmiter, R.D., and Brinster, R.L. (1985). The c-myc oncogene driven by immunoglobulin enhancers induces lymphoid malignancy in transgenic mice. Nature *318*, 533-538.

Ambrosini, G., Cheema, H.S., Seelman, S., Teed, A., Sambol, E.B., Singer, S., and Schwartz, G.K. (2008). Sorafenib inhibits growth and mitogen-activated protein kinase signaling in malignant peripheral nerve sheath cells. Mol Cancer Ther *7*, 890-896.

Andersson, J., Sihto, H., Meis-Kindblom, J.M., Joensuu, H., Nupponen, N., and Kindblom, L.G. (2005). NF1-associated gastrointestinal stromal tumors have unique clinical, phenotypic, and genotypic characteristics. Am J Surg Pathol *29*, 1170-1176.

Angelov, L., Davis, A., O'Sullivan, B., Bell, R., and Guha, A. (1998). Neurogenic sarcomas: experience at the University of Toronto. Neurosurgery *43*, 56-64.

Anghileri, M., Miceli, R., Fiore, M., Mariani, L., Ferrari, A., Mussi, C., Lozza, L., Collini, P., Olmi, P., Casali, P.G., *et al.* (2006). Malignant peripheral nerve sheath tumors. Cancer *107*, 1065-1074.

Aoki, M., Nabeshima, K., Koga, K., Hamasaki, M., Suzumiya, J., Tamura, K., and Iwasaki, H. (2007). Imatinib mesylate inhibits cell invasion of malignant peripheral nerve sheath tumor induced by platelet-derived growth factor-BB. Lab Invest *87*, 767-779.

Bader, J.L., and Miller, R.W. (1978). Neurofibromatosis and childhood leukemia. J Pediatr *92*, 925-929.

Ballester, R., Marchuk, D., Boguski, M., Saulino, A., Letcher, R., Wigler, M., and Collins, F. (1990). The NF1 locus encodes a protein functionally related to mammalian GAP and yeast IRA proteins. Cell *63*, 851-859.

Baron, U., and Bujard, H. (2000). Tet repressor-based system for regulated gene expression in eukaryotic cells: principles and advances. Methods Enzymol *327*, 401-421.

Basu, T.N., Gutmann, D.H., Fletcher, J.A., Glover, T.W., Collins, F.S., and Downward, J. (1992). Aberrant regulation of ras proteins in malignant tumour cells from type 1 neurofibromatosis patients. Nature *356*, 713-715.

Bates, S., Bonetta, L., MacAllan, D., Parry, D., Holder, A., Dickson, C., and Peters, G. (1994). CDK6 (PLSTIRE) and CDK4 (PSK-J3) are a distinct subset of the cyclin-dependent kinases that associate with cyclin D1. Oncogene *9*, 71-79.

Bausch, B., Borozdin, W., Mautner, V.F., Hoffmann, M.M., Boehm, D., Robledo, M., Cascon, A., Harenberg, T., Schiavi, F., Pawlu, C., *et al.* (2007). Germline NF1 mutational spectra and loss-of-heterozygosity analyses in patients with pheochromocytoma and neurofibromatosis type 1. J Clin Endocrinol Metab *92*, 2784-2792.

Bennett, E., Thomas, N., and Upadhyaya, M. (2009). Neurofibromatosis type 1: its association with the Ras/MAPK pathway syndromes. Journal of Pediatric Neurology *7*, 105-115.

Berghmans, S., Murphey, R.D., Wienholds, E., Neuberg, D., Kutok, J.L., Fletcher, C.D., Morris, J.P., Liu, T.X., Schulte-Merker, S., Kanki, J.P., *et al.* (2005). tp53 mutant zebrafish develop malignant peripheral nerve sheath tumors. Proc Natl Acad Sci U S A *102*, 407-412.

Bernardis, V., Sorrentino, D., Snidero, D., Avellini, C., Paduano, R., Beltrami, C., Digito, F., and Bartoli, E. (1999). Intestinal Leiomyosarcoma and Gastroparesis Associated withvon Recklinghausen's Disease. Digestion *60*, 82-85.

Berner, J.M., Sorlie, T., Mertens, F., Henriksen, J., Saeter, G., Mandahl, N., Brogger, A., Myklebost, O., and Lothe, R.A. (1999). Chromosome band 9p21 is frequently altered in malignant peripheral nerve sheath tumors: studies of CDKN2A and other genes of the pRB pathway. Genes Chromosomes Cancer *26*, 151-160.

Bhargava, R., Parham, D., Lasater, O., Chari, R., Chen, G., and Fletcher, B. (1997). MR imaging differentiation of benign and malignant peripheral nerve sheath tumors: use of the target sign. Pediatric Radiology *27*, 124-129.

Biernaskie, J.A., McKenzie, I.A., Toma, J.G., and Miller, F.D. (2006). Isolation of skin-derived precursors (SKPs) and differentiation and enrichment of their Schwann cell progeny. Nat Protoc *1*, 2803-2812.

Birindelli, S., Perrone, F., Oggionni, M., Lavarino, C., Pasini, B., Vergani, B., Ranzani, G.N., Pierotti, M.A., and Pilotti, S. (2001). Rb and TP53 pathway alterations in sporadic and NF1-related malignant peripheral nerve sheath tumors. Lab Invest *81*, 833-844.

Bollag, G., Clapp, D.W., Shih, S., Adler, F., Zhang, Y.Y., Thompson, P., Lange, B.J., Freedman, M.H., McCormick, F., and Jacks, T. (1996). Loss of NF1 results in activation of the Ras signaling pathway and leads to aberrant growth in haematopoietic cells. Nature genetics *12*, 144-148.

Brannan, C.I., Perkins, A.S., Vogel, K.S., Ratner, N., Nordlund, M.L., Reid, S.W., Buchberg, A.M., Jenkins, N.A., Parada, L.F., and Copeland, N.G. (1994). Targeted disruption of the neurofibromatosis type-1 gene leads to developmental abnormalities in heart and various neural crest-derived tissues. Genes Dev *8*, 1019-1029.

Brazil, D.P., and Hemmings, B.A. (2001). Ten years of protein kinase B signalling: a hard Akt to follow. Trends in Biochemical Sciences *26*, 657.

Brems, H., Beert, E., de Ravel, T., and Legius, E. (2009). Mechanisms in the pathogenesis of malignant tumours in neurofibromatosis type 1. Lancet Oncol *10*, 508-515.

Brenner, D.E., Wiernik, P.H., Wesley, M., and Bachur, N.R. (1984). Acute doxorubicin toxicity relationship to pretreatment liver function, response, and pharmacokinetics in patients with acute nonlymphocytic leukemia. Cancer *53*, 1042-1048.

Brinster, R.L., Chen, H.Y., Messing, A., van Dyke, T., Levine, A.J., and Palmiter, R.D. (1984). Transgenic mice harboring SV40 T-antigen genes develop characteristic brain tumors. Cell *37*, 367-379.

Brocard, J., Warot, X., Wendling, O., Messaddeq, N., Vonesch, J.L., Chambon, P., and Metzger, D. (1997). Spatio-temporally controlled site-specific somatic mutagenesis in the mouse. Proc Natl Acad Sci U S A *94*, 14559-14563.

Buchberg, A.M., Buckwalter, M.S., and Camper, S.A. (1992). Mouse chromosome 11. Mamm Genome *3 Spec No*, S162-181.

Buchstaller, J., McKeever, Paul E., and Morrison, Sean J. (2012). Tumorigenic Cells Are Common in Mouse MPNSTs but Their Frequency Depends upon Tumor Genotype and Assay Conditions. Cancer Cell *21*, 240-252.

Buranasinsup, S., Sila-Asna, M., Bunyaratvej, N., and Bunyaratvej, A. (2006). In vitro osteogenesis from human skin-derived precursor cells. Dev Growth Differ *48*, 263-269.

Cantley, L.C., and Neel, B.G. (1999). New insights into tumor suppression: PTEN suppresses tumor formation by restraining the phosphoinositide 3-kinase/AKT pathway. Proceedings of the National Academy of Sciences *96*, 4240-4245.

Cardona, S., Schwarzbach, M., Hinz, U., Dimitrakopoulou-Strauss, A., Attigah, N., Mechtersheimer, G., and Lehnert, T. (2003). Evaluation of F18-deoxyglucose positron emission tomography (FDG-PET) to assess the nature of neurogenic tumours. European journal of surgical oncology *29*, 536-541.

Cawthon, R.M., Weiss, R., Xu, G., Viskochil, D., Culver, M., Stevens, J., Robertson, M., Dunn, D., Gesteland, R., and O'Connell, P. (1990). A major segment of the neurofibromatosis type 1 gene: cDNA sequence, genomic structure, and point mutations. Cell *62*, 193-201.

Cichowski, K., and Jacks, T. (2001). NF1 tumor suppressor gene function: narrowing the GAP. Cell *104*, 593-604.

Cichowski, K., Shih, T.S., Schmitt, E., Santiago, S., Reilly, K., McLaughlin, M.E., Bronson, R.T., and Jacks, T. (1999). Mouse models of tumor development in neurofibromatosis type 1. Science *286*, 2172-2176.

Clarke, A., Purdie, C., Harrison, D., Morris, R., Bird, C., Hooper, M., and Wyllie, A. (1993). Thymocyte apoptosis induced by p53-dependent and independent pathways. Nature *362*, 849-852.

Coffin, C.M., Cassity, J., Viskochil, D., Randall, R.L., and Albritton, K. (2004). Non-neurogenic sarcomas in four children and young adults with neurofibromatosis type 1. Am J Med Genet A *127A*, 40-43.

Coleman, M.L., Sahai, E.A., Yeo, M., Bosch, M., Dewar, A., and Olson, M.F. (2001). Membrane blebbing during apoptosis results from caspase-mediated activation of ROCK I. Nat Cell Biol *3*, 339-345.

Crowe, F.W., Schull, W.J., and Neel, J.V. (1956). A Clinical Pathological and Genetic Study of Multiple Neurofibromatosis. Frank W. Crowe,... William J. Schull,... James V. Neel (Ch. C. Thomas).

Cunha, K.S.G., Barboza, E.P., and Da Fonseca, E.C. (2003). Identification of growth hormone receptor in localised neurofibromas of patients with neurofibromatosis type 1. Journal of Clinical Pathology *56*, 758-763.

D'Adamo, D.R., Anderson, S.E., Albritton, K., Yamada, J., Riedel, E., Scheu, K., Schwartz, G.K., Chen, H., and Maki, R.G. (2005). Phase II study of doxorubicin and bevacizumab for patients with metastatic soft-tissue sarcomas. J Clin Oncol *23*, 7135-7142.

Dasgupta, B., Yi, Y., Chen, D.Y., Weber, J.D., and Gutmann, D.H. (2005). Proteomic analysis reveals hyperactivation of the mammalian target of rapamycin pathway in neurofibromatosis 1-associated human and mouse brain tumors. Cancer Res *65*, 2755-2760.

De Raedt, T., Walton, Z., Yecies, Jessica L., Li, D., Chen, Y., Malone, Clare F., Maertens, O., Jeong, Seung M., Bronson, Roderick T., Lebleu, V., *et al.* (2011).

Exploiting Cancer Cell Vulnerabilities to Develop a Combination Therapy for Ras-Driven Tumors. Cancer Cell *20*, 400-413.

DeClue, J.E., Papageorge, A.G., Fletcher, J.A., Diehl, S.R., Ratner, N., Vass, W.C., and Lowy, D.R. (1992). Abnormal regulation of mammalian p21ras contributes to malignant tumor growth in von Recklinghausen (type 1) neurofibromatosis. Cell *69*, 265-273.

Dilworth, J.T., Kraniak, J.M., Wojtkowiak, J.W., Gibbs, R.A., Borch, R.F., Tainsky, M.A., Reiners, J.J., Jr., and Mattingly, R.R. (2006). Molecular targets for emerging anti-tumor therapies for neurofibromatosis type 1. Biochem Pharmacol *72*, 1485-1492.

Donehower, L.A., Harvey, M., Slagle, B.L., McArthur, M.J., Montgomery, C.A., Jr., Butel, J.S., and Bradley, A. (1992). Mice deficient for p53 are developmentally normal but susceptible to spontaneous tumours. Nature *356*, 215-221.

Ducatman, B.S., Scheithauer, B.W., Piepgras, D.G., Reiman, H.M., and Ilstrup, D.M. (1986). Malignant peripheral nerve sheath tumors. A clinicopathologic study of 120 cases. Cancer *57*, 2006-2021.

Dugoff, L., and Sujansky, E. (1996). Neurofibromatosis type 1 and pregnancy. Am J Med Genet *66*, 7-10.

Dupuy, A.J., Akagi, K., Largaespada, D.A., Copeland, N.G., and Jenkins, N.A. (2005). Mammalian mutagenesis using a highly mobile somatic Sleeping Beauty transposon system. Nature *436*, 221-226.

Egan, S.E., Giddings, B.W., Brooks, M.W., Buday, L., Sizeland, A.M., and Weinberg, R.A. (1993). Association of Sos Ras exchange protein with Grb2 is implicated in tyrosine kinase signal transduction and transformation. Nature *363*, 45-51.

Evans, D.G.R., Baser, M.E., McGaughran, J., Sharif, S., Howard, E., and Moran, A. (2002). Malignant peripheral nerve sheath tumours in neurofibromatosis 1. Journal of medical genetics *39*, 311-314.

Feil, R., Wagner, J., Metzger, D., and Chambon, P. (1997). Regulation of Cre recombinase activity by mutated estrogen receptor ligand-binding domains. Biochem Biophys Res Commun *237*, 752-757.

Fernandes, K.J., Kobayashi, N.R., Gallagher, C.J., Barnabe-Heider, F., Aumont, A., Kaplan, D.R., and Miller, F.D. (2006). Analysis of the neurogenic potential of multipotent skin-derived precursors. Exp Neurol *201*, 32-48.

Fernandes, K.J., McKenzie, I.A., Mill, P., Smith, K.M., Akhavan, M., Barnabe-Heider, F., Biernaskie, J., Junek, A., Kobayashi, N.R., Toma, J.G., *et al.* (2004). A dermal niche for multipotent adult skin-derived precursor cells. Nat Cell Biol *6*, 1082-1093.

Fernandes, K.J., Toma, J.G., and Miller, F.D. (2008). Multipotent skin-derived precursors: adult neural crest-related precursors with therapeutic potential. Philos Trans R Soc Lond B Biol Sci *363*, 185-198.

Ferner, R.E. (2007). Neurofibromatosis 1. Eur J Hum Genet *15*, 131-138.

Ferner, R.E., and Gutmann, D.H. (2002). International consensus statement on malignant peripheral nerve sheath tumors in neurofibromatosis. Cancer Res *62*, 1573-1577.

Ferrari, A., Bisogno, G., Macaluso, A., Casanova, M., D'Angelo, P., Pierani, P., Zanetti, I., Alaggio, R., Cecchetto, G., and Carli, M. (2007). Soft-tissue sarcomas in children and adolescents with neurofibromatosis type 1. Cancer *109*, 1406-1412.

Fesik, S.W. (2005). Promoting apoptosis as a strategy for cancer drug discovery. Nat Rev Cancer *5*, 876-885.

Fishbein, L., Zhang, X., Fisher, L.B., Li, H., Campbell-Thompson, M., Yachnis, A., Rubenstein, A., Muir, D., and Wallace, M.R. (2007). In vitro studies of steroid hormones in neurofibromatosis 1 tumors and schwann cells. Molecular Carcinogenesis *46*, 512-523.

Gorman, C., and Bullock, C. (2000). Site-specific gene targeting for gene expression in eukaryotes. Curr Opin Biotechnol *11*, 455-460.

Greenblatt, M.S., Bennett, W.P., Hollstein, M., and Harris, C.C. (1994). Mutations in the p53 tumor suppressor gene: clues to cancer etiology and molecular pathogenesis. Cancer Res *54*, 4855-4878.

Gregorian, C., Nakashima, J., Dry, S.M., Nghiemphu, P.L., Smith, K.B., Ao, Y., Dang, J., Lawson, G., Mellinghoff, I.K., Mischel, P.S., *et al.* (2009). PTEN dosage is essential for neurofibroma development and malignant transformation. Proceedings of the National Academy of Sciences *106*, 19479-19484.

Grobmyer, S.R., Reith, J.D., Shahlaee, A., Bush, C.H., and Hochwald, S.N. (2008). Malignant peripheral nerve sheath tumor: molecular pathogenesis and current management considerations. Journal of surgical oncology *97*, 340-349.

Guha, A., Lau, N., Huvar, I., Gutmann, D., Provias, J., Pawson, T., and Boss, G. (1996). Ras-GTP levels are elevated in human NF1 peripheral nerve tumors. Oncogene *12*, 507-513.

Gutmann, D.H. (2001). The neurofibromatoses: when less is more. Hum Mol Genet *10*, 747-755.

Gutmann, D.H., Aylsworth, A., Carey, J.C., Korf, B., Marks, J., Pyeritz, R.E., Rubenstein, A., and Viskochil, D. (1997). The diagnostic evaluation and multidisciplinary management of neurofibromatosis 1 and neurofibromatosis 2. JAMA *278*, 51-57.

Hacker, G. (2000). The morphology of apoptosis. Cell Tissue Res *301*, 5-17.

Hakem, R., Hakem, A., Duncan, G.S., Henderson, J.T., Woo, M., Soengas, M.S., Elia, A., de la Pompa, J.L., Kagi, D., Khoo, W., *et al.* (1998). Differential requirement for caspase 9 in apoptotic pathways in vivo. Cell *94*, 339-352.

Hanahan, D. (1985). Heritable formation of pancreatic beta-cell tumours in transgenic mice expressing recombinant insulin/simian virus 40 oncogenes. Nature *315*, 115-122.

Hanahan, D., and Weinberg, R.A. (2011). Hallmarks of cancer: the next generation. Cell *144*, 646-674.

Harbour, J.W., Luo, R.X., Santi, A.D., Postigo, A.A., and Dean, D.C. (1999). Cdk Phosphorylation Triggers Sequential Intramolecular Interactions that Progressively Block Rb Functions as Cells Move through G1. Cell *98*, 859-869.

Hay, N., and Sonenberg, N. (2004). Upstream and downstream of mTOR. Genes Dev *18*, 1926-1945.

Hegedus, B., Banerjee, D., Yeh, T.H., Rothermich, S., Perry, A., Rubin, J.B., Garbow, J.R., and Gutmann, D.H. (2008). Preclinical cancer therapy in a mouse model of neurofibromatosis-1 optic glioma. Cancer Res *68*, 1520-1528.

Hennessy, B.T., Smith, D.L., Ram, P.T., Lu, Y., and Mills, G.B. (2005). Exploiting the PI3K/AKT pathway for cancer drug discovery. Nat Rev Drug Discov *4*, 988-1004.

Huson, S.M. (1999). What level of care for the neurofibromatoses? Lancet *353*, 1114-1116.

Huson, S.M., Compston, D.A., Clark, P., and Harper, P.S. (1989). A genetic study of von Recklinghausen neurofibromatosis in south east Wales. I. Prevalence, fitness, mutation rate, and effect of parental transmission on severity. J Med Genet *26*, 704-711.

Huson, S.M., Harper, P.S., and Compston, D.A. (1988). Von Recklinghausen neurofibromatosis. A clinical and population study in south-east Wales. Brain *111 ( Pt 6)*, 1355-1381.

Inoki, K., Li, Y., Zhu, T., Wu, J., and Guan, K.-L. (2002). TSC2 is phosphorylated and inhibited by Akt and suppresses mTOR signalling. Nature cell biology *4*, 648-657.

Jacks, T., Fazeli, A., Schmitt, E.M., Bronson, R.T., Goodell, M.A., and Weinberg, R.A. (1992). Effects of an Rb mutation in the mouse. Nature *359*, 295-300.

Jacks, T., Shih, T.S., Schmitt, E.M., Bronson, R.T., Bernards, A., and Weinberg, R.A. (1994). Tumour predisposition in mice heterozygous for a targeted mutation in Nf1. Nat Genet *7*, 353-361.

Jeffers, J.R., Parganas, E., Lee, Y., Yang, C., Wang, J., Brennan, J., MacLean, K.H., Han, J., Chittenden, T., Ihle, J.N., *et al.* (2003). Puma is an essential mediator of p53-dependent and -independent apoptotic pathways. Cancer Cell *4*, 321-328.

Jessen, W.J., Miller, S.J., Jousma, E., Wu, J., Rizvi, T.A., Brundage, M.E., Eaves, D., Widemann, B., Kim, M.O., Dombi, E., *et al.* (2013). MEK inhibition exhibits efficacy in human and mouse neurofibromatosis tumors. J Clin Invest *123*, 340-347.

Jhanwar, S.C., Chen, Q., Li, F.P., Brennan, M.F., and Woodruff, J.M. (1994). Cytogenetic analysis of soft tissue sarcomas. Recurrent chromosome abnormalities in malignant peripheral nerve sheath tumors (MPNST). Cancer Genet Cytogenet *78*, 138-144.

Johannessen, C.M., Reczek, E.E., James, M.F., Brems, H., Legius, E., and Cichowski, K. (2005). The NF1 tumor suppressor critically regulates TSC2 and mTOR. Proc Natl Acad Sci U S A *102*, 8573-8578.

Johansson, G., Mahller, Y.Y., Collins, M.H., Kim, M.-O., Nobukuni, T., Perentesis, J., Cripe, T.P., Lane, H.A., Kozma, S.C., Thomas, G., *et al.* (2008). Effective in vivo targeting of the mammalian target of rapamycin pathway in malignant peripheral nerve sheath tumors. Molecular Cancer Therapeutics *7*, 1237-1245.

Joseph, N.M., Mosher, J.T., Buchstaller, J., Snider, P., McKeever, P.E., Lim, M., Conway, S.J., Parada, L.F., Zhu, Y., and Morrison, S.J. (2008). The loss of Nf1 transiently promotes self-renewal but not tumorigenesis by neural crest stem cells. Cancer Cell *13*, 129-140.

Joseph, N.M., Mukouyama, Y.S., Mosher, J.T., Jaegle, M., Crone, S.A., Dormand, E.L., Lee, K.F., Meijer, D., Anderson, D.J., and Morrison, S.J. (2004). Neural crest

stem cells undergo multilineage differentiation in developing peripheral nerves to generate endoneurial fibroblasts in addition to Schwann cells. Development *131*, 5599-5612.

Kahn, H.J., Marks, A., Thom, H., and Baumal, R. (1983). Role of antibody to S100 protein in diagnostic pathology. Am J Clin Pathol *79*, 341-347.

Kandel, E.S., and Hay, N. (1999). The regulation and activities of the multifunctional serine/threonine kinase Akt/PKB. Experimental Cell Research *253*, 210.

Kastan, M.B., and Bartek, J. (2004). Cell-cycle checkpoints and cancer. Nature *432*, 316-323.

Kastan, M.B., Onyekwere, O., Sidransky, D., Vogelstein, B., and Craig, R.W. (1991). Participation of p53 Protein in the Cellular Response to DNA Damage. Cancer Research *51*, 6304-6311.

Katz, D., Lazar, A., and Lev, D. (2009). Malignant peripheral nerve sheath tumour (MPNST): the clinical implications of cellular signalling pathways. Expert Rev Mol Med *11*, e30.

Katz, M.E., and McCormick, F. (1997). Signal transduction from multiple Ras effectors. Curr Opin Genet Dev *7*, 75-79.

Keng, V.W., Rahrmann, E.P., Watson, A.L., Tschida, B.R., Moertel, C.L., Jessen, W.J., Rizvi, T.A., Collins, M.H., Ratner, N., and Largaespada, D.A. (2012a). PTEN and NF1 inactivation in Schwann cells produces a severe phenotype in the peripheral nervous system that promotes the development and malignant progression of peripheral nerve sheath tumors. Cancer Res *72*, 3405-3413.

Keng, V.W., Watson, A.L., Rahrmann, E.P., Li, H., Tschida, B.R., Moriarity, B.S., Choi, K., Rizvi, T.A., Collins, M.H., Wallace, M.R., *et al.* (2012b). Conditional Inactivation of Pten with EGFR Overexpression in Schwann Cells Models Sporadic MPNST. Sarcoma *2012*, 620834.

Kioussi, C., and Gruss, P. (1996). Making of a Schwann. Trends in Genetics *12*, 84-86.

Korf, B.R. (1999). Plexiform neurofibromas. Am J Med Genet *89*, 31-37.

Kourea, H.P., Orlow, I., Scheithauer, B.W., Cordon-Cardo, C., and Woodruff, J.M. (1999). Deletions of the INK4A gene occur in malignant peripheral nerve sheath tumors but not in neurofibromas. Am J Pathol *155*, 1855-1860.

Kroep, J.R., Ouali, M., Gelderblom, H., Le Cesne, A., Dekker, T.J., Van Glabbeke, M., Hogendoorn, P.C., and Hohenberger, P. (2011). First-line chemotherapy for

malignant peripheral nerve sheath tumor (MPNST) versus other histological soft tissue sarcoma subtypes and as a prognostic factor for MPNST: an EORTC soft tissue and bone sarcoma group study. Ann Oncol *22*, 207-214.

Lakkis, M.M., and Tennekoon, G.I. (2000). Neurofibromatosis type 1. I. General overview. J Neurosci Res *62*, 755-763.

Le, L.Q., and Parada, L.F. (2007). Tumor microenvironment and neurofibromatosis type I: connecting the GAPs. Oncogene *26*, 4609-4616.

Le, L.Q., Shipman, T., Burns, D.K., and Parada, L.F. (2009). Cell of origin and microenvironment contribution for NF1-associated dermal neurofibromas. Cell Stem Cell *4*, 453-463.

Leverrier, Y., and Ridley, A.J. (2001). Apoptosis: caspases orchestrate the ROCK 'n' bleb. Nat Cell Biol *3*, E91-93.

Li, H., Velasco-Miguel, S., Vass, W.C., Parada, L.F., and DeClue, J.E. (2002). Epidermal growth factor receptor signaling pathways are associated with tumorigenesis in the Nf1:p53 mouse tumor model. Cancer Res *62*, 4507-4513.

Li, Z., Jiang, H., Xie, W., Zhang, Z., Smrcka, A.V., and Wu, D. (2000). Roles of PLC-beta2 and -beta3 and PI3Kgamma in chemoattractant-mediated signal transduction. Science *287*, 1046-1049.

Lin, B.T., Weiss, L.M., and Medeiros, L.J. (1997). Neurofibroma and cellular neurofibroma with atypia: a report of 14 tumors. The American Journal of Surgical Pathology *21*, 1443-1449.

Listernick, R., Louis, D.N., Packer, R.J., and Gutmann, D.H. (1997). Optic pathway gliomas in children with neurofibromatosis 1: consensus statement from the NF1 Optic Pathway Glioma Task Force. Ann Neurol *41*, 143-149.

Lowenstein, E.J., Daly, R.J., Batzer, A.G., Li, W., Margolis, B., Lammers, R., Ullrich, A., Skolnik, E.Y., Bar-Sagi, D., and Schlessinger, J. (1992). The SH2 and SH3 domain-containing protein GRB2 links receptor tyrosine kinases to ras signaling. Cell *70*, 431-442.

Lu, J., Ma, Z., Hsieh, J.-C., Fan, C.-W., Chen, B., Longgood, J.C., Williams, N.S., Amatruda, J.F., Lum, L., and Chen, C. (2009). Structure–activity relationship studies of small-molecule inhibitors of Wnt response. Bioorganic & Medicinal Chemistry Letters *19*, 3825-3827.

Lundberg, A.S., and Weinberg, R.A. (1998). Functional inactivation of the retinoblastoma protein requires sequential modification by at least two distinct cyclin-cdk complexes. Mol Cell Biol *18*, 753-761.

Malumbres, M., and Barbacid, M. (2001). Milestones in cell division: to cycle or not to cycle: a critical decision in cancer. Nature Reviews Cancer *1*, 222-231.

Malumbres, M., and Barbacid, M. (2005). Mammalian cyclin-dependent kinases. Trends in Biochemical Sciences *30*, 630-641.

Malumbres, M., and Barbacid, M. (2009). Cell cycle, CDKs and cancer: a changing paradigm. Nat Rev Cancer *9*, 153-166.

Mandal, D., Moitra, P.K., Saha, S., and Basu, J. (2002). Caspase 3 regulates phosphatidylserine externalization and phagocytosis of oxidatively stressed erythrocytes. FEBS Lett *513*, 184-188.

Manning, B.D., Tee, A.R., Logsdon, M.N., Blenis, J., and Cantley, L.C. (2002). Identification of the tuberous sclerosis complex-2 tumor suppressor gene product tuberin as a target of the phosphoinositide 3-kinase/akt pathway. Molecular Cell *10*, 151-162.

Mao, C., Shah, A., Hanson, D.J., and Howard, J.M. (1995). Von Recklinghausen's disease associated with duodenal somatostatinoma: contrast of duodenal versus pancreatic somatostatinomas. J Surg Oncol *59*, 67-73.

Mattingly, R.R., Kraniak, J.M., Dilworth, J.T., Mathieu, P., Bealmear, B., Nowak, J.E., Benjamins, J.A., Tainsky, M.A., and Reiners, J.J., Jr. (2006). The mitogen-activated protein kinase/extracellular signal-regulated kinase kinase inhibitor PD184352 (CI-1040) selectively induces apoptosis in malignant schwannoma cell lines. J Pharmacol Exp Ther *316*, 456-465.

Mayes, D.A., Rizvi, T.A., Cancelas, J.A., Kolasinski, N.T., Ciraolo, G.M., Stemmer-Rachamimov, A.O., and Ratner, N. (2011). Perinatal or Adult Nf1 Inactivation Using Tamoxifen-Inducible PlpCre Each Cause Neurofibroma Formation. Cancer Res *71*, 4675-4685.

McKenzie, I.A., Biernaskie, J., Toma, J.G., Midha, R., and Miller, F.D. (2006). Skin-derived precursors generate myelinating Schwann cells for the injured and dysmyelinated nervous system. J Neurosci *26*, 6651-6660.

McLaughlin, M.E., and Jacks, T. (2003). Progesterone Receptor Expression in Neurofibromas. Cancer Research *63*, 752-755.

Menon, A.G., Anderson, K.M., Riccardi, V.M., Chung, R.Y., Whaley, J.M., Yandell, D.W., Farmer, G.E., Freiman, R.N., Lee, J.K., Li, F.P., *et al.* (1990). Chromosome 17p deletions and p53 gene mutations associated with the formation of malignant neurofibrosarcomas in von Recklinghausen neurofibromatosis. Proc Natl Acad Sci U S A *87*, 5435-5439.

Mo, W., Chen, J., Patel, A., Zhang, L., Chau, V., Li, Y., Cho, W., Lim, K., Xu, J., Lazar, Alexander J., *et al.* (2013). CXCR4/CXCL12 Mediate Autocrine Cell- Cycle Progression in NF1-Associated Malignant Peripheral Nerve Sheath Tumors. Cell *152*, 1077-1090.

Morrison, S.J., White, P.M., Zock, C., and Anderson, D.J. (1999). Prospective identification, isolation by flow cytometry, and in vivo self-renewal of multipotent mammalian neural crest stem cells. Cell *96*, 737-749.

Mousley, C.J., Tyeryar, K.R., Vincent-Pope, P., and Bankaitis, V.A. (2007). The Sec14-superfamily and the regulatory interface between phospholipid metabolism and membrane trafficking. Biochimica et Biophysica Acta (BBA) - Molecular and Cell Biology of Lipids *1771*, 727-736.

Nagy, A. (2000). Cre recombinase: the universal reagent for genome tailoring. Genesis *26*, 99-109.

Nicholson, D.W., Ali, A., Thornberry, N.A., Vaillancourt, J.P., Ding, C.K., Gallant, M., Gareau, Y., Griffin, P.R., Labelle, M., Lazebnik, Y.A., *et al.* (1995). Identification and inhibition of the ICE/CED-3 protease necessary for mammalian apoptosis. Nature *376*, 37-43.

Nielsen, G.P., Stemmer-Rachamimov, A.O., Ino, Y., Møller, M.B., Rosenberg, A.E., and Louis, D.N. (1999). Malignant Transformation of Neurofibromas in Neurofibromatosis 1 Is Associated with CDKN2A/p16 Inactivation. The American Journal of Pathology *155*, 1879-1884.

Ozonoff, S. (1999). Cognitive impairment in neurofibromatosis type 1. Am J Med Genet *89*, 45-52.

Palmero, I., Pantoja, C., and Serrano, M. (1998). p19ARF links the tumour suppressor p53 to Ras. Nature *395*, 125-126.

Peled, A., Zipori, D., and Rotter, V. (1996). Cooperation between p53-dependent and p53-independent apoptotic pathways in myeloid cells. Cancer Res *56*, 2148-2156.

Peng, X.-d., Xu, P.-Z., Chen, M.-L., Hahn-Windgassen, A., Skeen, J., Jacobs, J., Sundararajan, D., Chen, W.S., Crawford, S.E., and Coleman, K.G. (2003). Dwarfism, impaired skin development, skeletal muscle atrophy, delayed bone

development, and impeded adipogenesis in mice lacking Akt1 and Akt2. Genes & Development *17*, 1352-1365.

Perrone, F., Tabano, S., Colombo, F., Dagrada, G., Birindelli, S., Gronchi, A., Colecchia, M., Pierotti, M.A., and Pilotti, S. (2003). p15INK4b, p14ARF, and p16INK4a inactivation in sporadic and neurofibromatosis type 1-related malignant peripheral nerve sheath tumors. Clin Cancer Res *9*, 4132-4138.

Pinsk, I., Dukhno, O., Ovnat, A., and Levy, I. (2003). Gastrointestinal complications of von Recklinghausen's disease: two case reports and a review of the literature. Scand J Gastroenterol *38*, 1275-1278.

Quelle, D.E., Zindy, F., Ashmun, R.A., and Sherr, C.J. (1995). Alternative reading frames of the INK4a tumor suppressor gene encode two unrelated proteins capable of inducing cell cycle arrest. Cell *83*, 993-1000.

Rahrmann, E.P., Watson, A.L., Keng, V.W., Choi, K., Moriarity, B.S., Beckmann, D.A., Wolf, N.K., Sarver, A., Collins, M.H., Moertel, C.L., *et al.* (2013). Forward genetic screen for malignant peripheral nerve sheath tumor formation identifies new genes and pathways driving tumorigenesis. Nat Genet.

Reuss, D.E., Mucha, J., Hagenlocher, C., Ehemann, V., Kluwe, L., Mautner, V., and von Deimling, A. (2013). Sensitivity of malignant peripheral nerve sheath tumor cells to TRAIL is augmented by loss of NF1 through modulation of MYC/MAD and is potentiated by curcumin through induction of ROS. PLoS One *8*, e57152.

Ridley, A.J., Paterson, H.F., Noble, M., and Land, H. (1988). Ras-mediated cell cycle arrest is altered by nuclear oncogenes to induce Schwann cell transformation. EMBO J *7*, 1635-1645.

Rossant, J., and McMahon, A. (1999). "Cre"-ating mouse mutants-a meeting review on conditional mouse genetics. Genes Dev *13*, 142-145.

Rozakis-Adcock, M., McGlade, J., Mbamalu, G., Pelicci, G., Daly, R., Li, W., Batzer, A., Thomas, S., Brugge, J., Pelicci, P.G., *et al.* (1992). Association of the Shc and Grb2/Sem5 SH2-containing proteins is implicated in activation of the Ras pathway by tyrosine kinases. Nature *360*, 689-692.

Ruggieri, M., and Huson, S.M. (1999). The neurofibromatoses. An overview. Ital J Neurol Sci *20*, 89-108.

Ruggieri, M., and Packer, R.J. (2001). Why do benign astrocytomas become malignant in NF1? Neurology *56*, 827-829.

Sarbassov, D.D., Guertin, D.A., Ali, S.M., and Sabatini, D.M. (2005). Phosphorylation and Regulation of Akt/PKB by the Rictor-mTOR Complex. Science *307*, 1098-1101.

Scheid, M.P., and Woodgett, J.R. (2001). PKB/AKT: functional insights from genetic models. Nature Reviews Molecular Cell Biology *2*, 760-768.

Sebbagh, M., Renvoize, C., Hamelin, J., Riche, N., Bertoglio, J., and Breard, J. (2001). Caspase-3-mediated cleavage of ROCK I induces MLC phosphorylation and apoptotic membrane blebbing. Nat Cell Biol *3*, 346-352.

Serra, E., Puig, S., Otero, D., Gaona, A., Kruyer, H., Ars, E., Estivill, X., and Lázaro, C. (1997). Confirmation of a Double-Hit Model for the NF1Gene in Benign Neurofibromas. The American Journal of Human Genetics *61*, 512-519.

Serrano, M., Hannon, G.J., and Beach, D. (1993). A new regulatory motif in cell-cycle control causing specific inhibition of cyclin D/CDK4. Nature *366*, 704-707.

Sharif, S., Ferner, R., Birch, J.M., Gillespie, J.E., Gattamaneni, H.R., Baser, M.E., and Evans, D.G.R. (2006). Second primary tumors in neurofibromatosis 1 patients treated for optic glioma: substantial risks after radiotherapy. Journal of clinical oncology *24*, 2570-2575.

Sherr, C.J. (1995). D-type cyclins. Trends Biochem Sci *20*, 187-190.

Sherr, C.J., and Roberts, J.M. (1999). CDK inhibitors: positive and negative regulators of G1-phase progression. Genes Dev *13*, 1501-1512.

Side, L., Taylor, B., Cayouette, M., Conner, E., Thompson, P., Luce, M., and Shannon, K. (1997). Homozygous inactivation of the NF1 gene in bone marrow cells from children with neurofibromatosis type 1 and malignant myeloid disorders. N Engl J Med *336*, 1713-1720.

Slee, E.A., Adrain, C., and Martin, S.J. (2001). Executioner caspase-3, -6, and -7 perform distinct, non-redundant roles during the demolition phase of apoptosis. J Biol Chem *276*, 7320-7326.

Slomiany, M.G., Dai, L., Bomar, P.A., Knackstedt, T.J., Kranc, D.A., Tolliver, L., Maria, B.L., and Toole, B.P. (2009). Abrogating Drug Resistance in Malignant Peripheral Nerve Sheath Tumors by Disrupting Hyaluronan-CD44 Interactions with Small Hyaluronan Oligosaccharides. Cancer Research *69*, 4992-4998.

Stefansson, K., Wollmann, R., and Jerkovic, M. (1982). S-100 protein in soft-tissue tumors derived from Schwann cells and melanocytes. Am J Pathol *106*, 261-268.

Stemple, D.L., and Anderson, D.J. (1992). Isolation of a stem cell for neurons and glia from the mammalian neural crest. Cell *71*, 973-985.

Stewart, T.A., Pattengale, P.K., and Leder, P. (1984). Spontaneous mammary adenocarcinomas in transgenic mice that carry and express MTV/myc fusion genes. Cell *38*, 627-637.

Straetemans, R., O'Brien, T., Wouters, L., Van Dun, J., Janicot, M., Bijnens, L., Burzykowski, T., and Aerts, M. (2005). Design and analysis of drug combination experiments. Biom J *47*, 299-308.

Strasser, A., Harris, A.W., Jacks, T., and Cory, S. (1994). DNA damage can induce apoptosis in proliferating lymphoid cells via p53-independent mechanisms inhibitable by Bcl-2. Cell *79*, 329-339.

Stumpf, D., Alksne, J., Annegers, J., Brown, S., Conneally, P., Housman, D., Leppert, M., Miller, J., Moss, M., and Pileggi, A. (1988). Neurofibromatosis. Conference statement. National institutes of health consensus development conference. Arch Neurol *45*, 575-578.

Suster, S., Fisher, C., and Moran, C.A. (1998). Expression of bcl-2 oncoprotein in benign and malignant spindle cell tumors of soft tissue, skin, serosal surfaces, and gastrointestinal tract. Am J Surg Pathol *22*, 863-872.

Symonds, H., Krall, L., Remington, L., Saenz-Robles, M., Lowe, S., Jacks, T., and Van Dyke, T. (1994). p53-dependent apoptosis suppresses tumor growth and progression in vivo. Cell *78*, 703-711.

Szudek, J., Birch, P., Riccardi, V.M., Evans, D.G., and Friedman, J.M. (2000). Associations of clinical features in neurofibromatosis 1 (NF1). Genet Epidemiol *19*, 429-439.

Takahashi, K., and Yamanaka, S. (2006). Induction of pluripotent stem cells from mouse embryonic and adult fibroblast cultures by defined factors. Cell *126*, 663-676.

Tam, S.W., Theodoras, A.M., Shay, J.W., Draetta, G.F., and Pagano, M. (1994). Differential expression and regulation of Cyclin D1 protein in normal and tumor human cells: association with Cdk4 is required for Cyclin D1 function in G1 progression. Oncogene *9*, 2663-2674.

Tanaka, Y., Yoshihara, K., Itaya, A., Kamiya, T., and Koide, S. (1984). Mechanism of the inhibition of Ca2+, Mg2+-dependent endonuclease of bull seminal plasma induced by ADP-ribosylation. Journal of Biological Chemistry *259*, 6579-6585.

Tewari, M., Quan, L.T., O'Rourke, K., Desnoyers, S., Zeng, Z., Beidler, D.R., Poirier, G.G., Salvesen, G.S., and Dixit, V.M. (1995). Yama/CPP32 beta, a mammalian homolog of CED-3, is a CrmA-inhibitable protease that cleaves the death substrate poly(ADP-ribose) polymerase. Cell *81*, 801-809.

Thornberry, N.A., and Lazebnik, Y. (1998). Caspases: enemies within. Science *281*, 1312-1316.

Toma, J.G., Akhavan, M., Fernandes, K.J., Barnabe-Heider, F., Sadikot, A., Kaplan, D.R., and Miller, F.D. (2001). Isolation of multipotent adult stem cells from the dermis of mammalian skin. Nat Cell Biol *3*, 778-784.

Toma, J.G., McKenzie, I.A., Bagli, D., and Miller, F.D. (2005). Isolation and characterization of multipotent skin-derived precursors from human skin. Stem Cells *23*, 727-737.

Tso, S.C., Qi, X., Gui, W.J., Chuang, J.L., Morlock, L.K., Wallace, A.L., Ahmed, K., Laxman, S., Campeau, P.M., Lee, B.H., *et al.* (2013). Structure-based design and mechanisms of allosteric inhibitors for mitochondrial branched-chain alpha-ketoacid dehydrogenase kinase. Proc Natl Acad Sci U S A *110*, 9728-9733.

Van Dyke, T., and Jacks, T. (2002). Cancer modeling in the modern era: progress and challenges. Cell *108*, 135-144.

Vauthey, J.-N., Woodruff, J.M., and Brennan, M.F. (1995). Extremity malignant peripheral nerve sheath tumors (neurogenic sarcomas): A 10-year experience. Annals of surgical oncology *2*, 126-131.

Vermes, I., Haanen, C., Steffens-Nakken, H., and Reutelingsperger, C. (1995). A novel assay for apoptosis. Flow cytometric detection of phosphatidylserine expression on early apoptotic cells using fluorescein labelled Annexin V. J Immunol Methods *184*, 39-51.

Villunger, A., Michalak, E.M., Coultas, L., Mullauer, F., Bock, G., Ausserlechner, M.J., Adams, J.M., and Strasser, A. (2003). p53- and drug-induced apoptotic responses mediated by BH3-only proteins puma and noxa. Science *302*, 1036-1038.

Viskochil, D., Buchberg, A.M., Xu, G., Cawthon, R.M., Stevens, J., Wolff, R.K., Culver, M., Carey, J.C., Copeland, N.G., and Jenkins, N.A. (1990). Deletions and a translocation interrupt a cloned gene at the neurofibromatosis type 1 locus. Cell *62*, 187-192.

Vlenterie, M., Flucke, U., Hofbauer, L.C., Timmers, H.J., Gastmeier, J., Aust, D.E., van der Graaf, W.T., Wesseling, P., Eisenhofer, G., and Lenders, J.W. (2013).

Pheochromocytoma and gastrointestinal stromal tumors in patients with neurofibromatosis type I. Am J Med *126*, 174-180.

Vogel, K.S., Klesse, L.J., Velasco-Miguel, S., Meyers, K., Rushing, E.J., and Parada, L.F. (1999). Mouse tumor model for neurofibromatosis type 1. Science *286*, 2176-2179.

Vogelstein, B., Lane, D., and Levine, A.J. (2000). Surfing the p53 network. Nature *408*, 307-310.

Wallace, M.R., Marchuk, D.A., Andersen, L.B., Letcher, R., Odeh, H.M., Saulino, A.M., Fountain, J.W., Brereton, A., Nicholson, J., and Mitchell, A.L. (1990). Type 1 neurofibromatosis gene: identification of a large transcript disrupted in three NF1 patients. Science *249*, 181-186.

Walther, M.M., Herring, J., Enquist, E., Keiser, H.R., and Linehan, W.M. (1999). von Recklinghausen's disease and pheochromocytomas. J Urol *162*, 1582-1586.

Watson, A.L., Rahrmann, E.P., Moriarity, B.S., Choi, K., Conboy, C.B., Greeley, A.D., Halfond, A.L., Anderson, L.K., Wahl, B.R., Keng, V.W., *et al.* (2013). Canonical Wnt/beta-catenin Signaling Drives Human Schwann Cell Transformation, Progression, and Tumor Maintenance. Cancer Discov *3*, 674-689.

Wei, M.C., Zong, W.X., Cheng, E.H., Lindsten, T., Panoutsakopoulou, V., Ross, A.J., Roth, K.A., MacGregor, G.R., Thompson, C.B., and Korsmeyer, S.J. (2001). Proapoptotic BAX and BAK: a requisite gateway to mitochondrial dysfunction and death. Science *292*, 727-730.

Weiss, B., Bollag, G., and Shannon, K. (1999). Hyperactive Ras as a therapeutic target in neurofibromatosis type 1. Am J Med Genet *89*, 14-22.

Williams, N.S., Burgett, A.W.G., Atkins, A.S., Wang, X., Harran, P.G., and McKnight, S.L. (2007). Therapeutic anticancer efficacy of a synthetic diazonamide analog in the absence of overt toxicity. Proceedings of the National Academy of Sciences *104*, 2074-2079.

Wittinghofer, A. (1998). Signal transduction via Ras. Biol Chem *379*, 933-937.

Wolf, B.B., and Green, D.R. (1999). Suicidal tendencies: apoptotic cell death by caspase family proteinases. J Biol Chem *274*, 20049-20052.

Wu, J., Williams, J.P., Rizvi, T.A., Kordich, J.J., Witte, D., Meijer, D., Stemmer-Rachamimov, A.O., Cancelas, J.A., and Ratner, N. (2008). Plexiform and dermal neurofibromas and pigmentation are caused by Nf1 loss in desert hedgehog-expressing cells. Cancer Cell *13*, 105-116.

Xu, G., Lin, B., Tanaka, K., Dunn, D., Wood, D., Gesteland, R., White, R., Weiss, R., and Tamanoi, F. (1990a). The catalytic domain of the neurofibromatosis type 1 gene product stimulates< i> ras</i> GTPase and complements< i> ira</i> mutants of S. cerevisiae. Cell *63*, 835-841.

Xu, G., O'Connell, P., Viskochil, D., Cawthon, R., Robertson, M., Culver, M., Dunn, D., Stevens, J., Gesteland, R., White, R., *et al.* (1990b). The neurofibromatosis type 1 gene encodes a protein related to GAP. Cell *62*, 599-608.

Yang, F.C., Ingram, D.A., Chen, S., Hingtgen, C.M., Ratner, N., Monk, K.R., Clegg, T., White, H., Mead, L., Wenning, M.J., *et al.* (2003). Neurofibromin-deficient Schwann cells secrete a potent migratory stimulus for Nf1+/- mast cells. J Clin Invest *112*, 1851-1861.

Yang, F.C., Ingram, D.A., Chen, S., Zhu, Y., Yuan, J., Li, X., Yang, X., Knowles, S., Horn, W., Li, Y., *et al.* (2008). Nf1-dependent tumors require a microenvironment containing Nf1+/-- and c-kit-dependent bone marrow. Cell *135*, 437-448.

Yoshihara, K., Tanigawa, Y., Burzio, L., and Koide, S.S. (1975). Evidence for adenosine diphosphate ribosylation of Ca2+, Mg2+-dependent endonuclease. Proc Natl Acad Sci U S A *72*, 289-293.

Yoshihara, K., Tanigawa, Y., and Koide, S.S. (1974). Inhibition of rat liver Ca2+, Mg2+-dependent endonuclease activity by nicotinamide adenine dinucleotide and poly (adenosine diphosphate ribose) synthetase. Biochem Biophys Res Commun *59*, 658-665.

Yu, J., and Zhang, L. (2003). No PUMA, no death: Implications for p53-dependent apoptosis. Cancer Cell *4*, 248-249.

Zheng, H., Chang, L., Patel, N., Yang, J., Lowe, L., Burns, D.K., and Zhu, Y. (2008). Induction of abnormal proliferation by nonmyelinating schwann cells triggers neurofibroma formation. Cancer Cell *13*, 117-128.

Zhu, Y., Ghosh, P., Charnay, P., Burns, D.K., and Parada, L.F. (2002). Neurofibromas in NF1: Schwann cell origin and role of tumor environment. Science *296*, 920-922.

Zimmer, D.B., Cornwall, E.H., Landar, A., and Song, W. (1995). The S100 protein family: history, function, and expression. Brain Res Bull *37*, 417-429.

Zinnamosca, L., Petramala, L., Cotesta, D., Marinelli, C., Schina, M., Cianci, R., Giustini, S., Sciomer, S., Anastasi, E., Calvieri, S., *et al.* (2011). Neurofibromatosis type 1 (NF1) and pheochromocytoma: prevalence, clinical and cardiovascular aspects. Arch Dermatol Res *303*, 317-325.

Zou, C., Smith, K.D., Liu, J., Lahat, G., Myers, S., Wang, W.-L., Zhang, W., McCutcheon, I.E., Slopis, J.M., and Lazar, A.J. (2009a). Clinical, pathological, and molecular variables predictive of malignant peripheral nerve sheath tumor outcome. Annals of surgery *249,* 1014-1022.

Zou, C.Y., Smith, K.D., Zhu, Q.-S., Liu, J., McCutcheon, I.E., Slopis, J.M., Meric-Bernstam, F., Peng, Z., Bornmann, W.G., Mills, G.B., *et al.* (2009b). Dual targeting of AKT and mammalian target of rapamycin: A potential therapeutic approach for malignant peripheral nerve sheath tumor. Molecular Cancer Therapeutics *8,* 1157-1168.

Zvulunov, A., Barak, Y., and Metzker, A. (1995). Juvenile xanthogranuloma, neurofibromatosis, and juvenile chronic myelogenous leukemia. World statistical analysis. Arch Dermatol *131,* 904-908.